# VISCOUS AND NONLINEAR EFFECTS IN THE OSCILLATIONS OF DROPS AND BUBBLES

Thesis by

Andrea Prosperetti

In Partial Fulfillment of the Requirements

for the Degree of

Doctor of Philosophy

California Institute of Technology

Pasadena, California

1974

(Submitted May 9, 1974)

Son of man,

You cannot say, or guess, for you know only

A heap of broken images

T. S. Eliot, The Waste Land

ACKNOWLEDGMENTS

I wish to thank Professor Milton S. Plesset for all he taught me, about physics, life, and myself. His guidance and friendship in the past three years have resulted in a most effective encouragement and have had a determining influence on my development. For all this I feel deeply grateful to him. I also wish to myself that whatever fragment of his style of scientific research I may have assimilated, I will not lose in time.

Of the many other persons at Caltech that have helped me in the struggle from Darkness to Knowledge I wish to thank in particular Professors Thomas K. Caughey, Paco A. Lagerstrom, and Theodore Y. Wu.

Miss Cecilia S. Lin has neglected her artistic pursuits to draw the figures of this thesis, and Miss Helen F. Burrus and Mrs. Barbara J. Hawk have transformed a messy handwriting into a neat typescript. To them goes my appreciation and gratitude.

## ABSTRACT

The thesis is divided into three parts. In Part I the nonlinear oscillations of a spherical gas bubble in an incompressible, viscous liquid are investigated analytically by means of an asymptotic method. The effect of surface tension is included, and it is shown that thermal and acoustic damping can be accounted for by the suitable redefinition of one parameter. Approximate analytical solutions for the steady state oscillations are presented for the fundamental mode as well as for the first and second subharmonic and for the first and second harmonic. The transient behaviour is also briefly considered. The first subharmonic is studied in particular detail, and a new explanation of its connection with acoustic cavitation is proposed. The approximate analytical results are compared with some numerical ones and a good agreement is found.

In Part II the characteristics of subharmonic and ultraharmonic modes appearing in the forced, steady state oscillations of weakly nonlinear systems are considered from the physical, rather than mathematical, viewpoint. A simple explanation of the differences between the two modes, and in particular of the threshold effect usually exhibited by subharmonic oscillations, is presented. The principal resonance in the case of weak excitation is also briefly considered.

Finally, in Part III the problem of two viscous, incompressible fluids separated by a nearly spherical free surface is considered in general terms as an initial value problem to first order in the perturbation of the spherical symmetry. As an example of the applications

of the theory, the free oscillations of a viscous drop are studied in some detail. In particular, it is shown that the normal mode analysis of this problem available in the literature does not furnish a solution correct for all times, but only an asymptotic one valid as $t \to \infty$.

TABLE OF CONTENTS

# PART I

# NONLINEAR OSCILLATIONS OF GAS BUBBLES IN VISCOUS, INCOMPRESSIBLE LIQUIDS

## 1. Introduction

Because of the highly non-linear nature of the governing equations, the oscillations of a bubble in a liquid present a difficult mathematical problem. Several authors have tried to circumvent this obstacle in part by means of linearized treatments. Thus Minnaert derived in 1933 an expression for the natural frequency of a spherical gas bubble in an incompressible, non viscous liquid[1], and two years later Smith gave the first analysis of the forced oscillations[2]. More recently, Plesset and Hsieh[3] investigated the thermodynamic characteristics of a gas bubble in forced oscillations clarifying the conditions under which an adiabatic or isothermal behavior would dominate. Among the other studies based on the linearized theory (for a recent review see[13]), the works by Devin [4] and by Chapman and Plesset[5] on the damping mechanisms of the free oscillations of gas bubbles should also be mentioned here for their connection with the present study.

The linearized theory has contributed a considerable amount of understanding of many physical mechanisms involved in this phenomenon, but unfortunately many of the points of practical interest are closely connected in an essential way with the non-linear nature of the phenomenon. A typical example is the process of acoustic cavitation, in which stability problems as well as higher and lower harmonics of the driving pressure frequency play a central role (see e. g. Ref. [6]). Numerical investigations of the bubble equation date back at least to the early fifties, when Noltingk and Neppiras[7, 8] published several radius-versus-time curves for a spherical bubble

and investigated the effect of the various physical parameters on their characteristics. Other numerical results have been obtained, among others, by Robinson and Buchanan[9], Flynn[6], Borotnikova and Soloukhin[10], Solomon and Evans[11, 12], and Lauterborn[14-16, 31].

A first analytical attempt to study the nonlinear oscillations of a spherical gas bubble was made by Guth in 1956[17]. He neglected surface tension and damping, and obtained approximate solutions for the resonant and subharmonic oscillations. Recently, Eller and Flynn considered the same problem, and focused their attention on the generation of subharmonics by bubbles in a sound field[18]. They neglected surface tension and gave an approximate treatment of the effect of damping. An expression for the threshold of the subharmonic was established in an indirect way by an investigation of the stability of the purely harmonic solution. This close consideration of the subharmonic mode of oscillation has been motivated by the experimental observation that a strong signal at half the excitation frequency accompanies the onset of acoustic cavitation (see, e. g. [19, 20] and references quoted therein. This topic is considered in greater detail below in Section 6, especially Subsection 6. 5). In this study, the nonlinear oscillations of a gas bubble about the equilibrium radius are investigated analytically by means of the Bogolyubov-Krylov asymptotic method. The bubble is assumed to remain spherical and to be immersed in an incompressible, viscous liquid subject to steady sinusoidal ambient pressure oscillations. The effects of surface tension and of viscous damping are included, and it is shown how the other two damping mechanisms (i. e. thermal and acoustic) can be accounted for

by the suitable redefinition of one parameter. The pressure-volume relationship of the gas in the bubble is approximated by a polytropic relation. Analytical results for the steady state oscillations are presented for the fundamental mode, as well as for the first and second subharmonics and for the first and second harmonics. The first subharmonic is considered in particular detail. It is shown that Eller and Flynn's results (which are corrected here for surface tension) are not complete for what concerns the appearance of the subharmonic mode, and an explanation of the connection of this with the onset of acoustic cavitation is proposed. The approximate analytical results are compared with some numerical ones and a good agreement is found.

In Section 2 the problem is stated in mathematical form and the various hypotheses and approximations are discussed. In Section 3 an approximation to the bubble equation is derived and suitable non-dimensional variables are introduced, reducing the number of parameters in the problem to four. The analytical method used in the solution of the approximate equation is briefly described in Section 4, and Section 5 contains some preliminary computations. Section 6 presents in detail the results for the first subharmonic, and Section 7 and 8 for the other harmonics and for the resonant oscillations respectively. In Section 9 the approximate analytical results are compared with the numerical ones. Finally, Section 10 presents some concluding remarks on some features of the analytical results which are experimentally verified.

Unfortunately the derivation of the results given here requires a considerable amount of computation. In the presentation an effort

has been made to separate as far as possible the computational part from the discussion of results.

## 2. Statement of the problem

We study the non-linear oscillations of a gas bubble assuming that the motion is spherically symmetric and that the effects of compressibility may be neglected. Since under these hypotheses the velocity field is purely radial and divergenceless, viscosity enters only in the continuity of the normal stress across the gas-liquid interface. Rayleigh's equation of motion for the bubble wall can then be written as[21]:

$$R\frac{d^2R}{dt^2} + \frac{3}{2}\left(\frac{dR}{dt}\right)^2 = \frac{1}{\rho}\left\{p_i - p(t) - \frac{2\sigma}{R} - \frac{4\mu}{R}\frac{dR}{dt}\right\} \qquad (2.1)$$

where $R$ is the instantaneous radius of the bubble, $p_i$ its internal pressure, and $p(t)$, the ambient pressure, oscillates with angular frequency $\Omega$:

$$p(t) = p_\infty(1 - \eta\cos\Omega t) \quad . \qquad (2.2)$$

This expression is a close approximation to the pressure distribution in a liquid subject to a sound field the wavelength of which is large as compared with the bubble radius. The nature of the liquid is described by its density $\rho$, surface tension $\sigma$, and viscosity $\mu$. The experimental situation envisaged here is that of a small gas bubble introduced in a body of liquid. Hence it will be assumed that the amount of vapor present in the bubble is negligible, and that $p_i$ can be written in the form:

$$p_i = p_o\left(\frac{R_o}{R}\right)^{3\gamma} \tag{2.3}$$

where $\gamma$ is a polytropic exponent and $p_o$ the internal pressure corresponding to the equilibrium radius $R_o$.

The conditions under which Eq. (2.3) is valid need further consideration. First of all, it should be noted that a relation of this type is acceptable only insofar as thermal damping can be neglected, since this effect produces a phase difference between pressure and volume variations[3, 5]. As can be deduced from Fig. 1 of Ref. [5], in water this will be the case for bubbles smaller than about $10^{-4}$cm.† Even if Eq. (2.3) is not strictly applicable to bubbles of larger radii, the results obtained for these will nevertheless be approximately valid if referred to the average behavior of the bubbles rather than to the instantaneous one.[3] Since our main concern in this study is the derivation of the steady-state amplitude response, it seems reasonable that the results presented here are of some value also in the domain where Eq. (2.3) is, rigorously speaking, invalid. In this domain, however, thermal dissipation should be considered. In principle this can be done by applying the same asymptotic method used here to the complete set of equations describing the phenomenon, i.e., the equation of energy and the equation of state of the gas, together with Eq. (2.1). This procedure would require very complicated

† For a bubble of this size, in water, the behavior will be approximately isothermal for frequencies of oscillation greater than $3 \times 10^9$ hertz and smaller than $3 \times 10^7$ hertz, and approximately adiabatic for frequencies of about $3 \times 10^8$ hertz [22].

and tedious computations. An approximate treatment can be obtained more easily by letting the parameter $\mu$ in Eq. (2.1) be the sum of the viscosity of the liquid plus a "thermal viscosity" suitably defined. In this way the interaction of the two dissipation mechanisms is neglected. Since, however, in the present study only terms proportional to $\mu$ are retained, while terms of order $\mu^2$ and higher are dropped, the resulting approximation would be consistent with the other ones employed. It may also be expected that the results obtained in this way would be equivalent to the ones of a more complete study, carried out to the same order of accuracy. A suitable definition of $\mu_{thermal}$ is already available in the literature, e.g., in the papers by Devin [4] and by Chapman and Plesset[5]. As an example we give here the expression that can be deduced from Eq. (27) of the latter authors:

$$\mu_{thermal} = \frac{1}{4}\,\rho\Omega R_o^2\,\frac{Im\{G\}}{Re\{G\} - \frac{2\sigma}{R_o}} \quad . \tag{2.4}$$

Here $R_o$ is the equilibrium radius of the bubble and $G$ a function defined in Eq. (24) of the paper. In a similar way, the acoustic damping can be introduced through an effective "acoustic viscosity" given by [4, 5]:

$$\mu_{acoustic} = \frac{1}{4}\,\frac{\rho\Omega^2 R_o^3}{c} \tag{2.5}$$

where $c$ is the velocity of sound in the liquid. The acoustic damping can also be treated by applying the asymptotic method to an equation similar to Eq. (2.1), in which additional terms describe the energy loss due to the compressibility of the liquid; for an example of such

an equation see Ref. [23]. The computations in this case would not be more complicated than the ones described here. This line, however, has not been pursued since the acoustic damping is by far the smallest among the three dissipative mechanisms [5], and can be ignored altogether in the vast majority of cases.

We will be concerned with the oscillations of the bubble about its equilibrium radius determined by:

$$p_o - p_\infty = \frac{2\sigma}{R_o} \quad . \tag{2.6}$$

It is implicit in this statement that the physical mechanisms that may alter the value of $R_o$ will be disregarded. We refer in particular to the process of rectified diffusion [29, 30]. From Table I of Ref. [29] it can be seen that the time scale for this process is by many orders of magnitude larger than the period of oscillation of a bubble. This means that the steady state regime is reached long before $R_o$ undergoes any significant change. The only effect of rectified diffusion will therefore be an exceedingly slow parametric change in the value of $R_o$ in the equations presented below. This conclusion is also substantiated by the findings of Ref. [30], in which it is shown that the growth by rectified diffusion can essentially be decoupled from the oscillations of the bubble. It is worth noting here that, as is apparent from formula (3.10) below, an increasing value of $R_o$ corresponds to a decreasing value of the natural frequency of the bubble $\Omega_o$.

## 3. Derivation of the approximate equation

Since we are interested in the oscillations of the bubble about

the equilibrium radius $R_o$ determined by Eq. (2.6), we let

$$R = R_o(1+X) \quad . \tag{3.1}$$

In Eq. (2.1) we also make the following change in the time scale:

$$\tau = \frac{1}{R_o}\left(\frac{p_o}{\rho}\right)^{\frac{1}{2}} t \quad . \tag{3.2}$$

In terms of $X, \tau$ Eq. (2.1) becomes:

$$\ddot{X} + \frac{3}{2}\frac{\dot{X}^2}{1+X} = (1+X)^{-(3\gamma+1)} - (1-w)(1-\eta\cos\omega\tau)(1+X)^{-1}$$

$$-w(1+X)^{-2} - 2b\,\dot{X}(1+X)^{-2} \tag{3.3}$$

where dots denote derivatives with respect to the dimensionless time $\tau$ and:

$$w = \frac{2\sigma}{R_o p_o} \tag{3.4a}$$

$$b = \frac{2\mu}{R_o\sqrt{\rho p_o}} \tag{3.4b}$$

$$\omega = R_o\left(\frac{\rho}{p_o}\right)^{\frac{1}{2}}\Omega \quad . \tag{3.4c}$$

In writing Eq. (3.3) use has been made of the fact that in terms of the Weber number w condition (2.6) reads:

$$\frac{p_\infty}{p_o} = 1 - w \quad . \tag{3.5}$$

The Bogolyubov-Krylov asymptotic method cannot be applied directly to an equation in which denominators involve the dependent variable. It is therefore necessary to make a power series

expansion of Eq. (3.3) based on the assumption that X is small in comparison to unity. When this is done terms of order unity cancel. If we further let:

$$X = \epsilon x \tag{3.6a}$$

$$b = \epsilon B \tag{3.6b}$$

$$(1-w)\eta = \xi = \epsilon P \tag{3.6c}$$

where the positive parameter $\epsilon$ is such that $x, B$ and $P$ are of order unity, Eq. (3.3) becomes:

$$\ddot{x} + \omega_o^2 x = P\cos\omega\tau + \sum_{i=1}^{\infty}(-1)^i \epsilon^i \left\{ \frac{3}{2}\dot{x}^2 x^{i-1} - a_i x^{i+1} + x^i P\cos\omega\tau + 2Bi\dot{x}\,x^{i-1} \right\} \tag{3.7}$$

where:

$$a_i = \begin{pmatrix} 3\gamma+i+1 \\ i+1 \end{pmatrix} - (i+1)w - 1 \tag{3.8}$$

$$\omega_o^2 = 3\gamma - w \quad . \tag{3.9}$$

It should be noted that once that this expression for the resonance frequency of the bubble is converted back into dimensional form it reads:

$$\Omega_o^2 = \frac{1}{\rho R_o^2}\left\{ 3\gamma p_o - \frac{2\sigma}{R_o} \right\} \tag{3.10}$$

which is a well-known result [5]. In particular, if the surface tension vanishes, Minnaert's expression is recovered [1]. Since the damping force is assumed to be of higher order than the driving force, the shift in frequency due to viscosity is absent from Eq. (3.10).

If Eq. (3.7) could be solved exactly keeping all terms, this shift would be recovered in the form of a power series in b. It will turn out however that in the domain of validity of our approximations, the parameter b is small, and that the effect of the shift would be completely masked by that of the nonlinearity.

In the following only the first two terms of the sum in (3.7) will be retained. Written out explicitly then, the equation to which the asymptotic method will be applied is:

$$\ddot{x} + \omega_o^2 x = P \cos \omega \tau + \epsilon \{-\frac{3}{2}\dot{x}^2 + a_1 x^2 - xP\cos \omega\tau - 2B\dot{x}\}$$

$$+ \epsilon^2 \{\frac{3}{2}\dot{x}^2 x - a_2 x^3 + x^2 P \cos \omega\tau + 4B x\dot{x}\} \quad . \qquad (3.11)$$

The coefficients $a_1$, $a_2$ are given by the expressions:

$$a_1 = \frac{9}{2}\gamma(\gamma + 1) - 2w \qquad (3.12a)$$

$$a_2 = \frac{1}{2}\gamma(9\gamma^2 + 18\gamma + 11) - 3w \quad . \qquad (3.12b)$$

## 4. Outline of the asymptotic method

We give now a very brief sketch of the Bogolyubov-Krylov asymptotic method. A satisfactory exposition would be out of place here: standard references are the books by Bogolyubov and Krylov[24] and by Bogolyubov and Mitropolsky[25]. A more recent method that can equally well be applied to the problem studied here is exposed in a book by Cole[26] and in a paper by Kevorkian[27]. The equivalence of the two methods has been shown by Morrison[28].

Consider a general nonlinear differential equation of the form:

$$\ddot{y} + \omega_o^2 y = \epsilon F^{(1)}(y, \dot{y}; \omega\tau) + \epsilon^2 F^{(2)}(y, \dot{y}; \omega\tau) + \ldots \qquad (4.1)$$

where the functions $F^{(i)}$ have period $2\pi$ in the variable $\omega\tau$ and $0 < \epsilon \ll 1$. The Bogolyubov-Krylov method consists in looking for an approximate solution of this equation in the form of an asymptotic series:

$$y = y_o + \epsilon y_1 + \epsilon^2 y_2 + \ldots \qquad (4.2)$$

where:

$$y_o = A(\tilde{\tau}) \cos [\nu\tau + \varphi(\tilde{\tau})] \qquad (4.2a)$$

In this expression $\nu$ is a multiple or submultiple of the driving frequency $\omega$ close to the resonant frequency $\omega_o$, and

$$\tilde{\tau} = \epsilon\tau( 1 + \epsilon\sigma_2 + \epsilon^2 \sigma_3 + \ldots )$$

is a "slow" time scale, whose explicit appearance in (4.2a) indicates the slow time variation of the two functions $A$ and $\varphi$. It will be apparent from the following that, at this stage, we are at liberty to impose one arbitrary relation between $A$ and $\varphi$. It is convenient to choose:

$$\dot{A} \cos (\nu\tau + \varphi) - A\dot{\varphi} \sin (\nu\tau + \varphi) = 0 \qquad (4.3)$$

because then the other relation that will be derived below, Eq. (4.6), involves only first derivatives of $A$ and $\varphi$. Denoting differentiation with respect to $\tilde{\tau}$ by a prime, upon substitution of (4.2) into (4.1), we obtain:

$$-\nu\epsilon(1+\epsilon\sigma_2+\epsilon^2\sigma_3+\ldots)[A'\sin(\nu\tau+\varphi)+A\varphi'\cos(\nu\tau+\varphi)]$$

$$+(\omega_o^2-\nu^2)A\cos(\nu\tau+\varphi)+\epsilon(\ddot{y}_1+\omega_o^2 y_1)+\epsilon^2(\ddot{y}_2+\omega_o^2 y_2)+\ldots$$

$$=\epsilon F^{(1)}+\epsilon^2 F^{(2)}+\ldots \tag{4.4}$$

Notice first of all that, for $A'$ and $\varphi'$ to be of order 1 (and consequently $\dot{A}$ and $\dot{\varphi}$ of order $\epsilon$) $\omega_o^2-\nu^2$ must be small (of order $\epsilon$) as was assumed above. If this is the case then, with:

$$\theta=\nu\tau+\varphi(\tilde{\tau}) \tag{4.5}$$

we get from (4.4):

$$\ddot{y}_1+\omega_o^2 y_1=(\nu^2-\omega_o^2)\epsilon^{-1}A\cos\theta$$

$$+\nu[A'\sin\theta+A\varphi'\cos\theta]+F^{(1)}(y_o,\dot{y}_o;\omega\tau) \tag{4.4a}$$

$$\ddot{y}_2+\omega_o^2 y_2=\nu\sigma_2[A'\sin\theta+A\varphi'\cos\theta]+F^{(2)}(y_o,\dot{y}_o;\omega\tau)$$

$$+F_1^{(1)}(y_o,\dot{y}_o;\omega\tau)y_1+F_2^{(1)}(y_o,\dot{y}_o;\omega\tau)\dot{y}_1 \tag{4.4b}$$

and so on, where the subscript i on the F's denotes differentiation with respect to the i-th argument. Now, in order for $y_1, y_2, \ldots$ to be of order one, as implicitly assumed in writing down the expansion (4.2), the right hand sides of these equations should be free of terms

frequency $\omega_o$ is included in the first term of the expansion.

Finally, consideration must be given to the solution of the system of equations for $A$ and $\varphi$ by the method of averaging [24, 25]. This system has the form:

$$\begin{cases} -\nu\dot{A}\sin\theta - \nu A\dot{\varphi}\cos\theta = h(A,\varphi;\theta) & (4.9a) \\ \nu\dot{A}\cos\theta - \nu A\dot{\varphi}\sin\theta = 0 & (4.9b) \end{cases}$$

where $\theta = \nu\tau + \varphi$. Multiplying Eq. (4.9a) by $\sin\theta$ and Eq. (4.9b) by $\cos\theta$, subtracting and integrating we have:

$$-\nu\int_o^{2\pi}\dot{A}d\theta = \int_o^{2\pi} h(A,\varphi;\theta)\sin\theta d\theta \qquad (4.10a)$$

and similarly multiplying (4.9a) by $\cos\theta$ and (4.9b) by $\sin\theta$

$$-\nu\int_o^{2\pi} A\dot{\varphi}d\theta = \int_o^{2\pi} h(A,\varphi;\theta)\cos\theta\, d\theta. \qquad (4.10b)$$

Now, since $\dot{A} = 0(\epsilon)$, $\dot{\varphi} = 0(\epsilon)$, $A, \varphi, \dot{A}, \dot{\varphi}$ can be considered approximately constant in performing the integrations so that one ends up with a system of the form:

$$\begin{cases} -2\nu\dot{A} = S(A,\varphi) & (4.11a) \\ -2\nu A\dot{\varphi} = C(A,\varphi) & (4.11b) \end{cases}$$

The initial conditions on Eq. (4.1) give, through (4.2), the initial conditions $A(\tau=o)$, $\varphi(\tau=o)$.

In order to apply the method outlined above to Eq. (3.11) when $\nu \neq \omega$ (i.e. in frequency ranges not near the fundamental resonance), a slight modification is necessary because of the presence of the forcing

term $P \cos \omega\tau$ in the RHS. It is easily verified that the substitution $x = x_o + y$, with $x_o$ given by:

$$x_o = \frac{P}{\omega_o^2 - \omega^2} \cos \omega\tau$$

reduces Eq. (3.11) to the general form (4.1). Accordingly, we let:

$$x = A \cos \theta + x_o + \epsilon x_1 + \epsilon^2 x_2 + \ldots$$

Then Eqs. (4.4a) and (4.4b) become:

$$\ddot{x}_1 + \omega_o^2 x_1 = -\frac{3}{2}(\dot{x}_o - \nu A \sin\theta)^2 + a_1 (A \cos\theta + x_o)^2$$

$$- P \cos\omega\tau\,(A \cos\theta + x_o) - 2B(\dot{x}_o - \nu A \sin\theta) \qquad (4.12)$$

$$\ddot{x}_2 + \omega_o^2 x_2 = -3\dot{x}_1(\dot{x}_o - \nu A \sin\theta) + 2a_1 x_1 (A \cos\theta + x_o)$$

$$- P x_1 \cos\omega\tau - 2B\dot{x}_1$$

$$+ \frac{3}{2}(-\nu A \sin\theta + \dot{x}_o)^2 (A \cos\theta + x_o) \qquad (4.13)$$

$$- a_2 (A \cos\theta + x_o)^3 + P \cos\omega\tau\,(A \cos\theta + x_o)^2$$

$$+ 4B(A \cos\theta + x_o)(-\nu A \sin\theta + \dot{x}_o).$$

5. Subharmonics and harmonics. Preliminary computations

To second order in $\epsilon$ the approximate Eq. (3.11) studied here possesses -- apart from the resonance for $\omega \simeq \omega_o$ -- two subharmonics for $\omega \simeq 2\omega_o$, $\omega \simeq 3\omega_o$ and two harmonics for $\omega \simeq \omega_o/2$, $\omega \simeq \omega_o/3$. The discussion of the main resonance is deferred to Section 8 whereas the other resonances will be considered here and in the following two Sections.

According to the preceding discussion, we select the frequency $\nu$ in the first term of the expansion as follows:

$$\nu = \omega/2 \quad \text{in the first subharmonic region} \tag{5.1}$$

$$\nu = \omega/3 \quad \text{in the second subharmonic region} \tag{5.2}$$

$$\nu = 2\omega \quad \text{in the first harmonic region} \tag{5.3a}$$

$$\nu = 3\omega \quad \text{in the second harmonic region.} \tag{5.3b}$$

Equation (4.12) for $x_1$ becomes:

$$\ddot{x}_1 + \omega_o^2 x_1 = \frac{1}{2} A^2 \left( a_1 - \frac{3}{2} \nu^2 \right) + \frac{1}{2} \frac{P^2}{\omega_o^2 - \omega^2} \left( \frac{a_1 - \frac{3}{2} \omega^2}{\omega_o^2 - \omega^2} - 1 \right)$$

$$+ \frac{1}{2} A^2 \left( a_1 + \frac{3}{2} \nu^2 \right) \cos 2\theta + AP \left( \frac{a_1 + \frac{3}{2} \omega \nu}{\omega_o^2 - \omega^2} - \frac{1}{2} \right) \cos(\omega\tau + \theta)$$

$$+ 2\, BP \frac{\omega}{\omega_o^2 - \omega^2} \sin \omega\tau + \underbrace{2\nu BA \sin \theta}_{①} \qquad (5.4)$$

$$+ \underbrace{AP \left( \frac{a_1 - \frac{3}{2} \omega\nu}{\omega_o^2 - \omega^2} - \frac{1}{2} \right) \cos(\omega\tau - \theta)}_{②}$$

$$+ \underbrace{\frac{1}{2} \frac{P^2}{\omega_o^2 - \omega^2} \left( \frac{a_1 + \frac{3}{2} \omega^2}{\omega_o^2 - \omega^2} - 1 \right) \cos 2\omega\tau}_{③} \; .$$

The underlined terms will produce resonances in specific situations. It is easily seen by substitution for $\nu$ of the values given by (5.2) into the expression for $\theta$, $\theta = \nu\tau + \varphi$, that:

Term No. 1 resonates in all regions

Term No. 2 resonates for $\omega \simeq 2\omega_o$ (1st subharmonic region)

Term No. 3 resonates for $\omega \simeq \omega_o/2$ (1st harmonic region).

Therefore, in agreement with the procedure sketched in Section 4, in the subharmonic region, for example, terms 1 and 2 should be removed from (5.4) and added to the RHS of Eq. (4.6). After this, $x_1$ should be determined from Eq. (5.4) without those terms. The resultant expression for $x_1$ should then be inserted into Eq. (4.13) for $x_2$, the resonant terms removed and cast back into the RHS of (4.6) and so on.

We make the following definitions:

$$[\omega_o^2 - (\omega-\nu)^2]c_o = \frac{a_1 - \frac{3}{2}\omega\nu}{\omega_o^2 - \omega^2} - \frac{1}{2} \tag{5.5a}$$

$$\omega_o^2 c_1 = \frac{1}{2}\frac{1}{\omega_o^2 - \omega^2}\left(\frac{a_1 - \frac{3}{2}\omega^2}{\omega_o^2 - \omega^2} - 1\right) \tag{5.5b}$$

$$(\omega_o^2 - 4\nu^2)c_2 = \frac{1}{2}\left(a_1 + \frac{3}{2}\nu^2\right) \tag{5.5c}$$

$$(\omega_o^2 - 4\omega^2)c_3 = \frac{1}{2}\frac{1}{\omega_o^2 - \omega^2}\left(\frac{a_1 + \frac{3}{2}\omega^2}{\omega_o^2 - \omega^2} - 1\right) \tag{5.5d}$$

$$[\omega_o^2 - (\omega+\nu)^2]c_4 = \frac{a_1 + \frac{3}{2}\omega\nu}{\omega_o^2 - \omega^2} - \frac{1}{2} \tag{5.5e}$$

$$\omega_o^2 c_5 = \frac{1}{2}\left(a_1 - \frac{3}{2}\nu^2\right) \tag{5.5f}$$

$$(\omega_o^2 - \omega^2)c_6 = \frac{2\omega}{\omega_o^2 - \omega^2} \quad . \tag{5.5g}$$

In terms of the quantities $c_i$'s, the (steady state) solution for $x_1$ is:

$$x_1 = P^2 c_1 + A^2 c_5 + A^2 c_2 \cos 2\theta + PAc_4 \cos(\omega\tau+\theta) + BPc_6 \sin\omega\tau$$

$$+ \begin{bmatrix} P^2 c_3 \cos 2\omega\tau & \text{in the first subharmonic region} \\ APc_o \cos(\omega\tau-\theta) & \text{in the first harmonic region} \\ APc_o \cos(\omega\tau-\theta) + P^2 c_3 \cos 2\omega\tau & \text{in other regions} \end{bmatrix} . \tag{5.6}$$

With the resonant terms removed from (5.4) added, Eq. (4.6) for the slowly varying quantities $A, \varphi$ becomes in the various regions, to first order in $\epsilon$:

$$-\nu\dot{A}\sin\theta-\nu A\dot{\phi}\cos\theta=(\nu^2-\omega_o^2)A\cos\theta+2\nu\epsilon BA\sin\theta$$

$$+\begin{cases}\beta_1\,\epsilon AP\cos(\omega\tau-\theta) & \text{first subharmonic region}\\ \beta_2\,\epsilon P^2\cos 2\omega\tau & \text{first harmonic region}\\ 0 & \text{other regions}\end{cases} \qquad (5.7)$$

where:

$$\beta_1=-\frac{a_1-\frac{3}{2}\omega\nu}{\omega_o^2-\omega^2}+\frac{1}{2} \qquad (5.8a)$$

$$\beta_2=\frac{1}{2}\frac{1}{\omega_o^2-\omega^2}\left(\frac{a_1+\frac{3}{2}\omega^2}{\omega_o^2-\omega^2}-1\right). \qquad (5.8b)$$

When expression (5.6) for $x_1$ is substituted into Eq. (4.13) for $x_2$ a somewhat complex equation results - - similar in structure to the RHS of Eq. (5.4) - - which needs not be written down. The resonating terms that are removed and added to the RHS of Eq. (5.7) are in the various regions:

$$\epsilon^2A(g_oA^2-g_1P^2)\cos\theta+\epsilon^2ABPg_4\sin(\omega\tau-\theta)\quad\text{first subharmonic}\quad(5.9a)$$

$$\epsilon^2A[g_oA^2+(-g_1+g_2)P^2]\cos\theta+\epsilon^2g_3BP^2\sin 2\omega\tau\quad\text{first harmonic}\quad(5.9b)$$

$$\epsilon^2A[g_oA^2+(-g_1+g_2)P^2]\cos\theta+\epsilon^2PA^2g_6\cos(\omega\tau-2\theta)\quad\text{second subharmonic}\quad(5.9c)$$

$$\epsilon^2A[g_oA^2+(-g_1+g_2)P^2]\cos\theta+\epsilon^2P^3g_5\cos 3\omega\tau\quad\text{second harmonic}\quad(5.9d)$$

The quantities $g_i$ are defined as follows:

$$g_o=a_1(2c_5+c_2)+\frac{3}{2}\nu^2\left(\frac{1}{4}-2c_2\right)-\frac{3}{4}a_2 \qquad (5.10a)$$

$$g_1 = -2a_1 c_1 - c_4\left(\frac{a_1 - \frac{3}{2}\omega(\omega+\nu)}{\omega_o^2-\omega^2} - \frac{1}{2}\right) - \frac{3}{2}\frac{\frac{1}{2}\omega^2 - a_2}{(\omega_o^2-\omega^2)^2} - \frac{1}{\omega_o^2-\omega^2} \qquad (5.10b)$$

$$g_2 = c_o\left(\frac{a_1 - \frac{3}{2}\omega(\omega-\nu)}{\omega_o^2-\omega^2} - \frac{1}{2}\right) \qquad (5.10c)$$

$$g_3 = c_6\left(\frac{a_1 + \frac{3}{2}\omega^2}{\omega_o^2-\omega^2} - \frac{1}{2}\right) - \frac{2\omega}{(\omega_o^2-\omega^2)^2} \qquad (5.10d)$$

$$g_4 = c_6\left(a_1 - \frac{3}{2}\omega\nu\right) + 2\frac{\nu-\omega}{\omega_o^2-\omega^2} \qquad (5.10e)$$

$$g_5 = c_3\left(\frac{a_1+3\omega^2}{\omega_o^2-\omega^2} - \frac{1}{2}\right) - \frac{1}{4(\omega_o^2-\omega^2)^2}\left(\frac{a_2 + \frac{3}{2}\omega^2}{\omega_o^2-\omega^2} - 1\right) \qquad (5.10f)$$

$$g_6 = c_o\left(a_1 - \frac{3}{2}\nu(\omega-\nu)\right) + c_2\left(\frac{a_1 - 3\nu\omega}{\omega_o^2-\omega^2} - \frac{1}{2}\right) + \frac{1}{4} + \frac{3}{4}\frac{\omega\nu - a_2 - \frac{1}{2}\nu^2}{\omega_o^2-\omega^2} \; . \qquad (5.10g)$$

Figures 5.1 through 5.8 present graphs of the $g_i$'s as functions of $\omega$ for some values of $\gamma$ and w. The strong variation of many of them illustrates the importance of retaining the full $\omega$ dependence in the analysis of the resonances.

In the following sections the various regions will be discussed in detail.

## 6. First subharmonic region

When averaged over $\theta$ in the manner described in Section 4, with $\nu = \frac{1}{2}\omega$, the system (4.11) determining the slowly varying terms $A, \varphi$ becomes:

$$\begin{cases} -\omega\dot{A} = \epsilon\omega BA - \epsilon\beta_1 PA\sin 2\varphi + \epsilon^2 BPA g_4 \cos 2\varphi & (6.1a) \\ -\omega A\dot{\varphi} = \left(\frac{1}{4}\omega^2 - \omega_o^2 - \epsilon^2 P^2 g_1\right) A + g_o\epsilon^2 A^3 - \epsilon\beta_1 PA\cos 2\varphi - \epsilon^2 BPA g_4 \sin 2\varphi \ . & (6.1b) \end{cases}$$

Note first that, with:

$$C = \epsilon A$$

and definitions (3.6b), (3.6c), $\epsilon$ disappears from Eqs. (6.1):

$$\begin{cases} -\omega\dot{C} = \omega bC - \beta_1 \xi C\sin 2\varphi + b\xi C g_4 \cos 2\varphi & (6.2a) \\ -\omega C\dot{\varphi} = \left(\frac{1}{4}\omega^2 - \omega_o^2 - \xi^2 g_1\right) C + g_o C^3 - \beta_1 \xi C\cos 2\varphi - b\xi C g_4 \sin 2\varphi \ . & (6.2b) \end{cases}$$

If $b > 0$, the functions $C(\tau)$ and $\varphi(\tau)$ solution of this system will tend asymptotically to definite values $C_o$ and $\varphi_o$ as $\tau \to \infty$. These values correspond to the critical points of the system, i.e., they satisfy Eqs. (6.1) with vanishing LHS. We begin the analysis by a study of these critical points. The unsteady solutions of (6.2) will be dealt with in subsection 6.4.

It should also be noted that in Eqs. (6.2) the pressure amplitude $\eta$ does not enter directly, but only through $\xi = (1-w)\eta$. The quantity $\xi$ appears here, and in the following, as an "effective pressure amplitude".

## 6.1 Steady state solution

The values $C_o$ and $\varphi_o$ corresponding to the singular points satisfy the equations:

$$\begin{cases} \beta_1 \xi C_o \sin 2\varphi_o - b\xi C_o g_4 \cos 2\varphi_o = \omega b C_o & (6.1.1a) \\ b\xi C_o g_4 \sin 2\varphi_o + \beta_1 \xi C_o \cos 2\varphi_o = \left(\frac{1}{4}\omega^2 - \omega_o^2 - \xi^2 g_1\right) C_o + g_o C_o^3 & (6.1.1b) \end{cases}$$

Obviously $C_o = 0$ is a solution of this system. The other solutions can be obtained by solving for $\sin\varphi_o$, $\cos\varphi_o$:

$$\sin 2\varphi_o = b\,\frac{\omega\beta_1 + g_4\left(\frac{1}{4}\omega^2 - \omega_o^2 - \xi^2 g_1 + g_o C_o^2\right)}{\xi(\beta_1^2 + b^2 g_4^2)} \qquad (6.1.2a)$$

$$\cos 2\varphi_o = \frac{\beta_1\left(\frac{1}{4}\omega^2 - \omega_o^2 - \xi^2 g_1 + g_o C_o^2\right) - \omega b^2 g_4}{\xi(\beta_1^2 + b^2 g_4^2)} \quad . \qquad (6.1.2b)$$

Substituting these into the closure condition $\sin^2 2\varphi_o + \cos^2 2\varphi_o = 1$, and rearranging, we get:

$$C_o = \left\{\frac{\omega_o^2 - \frac{1}{4}\omega^2 + \xi^2 g_1 \pm (\xi^2(\beta_1^2 + b^2 g_4^2) - \omega^2 b^2)^{\frac{1}{2}}}{g_o}\right\}^{\frac{1}{2}} \quad . \qquad (6.1.3)$$

The condition that the inner square root be real determines the frequency-dependent threshold for the subharmonic mode:

$$\xi_{\text{threshold}} = \frac{\omega b}{(\beta_1^2 + b^2 g_4^2)^{\frac{1}{2}}} \quad . \qquad (6.1.4)$$

From their definitions (5.8a) (5.10e) it is seen that in the subharmonic region there is a relation between $\beta_1$ and $g_4$:

$$g_4 = -\frac{2\omega}{\omega_o^2 - \omega^2}\,\beta_1 \quad . \qquad (6.1.5)$$

The expression for the threshold can then be written, by (3.6c):

$$\eta_{threshold} = \frac{\omega b}{(1-w)\beta_1 \sqrt{1 + \frac{4\omega^2 b^2}{(\omega_o^2 - \omega^2)^2}}} \qquad (6.1.6)$$

Another condition for the existence of the subharmonic comes from the requirement that $C_o^2$ be positive. Since $g_o > 0$, this implies

$$\omega_o^2 - \frac{1}{4}\omega^2 + \xi^2 g_1 \geqslant \pm (\xi^2(\beta_1^2 + b^2 g_4^2) - \omega^2 b^2)^{\frac{1}{2}} \quad . \qquad (6.1.7)$$

Figures 6.1, 6.2 and 6.3 show the two branches of the subharmonic peak (6.1.3) in some particular cases; a further discussion is deferred until subsection 6.4.

The above considerations concern the possibility of <u>existence</u> of the subharmonic mode, but by themselves they do not say anything about its <u>actual manifestation</u> in an experiment or in the numerical integration of the Rayleigh equation (2.1). This feature is connected with the stability of the harmonic mode and with the values of the initial conditions. These points will be discussed in the following subsections.

Clearly, once $C_o$ is known, Eqs.(6.1.2) determine two values of $\varphi_o$ differing by $\pi$. In the limit $b \to 0$, one of these will correspond to an oscillation in phase with the driving pressure and the other to an oscillation of opposite phase. Which one of these may be applicable to any specific case cannot be determined by a study of the steady state solution, but must be derived from an analysis of the complete initial value problem as will be seen below in subsection 6.3.

To second order in the displacement from the equilibrium radius, the solution for the steady state oscillations in presence of the

first subharmonic mode is now complete. By (5. 1), (5. 3) and (5. 6) it can be written out explicitly as:

$$X_{1/2}(\tau) = C_o \cos\left|\frac{1}{2}\ \omega\tau+\varphi_o\right| + \frac{\xi}{\omega_o^2-\omega^2}\ \cos\omega\tau + \xi^2\, c_1 + C_o^2\, c_5$$

$$+ C_o^2 c_2 \cos(\omega\tau+2\varphi_o) + \xi C_o c_4 \cos\left|\frac{3}{2}\ \omega\tau+\varphi_o\right| \qquad (6.1.8)$$

$$+ b\xi c_6 \sin\omega\tau + \xi^2 c_3 \cos 2\omega\tau \quad .$$

The solution for the radius is then (cf. (3. 11) ):

$$R(\tau) = R_o[\,1 + X_{1/2}(\tau)\,] \quad . \qquad (6.1.3)$$

## 6. 2 Stability of steady state solutions

In addition to the two solutions given by (6. 5), system (6. 3) has also the solution $C_o = 0$. To investigate the stability of the non-zero solutions we use Eqs. (6. 2) letting as usual:

$$C = C_o + \delta \qquad \varphi = \varphi_o + \beta \qquad (6.2.1)$$

where $C_o, \varphi_o$ are the steady state solutions and $\delta, \beta$ first order quantities. Linearizing system (6. 2) we get:

$$\begin{cases} \omega\dot{\delta} = 2\beta C_o\left|\frac{1}{4}\ \omega^2 - \omega_o^2 - \xi^2 g_1 + g_o C_o^2\right| & (6.2.2a) \\ -\omega C_o\dot{\beta} = g_o C_o^2\delta + \omega b C_o\beta \quad . & (6.2.2b) \end{cases}$$

As is well-known, the condition that the steady state solutions be stable is equivalent to the requirement that the following quadratic equation

has only negative roots:

$$\lambda^2 + b\lambda + 2\,\frac{g_o C_o^2}{\omega^2}\left(\frac{1}{4}\,\omega^2 - \omega_o^2 - \xi^2 g_1 + g_o C_o^2\right) = 0 \quad . \qquad (6.2.3)$$

Since $b$ and $g_o$ are positive, this will be insured if the term in parenthesis is non-negative, i.e. if:

$$\left(\frac{\omega}{2\omega_o}\right)^2 \geqslant 1 + \frac{1}{\omega_o^2}\,(g_1 \xi^2 - g_o C_o^2) \quad . \qquad (6.2.4)$$

Substituting for $C_o$ the two values given by (6.1.3), one finds that the larger one (plus sign in front of the radicand) always satisfies this relation, whereas the other one never does. The lower branch of the curve $C_o(\omega)$ is therefore unstable for all values of $\omega/\omega_o$ (Figs. 6.1, 6.2, 6.3).

We now turn to the investigation of the stability of the solution $C_o = 0$, i.e. of the harmonic mode of oscillation not containing the subharmonic. The technique applied above cannot be used for this analysis. In this case it is better to make recourse to the full equation (3.11). Details of the procedure are contained in the Appendix. The result is the following: the mode with $C_o = 0$ is stable if:

$$Q_{1/2} \equiv \omega_o^2 - \frac{1}{4}\,\omega^2 + \xi^2 g_7 \geqslant \sqrt{\xi^2(\beta_1^2 + b^2 g_8^2) - \omega^2 b^2} \quad . \qquad (6.2.5a)$$

if $Q_{1/2} \geqslant 0$, or if:

$$-Q_{1/2} \equiv -\omega_o^2 + \frac{1}{4}\,\omega^2 - \xi^2 g_7 \geqslant \sqrt{\xi^2(\beta_1^2 + b^2 g_8^2) - \omega^2 b^2} \quad . \qquad (6.2.5b)$$

If $Q_{1/2} \leqslant 0$. The functions $g_7, g_8$ are defined by:

$$g_7 = -2a_1 c_1 - \frac{1}{\omega_o^2 - \omega^2} + \frac{3}{2}\,\frac{a_2 - \frac{5}{4}\,\omega^2}{(\omega_o^2 - \omega^2)^2} \quad . \qquad (6.2.6a)$$

$$g_8 = c_6\left(a_1 - \frac{3}{4}\omega^2\right) - \frac{5}{2}\frac{\omega}{\omega_o^2-\omega^2} \quad . \qquad (6.2.6b)$$

Graphs of these two functions are presented in Figs. 6.4 and 6.5.

The meaning of these results is best illustrated by considering to begin with the first order approximation, which is:

$$\omega_o^2 - \frac{1}{4}\omega^2 \geqslant \sqrt{\xi^2\beta_1^2 - \omega^2 b^2} \qquad \text{if} \qquad \omega < 2\omega_o \qquad (6.2.7a)$$

$$-\left(\omega_o^2 - \frac{1}{4}\omega^2\right) \geqslant \sqrt{\xi^2\beta_1^2 - \omega^2 b^2} \qquad \text{if} \quad 2\omega_o < \omega \quad . \qquad (6.2.7b)$$

Conditions (6.1.7) for the existence of the subharmonic are, to first order

$$-\left(\omega_o^2 - \frac{1}{4}\omega^2\right) \leqslant \sqrt{\xi^2\beta_1^2 - \omega^2 b^2} \qquad \text{upper branch} \qquad (6.2.8a)$$

$$\omega_o^2 - \frac{1}{4}\omega^2 \geqslant \sqrt{\xi^2\beta_1^2 - \omega^2 b^2} \qquad \text{lower branch} \quad . \qquad (6.2.8b)$$

Hence to the left of the point $\omega/\omega_o = 2$, the upper (stable) branch exists where the harmonic solution is stable, and also in the small region

$$\omega_* \leqslant \omega \leqslant \omega_{**}$$

where $\omega_*$ and $\omega_{**}$ are respectively the values of $\omega$ that satisfy equations (6.1.7) with the equal signs (see Fig. 6.6). The lower (unstable) branch instead exists only where the harmonic solution is stable. Vice versa at the right of $\omega/\omega_o = 2$, the upper branch disappears at exactly the point where the harmonic solution begins to be stable, while the lower branch is not present; the situation is illustrated in Fig. 6.6.

If we now consider the full second order result, the picture is very little altered. First of all, it may be seen from Fig. 6.4 that the difference between $g_1$ and $g_7$ is quite small, with $g_1$ slightly greater than $g_7$. This has the consequence of shifting both $\omega_*$ and $\omega_{**}$ a little to the right. In the second place, as Fig. 6.5 shows, the function $g_8$ is somewhat bigger than $g_4$. However, because of the factor $b^2$ which is usually very small, this difference has practically no influence on the numerical values.

The implications of this analysis for the actual appearance of the subharmonic mode will be dealt with in the following subsection.

## 6.3 Unsteady solution and the influence of initial conditions

We study here the behavior of the unsteady solutions of the differential system (6.2). Consider first the undamped case, $b = 0$. In these conditions the system is Hamiltonian with a Hamiltonian function given by:

$$H = \frac{1}{4} g_o C^4 + \frac{1}{2}\left(\frac{1}{4}\omega^2 - \omega_o^2 - \xi^2 g_1\right) C^2 - \frac{1}{2}\beta_1 \xi C^2 \cos 2\varphi \quad . \tag{6.3.1}$$

Since the system can now be written:

$$\begin{cases} \omega C\dot{C} = \dfrac{\partial H}{\partial \varphi} & (6.3.2a) \\ \omega C\dot{\varphi} = -\dfrac{\partial H}{\partial C} \quad . & (6.3.2b) \end{cases}$$

it is readily verified that $dH/d\tau = 0$, so that the curves $H = \text{constant}$ are the unsteady, periodic solutions of (6.2). The value of $H$ is obviously determined by the initial conditions. In the phase plane

($u = C\cos\varphi$, $v = C\sin\varphi$) these curves are symmetric about both axes and are closed. Since a knowledge of the structure of this system of curves is useful for the discussion of the damped case, it will be described here. For $b = 0$ the singular points lie on the coordinate axes and are determined by:

$$\begin{cases} \sin 2\varphi_o = 0 & (6.3.3a) \\ C_o = \left( \dfrac{\omega_o^2 - \frac{1}{4}\omega^2 + \xi^2 g_1 + \beta_1 \xi \cos 2\varphi_o}{g_o} \right)^{\frac{1}{2}} . & (6.3.3b) \end{cases}$$

The stable ones correspond to $\varphi_o = 0, \pi$ and lie on the abscissa axis and the unstable ones $\left(\varphi_o = \frac{\pi}{2}, \frac{3}{2}\pi\right)$ are on the ordinate axis. The phase plane structure is important here only for the case in which the subharmonic mode can exist, but the harmonic mode is stable. Hence we confine the analysis to values of $\omega$ such that:

$$\omega_o^2 - \frac{1}{4}\omega^2 + \xi^2 g_1 > \beta_1 \xi > 0 .$$

The pattern corresponding to such a case is shown in Fig. 6.7. For H equal to $H_{cr}$, where:

$$H_{cr} = -\frac{1}{g_o}\left( \omega_o^2 - \frac{1}{4}\omega^2 + \xi^2 g_1 - \beta_1 \xi \right)^2 .$$

there are two trajectories touching each other at the unstable critical points: these are the separatrices. The inner separatrix labeled by $\infty_1$ in Fig. 6.7, encircles the origin, the outer, labeled by $\infty_2$, contains all stable singular points. As H grows away from $H_{cr}$ towards zero the inner branch becomes smaller until it shrinks to a point (the origin) for $H = 0$ (trajectories 114, 137 in the figure). At the same

time the outer one moves out encircling all singular points (trajectories 89 and 138) and eventually becomes a circle centered at the origin for H very large and positive. For values of H such that:

$$H_{min} = \frac{1}{g_o}\left|\omega_o^2 - \frac{1}{4}\omega^2 + \xi^2 g_1 + \beta_1 \xi\right|^2 \leqslant H \leqslant H_{cr} \qquad (6.3.4)$$

the trajectories encircle either one of the two stable singular points (trajectories 72, 86 and 119) and approach the ones corresponding to $H_{cr}$ as $H \to H_{cr}$, while they shrink to the singular points as H becomes closer and closer to $H_{min}$, the lower bound on the LHS of (6.3.4). If H is smaller than this lower bound, no real trajectory exists. From a study of the coefficients appearing in the locus (6.3.1) with varying $\omega$, it can be deduced that the size of the region bounded by the inner separatrix increases as $\omega/\omega_o$ decreases away from 2 (Fig. 6.8). Figure 6.9 shows instead how the two separatrices change when, for fixed $\omega/\omega_o$, $\eta$ is changed. It will be noted that, as $\eta$ increases, the region bounded by the inner separatrix gets smaller, while the regions bounded by the outer one get larger.

If now damping is introduced, it is found that H is no longer a constant of the motion, but that its time derivative is given by:

$$\frac{dH}{d\tau} = -\frac{b}{\omega} C^2 \left[ (\omega + \xi g_4 \cos 2\varphi)\left( g_o C^2 + \frac{1}{4}\omega^2 - \omega_o^2 - \xi^2 g_1 \right) - \beta_1 \xi (\omega \cos 2\varphi + \xi g_4) \right] . \qquad (6.3.5)$$

The expression on the RHS of this equation vanishes on the locus:

$$C^2 = \frac{1}{g_o}\left( \omega_o^2 - \frac{1}{4}\omega^2 + \xi^2 g_1 + \beta_1 \xi \frac{\omega \cos 2\varphi + \xi g_4}{\omega + \xi g_4 \cos 2\varphi} \right) \qquad (6.3.6)$$

which passes through the singular points, and is positive in the interior of it and negative in the exterior (dashed curve in Fig. 6. 7). The shape of the trajectories in the damped case can now be understood qualitatively. Assume first that the initial condition lies inside the inner separatrix (we shall call this Region I). In this region $\dot{H} > 0$, and H increases going towards the origin, so that the solution will spiral into the origin (curve a in Fig. 6. 10). The steady state oscillation of the bubble will then be free from the subharmonic mode. If the initial condition lies just outside the inner separatrix, but inside the outer one (Region II) again $\dot{H} > 0$ and the solution will cross the inner separatrix spiralling in this case too into the origin (curve b in Fig. 6. 10), so that the subharmonic component will be damped out. As the distance of the initial data from the inner separatrix is increased inside Region II, however, the solution will not be "captured" any more by Region I, but will eventually cross the locus of $\dot{H} = 0$. It can be seen from Fig. 6. 11 that $\dot{H}$ decreases very quickly outside this locus as C increases, whereas it is very small where it is positive. Therefore, roughly speaking, it may be said that H "loses" much more during the portion of the trajectory that lies outside the locus $\dot{H} = 0$, than it "gains" during the part that lies inside. The solution will therefore get farther and farther away from the origin, and will spiral into the non-zero singular point (curve c in Fig. 6. 10). The subharmonic component will then be present in the steady state oscillations. If the initial condition lies outside the region bounded by the outer separatrix (Region III) a variety of situations may arise, with the solution spiralling into any one of the three singular points (Fig. 6. 12). We may therefore say that, in an obvious sense, the phase plane is divided up into "domains

of influence" of the three stable singular points. Each of these domains is made up of all the trajectories that spiral into the same singular point as $\tau \to \infty$. The domain of influence of the origin contains Region I, bounded by the inner separatrix. The domain of influence of the other singular point to the right of the origin contains instead nearly all of Region II, bounded by the two separatrices, and so forth. Obviously these domains extend also beyond Regions I and II to cover the entire plane, but a detailed analysis of these outer regions is not necessary for our purposes. A sketch of their general structure is shown in Fig. 6.13.

The importance of the above for what concerns a possible explanation of the connection between subharmonic signal and onset of cavitation will be considered in subsection 6.5 below. Here we will only observe that integration of Eqs. (6.2) allows us to estimate the relaxation times of the system, and also the number of cycles of the driving pressure needed to reach the steady state amplitude to any prescribed accuracy. This information may be of great relevance for numerical integrations of the Rayleigh equation. The numbers labeling the curves in Fig. 6.7 express the period of the function $C(\tau)$ in units of $\omega\tau$. In Fig. 6.10 the numbers along the curves denote time in the same unit. It will be noted that, for small values of the damping coefficient b, the approach to the steady state solutions can take many cycles of the driving pressure oscillations. This may make very difficult and time consuming a numerical integration of the Rayleigh equation. The fact is also of some interest that the value of b selected for the examples of Fig. 6.10 is not particularly low, corresponding approximately to a bubble of radius $R_o \simeq 4 \times 10^{-4}$ cm in water at 20°C, if only the viscous damping is included.

## 6.4. Summary and discussion of results

Two conditions have been derived for the existence of a steady subharmonic response. One is that $\eta$ (the ratio between the maximum ambient pressure and its average value) be greater than a threshold value given by:

$$\eta_{threshold} = \frac{\omega b}{(1-w)\beta_1 \left( 1 + \frac{4\omega^2 b^2}{(\omega_o^2 - \omega^2)^2} \right)^{\frac{1}{2}}} \quad . \qquad (6.1.6)$$

The other is that $C_o$, the subharmonic amplitude, be real, i.e. that:

$$C_o^2 = \frac{\omega_o^2 - \frac{1}{4}\omega^2 + \xi^2 g_1 \pm (\xi^2(\beta^2 + b^2 g^2) - \omega^2 b^2)^{\frac{1}{2}}}{g_o} \geq 0 \quad . \qquad (6.4.1)$$

It should be kept in mind that these are approximate results, the validity of which breaks down when the predicted value of $C_o$ is too large. As will be seen in Section 9, comparison with results obtained by numerical integration of the complete Rayleigh equation (2.1) by Lauterborn shows that the results given by the asymptotic method are quantitatively accurate provided that $C_o$ is smaller than $\sim 0.4$; qualitatively their validity extends however much further, up to 1 and beyond. This defines implicitly a range of $\omega/\omega_o$ where Eqs. (6.1.6) and (6.4.1) are valid. Indeed, it can be seen from Fig. 5.1 that $g_o$ falls to zero for $\omega/\omega_o$ far away from 2, on both sides, so that the predicted $C_o$ increases without bound. Obviously the end points of the interval of frequencies in which the above formulae are valid are distant from such zeroes.

Figures 6. 1 and 6. 2 show the shape of the subharmonic peak given by Eq. (6. 1. 3) for $b = 0.05$, $\gamma = \frac{4}{3}$, $w = 0.3$, $\eta = 0.4$ and $0.6$.

It can be seen that there is a large interval of frequencies where the steady state subharmonic amplitude may either vanish or have a finite value. The appearance of a subharmonic mode in this frequency range is governed entirely by the initial conditions of the oscillation. A rough criterion for the ranges of initial radii $R_i$ and velocities $dR_i/dt$ that will give rise to a subharmonic component in the steady state regime can be obtained in the following way. If the component of frequency $\omega$ and all second order terms in (6. 1. 8) or (4. 2) are neglected(†) the solution of the Rayleigh equation is:

$$R \simeq R_o \{1 + C \cos (\tfrac{1}{2} \Omega t + \varphi)\}$$

from which:

$$R_i \simeq R_o \{1 + C_i \cos \varphi_i\}$$

$$\frac{dR_i}{dt} \simeq - \frac{1}{2} \Omega R_o C_i \sin \varphi_i$$

As appears from Fig. 6. 13, for small damping the "domain of influence" of the origin may be approximated by the region bounded by the inner separatrix in the undamped case. Computing the inner diameter of this curve with the aid of (6. 3. 3b) and the expression for $H_{cr}$, one can say that, if:

(†) In the subharmonic region the term $P/(\omega_o^2 - \omega^2) \cos \omega \tau$ is very small, because of the large denominator; see Fig. 9. 11.

$$\frac{1}{R_o}\left[(R_i - R_o)^2 + \frac{1}{\Omega_o^2}\left(\frac{dR_i}{dt}\right)^2\right]^{\frac{1}{2}} \lesssim \left(\frac{\omega_o^2 - \frac{1}{4}\omega^2}{g_o}\right)^{\frac{1}{2}} - \left(\frac{\beta_1 \xi}{g_o}\right)^{\frac{1}{2}} \qquad (6.4.2a)$$

then the steady state motion will not contain a subharmonic component. It should be noted however that this criterion is a conservative one if $dR_i/dt \neq 0$.

In the particular case $R_i = R_o$, a more accurate approximation would be:

$$\frac{1}{\Omega_o R_o}\left|\frac{dR_i}{dt}\right| \lesssim \left(\frac{\omega_o^2 - \frac{1}{4}\omega^2 - \beta_1 \xi}{g_o}\right)^{\frac{1}{2}} \qquad (6.4.2b)$$

This expression roughly applies also to the case in which steady oscillations at the impressed frequency $\Omega$ (i.e. oscillations given by Eq. (6.1.8) with $C_o = 0$) are perturbed by a short pulse. By use of (3.10), (6.4.2b) acquires the form:

$$\left|\frac{dR_i}{dt}\right| \lesssim \left(\frac{3\gamma p_o - 2\sigma/R_o}{\rho}\right)^{\frac{1}{2}}\left(\frac{\omega_o^2 - \frac{1}{4}\omega^2 - \beta_1 \xi}{g_o}\right)^{\frac{1}{2}}$$

The progressive decrease of the bounds (6.4.2a), (6.4.2b) as $\omega$ approaches $2\omega_o$ (i.e., for fixed driving frequency, as the bubble grows), and as the driving pressure amplitude $\xi$ is increased has been discussed in Subsection 6.3 above.

If the bubble equation is integrated with homogeneous initial conditions for increasing values of $\frac{\omega}{\omega_o}$, the subharmonic mode will set in abruptly only when the purely harmonic solution becomes unstable (see above Subsection 6.3). It should also be observed that,

since $\beta_1$ increases rapidly as $\omega/\omega_o$ decreases (Fig. 5.2), for a low enough value of $\eta$, a subharmonic component may be observed for some value of $\omega/\omega_o$ less than 2 if appropriate initial conditions are chosen, also if the harmonic solution is stable on the whole range. In this case the curve determined by (6.1.3) will not intersect the $C_o = 0$ axis (Fig. 6.3).

This discussion will be taken up again in the following subsection. Reverting now to Eq. (6.1.6) we note that if we let $\omega = 2\omega_o$ in it we obtain the approximate expression:

$$\eta_{threshold} \simeq \frac{12(3\gamma - w)^{3/2}\, b}{(1-w)(9\gamma^2 - w)\left[1 + \left(\frac{4b}{9\gamma - 3w}\right)^2\right]^{\frac{1}{2}}} \qquad (6.4.3)$$

Since the interval of instability of the purely harmonic solution is usually quite small, this expression for the threshold is adequate there. The complete result (6.1.6) however should be used for lower values of $\omega/\omega_o$.

Equations (6.4.1) and (6.4.3) coincide, up to the first order in $\eta$ and b, with Eller and Flynn's results[18]. The expressions obtained by these authors, however, do not contain either the effect of surface tension, which can be quite noticeable for small bubbles, or the full $\omega$ dependence. The discrepancy in the higher order terms derives presumably from the different nature of the two mathematical approximations.

## 6.5 Connection between subharmonic signal and acoustic cavitation

The sudden appearance of a strong signal at half the excitation frequency in a liquid at the onset of acoustic cavitation was first observed by Esche in 1952[32] and has since then been confirmed by many workers[19, 20, 33, 34]. It appears to be now established that this signal is connected in some as yet unexplained way with the presence of bubbles in the liquid, although other less important mechanisms may contribute to it (see e. g. Ref. [19] for a short summary and discussion). That the presence of bubbles of such radii that they resonate at the subharmonic frequency can result in a strong signal at half the frequency of the driving sound field has found further support in the results obtained by Neppiras[19, 20]. He made observations of single bubbles in a sound field oscillating at a frequency double the bubble's natural frequency and observed the characteristic sudden rise in the subharmonic signal as the driving pressure amplitude was increased. This threshold effect corresponds to condition (6. 1. 6) being fulfilled. To explain the coincidence between subharmonic signal and the onset of gaseous cavitation in an unprepared liquid in which no bubbles of definite size have been seeded, Neppiras conjectures that the subharmonically oscillating bubbles (which may form in the liquid because of rectified diffusion or coalescence of small bubbles) become unstable and collapse. This explanation, however, fails to account for the following features of the phenomenon:

(a) Experiments with single bubbles show that they can oscillate at the subharmonic frequency for long periods of time without evolving into transient cavities[19, 20]. Similarly, in experiments

with gassy liquids the subharmonic signal is present, without any visible streamers or white noise[19, 34].

(b) If bubbles grow from microscipic size by rectified difusion, they would reach a radius such that their natural frequency is equal to that of the sound field long before they would be in the subharmonic size range. Indeed, as Eq. (3.10) shows, if surface tension is neglected, the two radii would differ by a factor of two. It is therefore hard to understand why the instability manifests itself in the subharmonic oscillations rather than in the resonant ones, which are much more violent (see e.g. Sections 8 and 9 below).

(c) When the experiment is performed in a liquid in which several bubbles of the subharmonic size have been seeded, as the presure amplitude increases the subharmonic response presents a double-peak structure (see e.g. Fig. 17 of Ref. [19] or Fig. 5 of Ref. [10]). Neppiras interprets the first peak as corresponding to the subharmonic emission from the added bubbles, while the second, much higher one, would be caused by the bubbles of subharmonic size produced by the growth and agglomeration of microbubbles after the onset of cavitation. According to this explanation, the hypothesis must be made that at the threshold of acoustic cavitation there is a sudden and enormous increase in the number of bubbles of exactly the subharmonic size which, as can be seen from Eqs. (6.2.5), is rather sharply defined. An alternative interpretation of this phenomenon might make recourse to the existence of two unrelated thresholds, one for the subharmonic response of a

bubble of the correct radius and one for the onset of acoustic cavitation.

(d) At a sound frequency of a few tens of kHz, a bubble resonating at the subharmonic frequency would have a radius of the order of $10^{-1}$cm. Such relatively large bubbles have not always been observed in experiments in which the connection between subharmonic emission and onset of cavitation has been established.

Another recent result may be relevant for the explanation of the phenomenon in question. In the course of an extensive numerical investigation of nonlinear bubble oscillations, W. Lauterborn[31] has shown that a Fourier component of frequency $\omega/2$ is often present in bubbles whose natural frequency satisfies:

$$\frac{\omega}{\omega_o} \simeq \frac{2}{k} \qquad k = 1, 3, 4, 5, \ldots \tag{6.5.1}$$

For $k = 1$ this is the ordinary subharmonic oscillation in the sense discussed in the previous subsection. For $k > 1$, however, a spectral component at $\omega/2$ would be produced essentially as a subharmonic of the $k$-th harmonic, through a mechanism completely analogous to that which produces the ordinary subharmonic for $k = 1$. In this case, however, additional nonlinear couplings would have to come into play to transfer the energy from the mode $\omega$ to the mode $k\omega$, and from this to the mode $k\omega/(2k)$.

This mechanism for the generation of the subharmonic emission at $\omega/2$ looks attractive because it does not lend itself to the criticisms expressed in points (b) and (d) above, since bubbles satisfying (6.5.1)

with $k \geq 3$ would be smaller than resonating bubbles. Figure 6.14 taken from Ref. [31] shows the numerically computed response curve for the frequency region containing bubbles satisfying (6.5.1) with $k = 8$ and $k = 9$. It can be seen that even at this level of sound amplitude ($\eta = 0.8$, corresponding typically to conditions of weak cavitation), the peaks are rather broad, so that one can expect that at any time a nondegassed liquid would contain many bubbles capable of emitting the subharmonic signal.

If this is really the mechanism for the subharmonic emission, however, the connection between its appearance and the onset of cavitation would remain to be explained, and also a reason should be given for the absence of a strong subharmonic signal under non-cavitating conditions.

The analysis of the nonsteady behaviour of the subharmonic amplitude presented in this section may serve as a guide towards a satisfactory understanding of these features.

Equations (6.2.5) and Figs. 6.1, 6.2, show that the radii of bubbles that would enter spontaneously into subharmonic oscillations are rather sharply defined. This can be expected to be true also for the subharmonic emissions from bubbles satisfying (6.5.1). In fact, in view of the large number of couplings necessary to transfer energy from the frequency $\omega$ to the frequency $\omega/2$ if $k > 1$, one may expect that the domain of instability of the purely harmonic oscillations would be even narrower than that in the $\omega \simeq \omega_o/2$ region, thus demanding an even sharper "tuning" of the bubbles to emit spontaneously a subharmonic signal. However, as has been shown above, there exists

a much broader frequency domain in which, although the purely harmonic oscillation is stable, a subharmonic oscillation can also be present, provided that the initial conditions for the motion lie in a suitable range. In practice, this means that if the purely harmonic motion is sufficiently perturbed, the ensuing (steady) oscillations would contain a subharmonic component.

The weak shocks radiated by collapsing cavities in the vicinity of these bubbles seem to provide a very likely candidate for the agent of these perturbations. In this picture, the gas bubbles emitting the subharmonic signal would then act primarily as monitors of cavitation events, rather then be directly involved in them. This of course is not to say that, under particular conditions (especially in strong cavitation), they would not undergo a collapse, but only that their collapse is not essential to explain the connection between cavitation and subharmonic emission.

The above hypothesis has been based on the assumption that the transient behaviour of the first subharmonic models at least qualitatively the characteristics of the oscillations containing a subharmonic when (6. 5. 1) is satisfied. This appears to be plausible in view of the following considerations. It is very easy to show (see e. g. Ref. [35]) that the equations determining the amplitude $C_{\frac{1}{2}}$ for the Fourier component at half of the driving frequency for any nonlinearly oscillating system must possess the solution $C_{\frac{1}{2}} = 0$. Therefore, the problem of the occurrence of a nonzero subharmonic component is essentially the problem of the stability characteristics of the

subharmonic-free motion for the frequency region in the neighborhood of $\omega/2$. If this motion were given by:

$$x_o = \sum_{n=o}^{\infty} C_n \cos(n\omega\tau + \varphi_n) \qquad (6.5.2)$$

with $x_o$ an exact solution of:

$$\ddot{x} + F(x, \dot{x}) = P \cos \omega\tau \qquad (6.5.3)$$

then one way to perform the stability analysis would be to substitute:

$$x = x_o + \delta(\tau)$$

with:

$$\delta(\tau) = C_{\frac{1}{2}}(\tau) \cos\left(\tfrac{1}{2}\,\omega\tau + \varphi_{\frac{1}{2}}\right)$$

into (6.5.3), and to determine the conditions under which the perturbation $\delta$ would grow in time. Upon linearization of (6.5.3) about $x_o$, one would then obtain:

$$\ddot{\delta} + \left(\frac{\partial F}{\partial \dot{x}}\right)_{\dot{x}=\dot{x}_o} \dot{\delta} + \left(\frac{\partial F}{\partial x}\right)_{x=x_o} \delta = 0$$

which can be reduced to an equation of the Hill type(†). For fixed values of the pressure amplitude, the stability boundaries of this equation would be only a function of $\omega/\omega_o$, thus determining a narrow frequency interval corresponding to spontaneous growth of the subharmonic component. Since however the bubble is a "softening"

(†) See the Appendix for an example of this procedure.

oscillator, its effective resonant frequency is a decreasing function of the amplitude, so that the resonant peak leans towards lower frequencies in an amplitude-frequency plot. The configuration of the resonant region would thus be qualitatively equal to the one shown in Figs. 6.1, 6.2, and possibly, for relatively low driving amplitudes, in Fig. 6.3.

For an order of magnitude estimate of the perturbation induced by a collapsing cavity on a nearby bubble, one may approximate the weak shock by a delta function, since its duration is of the order of $10^{-6}$ - $10^{-7}$ secs. Integrating the Rayleigh equation, Eq. (2.1), over the interval $\Delta t$ we then get:

$$\frac{dR}{dt}(t+\Delta t) - \frac{dR}{dt}(t) = \frac{\tilde{p}(t)}{\rho R(t)} \qquad (6.5.4)$$

where $\tilde{p}$ is the intensity of the pressure pulse. The pressure field around a spherical bubble in an incompressible liquid is given by (see e.g. Ref. [6], p. 112):

$$p(r,t) = \frac{\bar{R}}{r}(\bar{p}-p_\infty) + \frac{\bar{R}}{r}\left(1 - \frac{\bar{R}^3}{r^3}\right)\frac{1}{2}\rho\bar{U}^2 + p_\infty \qquad (6.5.5)$$

The symbols $\bar{R}, \bar{p}, \bar{U}$ refer here to the radius, internal pressure and wall velocity of the collapsing bubble at time t. We then have:

$$\tilde{p}(t) = p(r,t)\Delta t$$

where r denotes the distance between the two bubbles. For $\bar{p} \sim 10^2$ bars, $\bar{U} \sim 10^4$ cm/sec, $\rho = 1$ g/cm$^3$, $\bar{R}/r \sim 10^{-1}$, $\Delta t \sim 10^{-6}$ sec, $R \sim 10^{-2}$ cm we obtain:

$$\left| \frac{dR}{dt} (t + \Delta t) - \frac{dR}{dt} (t) \right| \sim 1500 \text{ cm/sec.}$$

It can be seen that the order of magnitude of the pulse is large enough to produce a substantial perturbation in the motion of an oscillating bubble. The possibility of a mechanism of this kind is also confirmed by some experiments conducted by Bohn[36], who observed that under weak cavitation conditions gas bubbles smaller than resonance size can be excited to oscillate at their natural frequency by cavitation shocks. If the sound intensity is increased to strong cavitation conditions, these bubbles become unstable and break up. This effect, together with the lower transparency to sound of a strongly cavitating liquid, can be responsible for the observed decrease of the subharmonic signal at higher pressure amplitudes.

7. Other frequency regions

In the second harmonic and subharmonic regions the analysis follows a similar pattern. We present here the relevant equations and some examples, deferring a further discussion until Section 9. In the last subsection the non-resonant behavior is considered.

## 7.1 First harmonic

The system determining the slowly varying quantities $C = \epsilon A$ and $\varphi$ is in the first harmonic region ($\omega \sim \omega_o/2$):

$$\begin{cases} -4\omega\dot{C} = 4\omega bC + \xi^2\beta_2 \sin\varphi + b\xi^2 g_3 \cos\varphi & (7.1.1a) \\ -4\omega C\dot{\varphi} = C[4\omega^2 - \omega_o^2 - \xi^2(g_1 - g_2) + g_o C^2] & \\ \qquad -b\xi^2 g_3 \sin\varphi + \xi^2\beta_2 \cos\varphi. & (7.1.1b) \end{cases}$$

The singular points $C_o$, $\varphi_o$ are given by the equations

$$\sin\varphi_o = \frac{bC_o}{\xi^2} \frac{g_3(Q_2 + g_o C_o^2) - 4\omega\beta_2}{\beta_2^2 + b^2 g_3^2} \qquad (7.1.2a)$$

$$\cos\varphi_o = -\frac{C_o}{\xi^2} \frac{\beta_2(Q_2 + g_o C_o^2) + 4\omega b^2 g_3}{\beta_2^2 + b^2 g_3^2} \qquad (7.1.2b)$$

$$g_o^2 C_o^6 + 2g_o Q_2 C_o^4 + (Q_2^2 + 16b^2\omega^2)C_o^2 = \xi^4(\beta_2^2 + b^2 g_3^2) \qquad (7.1.3)$$

where:

$$Q_2 = 4\omega^2 - \omega_o^2 - \xi^2(g_1 - g_2) \quad .$$

Obviously there is no threshold for the first harmonic, and hence zero is not one of the possible values of $C_o$. Depending on the values of the coefficients, Eq. (7.3) can have either one or three real (positive) roots. In the latter case, a stability analysis shows that the intermediate root is unstable. Which one of the remaining two will appear in an experiment or in performing numerical computations is once again determined by the initial conditions, as was observed above in subsection 6.4. Examples of the harmonic peak are shown in Fig. 7.1, while Fig. 7.2 shows the behavior of the phase $\varphi_o$ across the resonance. The peaks are bent to the left, since the bubble is a "softening" oscillating system. Because of the relatively high damping, the peak labeled by $b = 0.1$ does not exhibit an unstable section of the response curve. For the other two values of b this section is present and is indicated by a dashed line in the figure. If damping is absent, system (7.1) is Hamiltonian, with a Hamiltonian function given by

$$H = \frac{1}{4} g_o C^4 + \frac{1}{2} Q_2 C^2 + \xi^2 \beta_2 C \cos\varphi \quad . \qquad (7.1.4)$$

As before, the lines $H = \text{constant}$ are a solution of (7.1.1) in the case of undamped oscillations.

The solution for X is in the first harmonic region:

$$X_2 = C_o \cos(2\omega\tau + \varphi_o) + \frac{\xi}{\omega_o^2 - \omega^2} \cos\omega\tau + \xi C_o c_o \cos(\omega\tau + \varphi_o) + \xi^2 c_1 + C_o^2 c_5$$
$$+ C_o^2 c_2 \cos(4\omega\tau + 2\varphi_o) + \xi C_o c_4 \cos(3\omega\tau + \varphi_o) + b\xi c_6 \sin\omega\tau \quad . \qquad (7.1.5)$$

## 7.2 Second harmonic

In the second harmonic region $(\omega \sim \omega_o/3)$ $C(\tau)$ and $\varphi(\tau)$ are solutions of:

$$\begin{cases} -6\omega\dot{C} = 6\omega b C + \xi^3 g_5 \sin\varphi & (7.2.1a) \\ -6\omega C\dot{\varphi} = C[g_o C^2 - \xi^2(g_1 - g_2) + 9\omega^2 - \omega_o^2] + \xi^3 g_5 \cos\varphi & (7.2.1b) \end{cases}$$

and the steady state values are determined by

$$\sin\varphi_o = -\frac{6\omega b C}{g_5 \xi^3} \qquad (7.2.2a)$$

$$\cos\varphi_o = -C\,\frac{Q_3 + g_o C^2}{g_5 \xi^3} \qquad (7.2.2b)$$

$$g_o^2 C_o^6 + 2Q_3 g_o C_o^4 + (Q_3^2 + 36\omega^2 b^2) C_o^2 - g_5^2 \xi^6 = 0 \qquad (7.2.3)$$

where:

$$Q_3 = 9\omega^2 - \omega_o^2 - \xi^2(g_1 - g_2) \quad .$$

The same remarks made for the first harmonic apply here too. In particular, the Hamiltonian of system (7.2.1) in the case of absence of damping is:

$$H = \frac{1}{4} g_o C^4 + \frac{1}{2} Q_3 C^2 + \xi^3 g_5 C \cos\varphi \quad . \qquad (7.2.4)$$

Figure 7.3 shows examples of the resonance peaks in this region. Comparing it with Fig. 7.1, it is evident that damping is much more effective on the second harmonic mode than on the first one, as should be expected on physical grounds. The phase exhibits a behavior analogous to that shown in Fig. 7.2.

The solution X is in this region:

$$X_3 = C\cos(3\omega\tau+\varphi_o) + \frac{\xi}{\omega_o^2-\omega^2}\cos\omega\tau + \xi C_o c_o \cos(2\omega\tau+\varphi_o)+\xi^2 c_1 + C_o^2 c_5$$

$$+ C_o^2 c_2 \cos(6\omega\tau+2\varphi_o)+\xi C_o c_4 \cos(4\omega\tau+\varphi_o)+\xi^2 c_3 \cos 2\omega\tau \qquad (7.2.5)$$

$$+ b\xi c_6 \sin\omega\tau \quad .$$

## 7.3 Second subharmonic

In the second subharmonic region ($\omega \simeq 3\omega_o$), the slowly varying functions $C(\tau)$, $\varphi(\tau)$ are determined by:

$$\begin{cases} -\frac{2}{3}\omega\dot{C} = \frac{2}{3}\omega bC + C^2\xi g_6 \sin 3\varphi & (7.3.1a) \\ -\frac{2}{3}\omega C\dot{\varphi} = \left[\frac{1}{9}\omega^2-\omega_o^2-\xi^2(g_1-g_2)\right]C+g_o C^3+C^2\xi g_6\cos 3\varphi \quad . & (7.3.1b) \end{cases}$$

The steady state solutions $C_o, \varphi_o$ are:

$$\sin 3\varphi_o = -\frac{2}{3}\frac{\omega b}{C_o \xi g_6} \qquad (7.3.2a)$$

$$\cos 3\varphi_o = -\frac{Q_{1/3}+g_o C_o^2}{C_o \xi g_6} \qquad (7.3.2b)$$

$$C_o^2\left\{g_o^2 C_o^4+(2Q_{1/3}g_o-\xi^2 g_6^2)C_o^2+\frac{4}{9}\omega^2 b^2+Q_{1/3}^2\right\} = 0 \qquad (7.3.3)$$

where

$$Q_{1/3} = \frac{1}{9}\omega^2-\omega_o^2-\xi^2(g_1-g_2) \quad .$$

Again, as in the case of the first subharmonic, $C_o = 0$ is a solution of (7.3.1). The condition that (7.3.3) has other solutions imposes a restriction on $\xi$, which is analogous to the threshold equation (6.1.6)

but more complicated in its analytical expression:

$$\xi \geqslant \xi_{threshold} = \left( 2g_o \frac{g_6 \left| \frac{\omega^2}{9} - \omega_o^2 \right| + \left| g_6^2 \left( \frac{\omega^2}{9} - \omega_o^2 \right)^2 + \frac{4}{9} \omega^2 b^2 [g_6^2 + 4g_o(g_1 - g_2)] \right|^{\frac{1}{2}}}{g_6 [g_6^2 + 4g_o(g_1 - g_2)]} \right)^{\frac{1}{2}} . \quad (7.3.4)$$

If this is satisfied, the solutions other than $C_o = 0$ are given by:

$$C_o = \left( \frac{-2Q_{1/3} g_o + \xi^2 g_6^2 \pm \left| \xi^4 g_6^4 - 4Q_{1/3} g_o g_6^2 \xi^2 - \frac{16}{9} g_o^2 \omega^2 b^2 \right|^{\frac{1}{2}}}{2g_o^2} \right)^{\frac{1}{2}} . \quad (7.3.5)$$

Of the two branches of this equation, the lower is unstable, exactly as in the first subharmonic case. The same phase plane analysis done there can be carried out here too. An additional complication in this case is that, as (7.3.2) show, the singular points corresponding to non-vanishing values of $C_o$ are three.

In view of the little practical interest in the second subharmonic mode (which however has been observed[20]), a detailed analysis is not presented here. We mention only the fact that, for fixed damping, the threshold for the second subharmonic is higher than that for the first, and that the response is lower. In the undamped case system (7.3.1) is Hamiltonian:

$$H = \frac{1}{4} g_o C^4 + \frac{1}{2} \left\{ \frac{1}{9} \omega^2 - \omega_o^2 - \xi^2 (g_1 - g_2) \right\} C^2 + \frac{1}{3} \xi g_6 C^3 \cos 3\varphi \quad . \quad (7.3.6)$$

The expression for the steady state oscillations is:

$$X_{1/3} = C_o \cos\left(\frac{\omega}{3}\tau + \varphi_o\right) + \frac{\xi}{\omega_o^2 - \omega^2}\cos\omega\tau + \xi C_o c_o \cos\left(\frac{2}{3}\omega\tau - \varphi_o\right) +$$

$$+ \xi^2 c_3 \cos 2\omega\tau + \xi^2 c_1 + C_o^2 c_5 + C_o^2 c_2 \cos\left(\frac{2}{3}\omega\tau + 2\varphi_o\right) + \qquad (7.3.7)$$

$$+ \xi C_o c_4 \cos\left(\frac{4}{3}\omega\tau + \varphi_o\right) + b\xi c_6 \sin\omega\tau \ .$$

## 7.4 Intermediate regions

In the regions between resonances the solution can be obtained just be letting $C_o$ tend to zero in any of the preceding expressions for X. In this way we obtain:

$$X_{int} = \frac{\xi}{\omega_o^2 - \omega^2}\cos\omega\tau + \xi^2 c_1 + b\xi c_6 \sin\omega\tau + \xi^2 c_3 \cos 2\omega\tau \ . \qquad (7.4.1)$$

As can be seen from their definitions (5.5), the functions of $c_i$ that enter in this expression do not depend on $\nu$, so that there is no ambiguity.

An analysis of the equations for $C_o$ given in the preceding subsection shows that $C_o \to 0$ as $\omega/\omega_o$ gets far from the resonant regions, so that the resonant solutions tend indeed to the form given by (7.4.1).

## 8. Resonant oscillations

In this section the resonant case in which the driving frequency $\omega$ is close to the natural frequency $\omega_o$ will be considered briefly. The general results are qualitatively very similar to the ones relative to the first and second harmonics, and the only reason to treat this case separately is that, as already noted in Section 4, a slightly different mathematical approach is necessary.

The suitable form for the asymptotic expansion of the solution $x$ is in this case given by (4. 2) with $\nu = \omega$:

$$x = A(\tau)\cos(\omega\tau + \varphi(\tau)) + \epsilon x_1 + \epsilon x_2 + \ldots \qquad (8.1)$$

The equation for $x_1$, corresponding to (4. 12), is:

$$\ddot{x}_1 + \omega_o^2 x_1 = 2\omega BA\sin\theta + \frac{1}{2}A^2(a_1 - \frac{3}{2}\omega^2) - \frac{1}{2}PA\cos\varphi$$
$$+ \frac{1}{2}A^2\left(a_1 + \frac{3}{2}\omega^2\right)\cos 2\theta - \frac{1}{2}PA\cos(2\theta - \varphi) \qquad (8.2)$$

where, as usual, $\theta = \omega\tau + \varphi$. The first term on the RHS of this equation should be removed and put back into the equation for the slowly varying terms. When this is done the (steady state) solution of Eq. (8. 2) results:

$$x_1 = \frac{1}{2}\frac{A^2\left(a_1 - \frac{3}{2}\omega^2\right) - PA\cos\varphi}{\omega_o^2} + \frac{1}{2}A^2\frac{a_1 + \frac{3}{2}\omega^2}{\omega_o^2 - 4\omega^2}\cos 2\theta$$

$$- \frac{1}{2}\frac{PA}{\omega_o^2 - 4\omega^2}\cos(2\theta - \varphi) \quad . \qquad (8.3)$$

This expression is now substituted into the equation for $x_2$, the resonant terms removed and cast back into the equation for the slowly varying terms. The system determining these, when averaged over $\theta$ in the way described in Section 4, is:

$$\begin{cases} -2\omega\dot{C} = 2\omega bC + \xi(1 - C^2 d_3)\sin\varphi + \dfrac{\xi^2}{4\omega_o^2}C\sin 2\varphi & (8.4a) \\ -2\omega C\dot{\varphi} = CQ_1 - d_1 C^3 + \xi(1 - C^2 d_2)\cos\varphi + \dfrac{\xi^2}{4\omega_o^2}C\cos 2\varphi \quad . & (8.4b) \end{cases}$$

Here $C = \epsilon A$, and the other quantities are defined as follows:

$$Q_1 = \omega^2 - \omega_o^2 + \frac{2\omega^2 - \omega_o^2}{2\omega_o^2(4\omega^2 - \omega_o^2)} \xi^2 \tag{8.5}$$

$$d_1 = -a_1\left(\frac{a_1 - \frac{3}{2}\omega^2}{\omega_o^2} + \frac{a_1 + \frac{3}{2}\omega^2}{2(\omega_o^2 - 4\omega^2)}\right) + \frac{3}{4}a_2 - \frac{3}{2}\omega^2\left(\frac{1}{4} - \frac{a_1 + \frac{3}{2}\omega^2}{\omega_o^2 - 4\omega^2}\right) \tag{8.6a}$$

$$d_2 = \frac{1}{4}\frac{3a_1 - \frac{9}{2}\omega^2}{\omega_o^2 - 4\omega^2} + \frac{3}{2}\frac{a_1 - \frac{1}{2}\omega^2}{\omega_o^2} - \frac{3}{4} \tag{8.6b}$$

$$d_3 = \frac{1}{4}\frac{a_1 - \frac{15}{2}\omega^2}{\omega_o^2 - 4\omega^2} + \frac{a_1 - \frac{3}{2}\omega^2}{2\omega_o^2} - \frac{1}{4} \tag{8.6c}$$

Graphs of the functions (8.6) are presented in Figs. 8.1 and 8.2. The equations for the singular points are in this case somewhat more complicated than before, but can readily be solved with the aid of a computer.

Examples of the resonant peak are shown in Fig. 8.3. The structure is qualitatively the same as that of the first and second harmonic, but the height of the peak is much greater, as is to be expected. In particular, if the excitation is strong enough, there are three values for the steady state amplitude, with the middle one unstable.

The (steady state) solution in the resonant region is:

$$X_1 = C_o\cos(\omega\tau + \varphi_o) + \frac{a_1 - \frac{3}{2}\omega^2}{2\omega_o^2}C_o^2 - \frac{\xi}{2\omega_o^2}C_o\cos\varphi_o +$$

$$+ \frac{a_1 + \frac{3}{2}\omega^2}{2(\omega_o^2 - 4\omega^2)} C_o^2 \cos(2\omega\tau + 2\varphi_o)$$

$$+ \frac{\xi}{2(4\omega^2 - \omega_o^2)} C_o \cos(2\omega\tau - \varphi_o) . \qquad (8.7)$$

9. Comparison with numerical results

W. Lauterborn has performed an extensive series of numerical computations of the response-frequency relation of an oscillating bubble. Since the equation that he has integrated numerically is exactly the same as Eq. (2.1), his results are particularly suitable for a check of the validity of the present analytical approach. Figs. 9.1 through 9.9 present a comparison of Lauterborn's results [ 31 ] with the analytical ones in a few cases. The figures are plots of $X_m = (R_{max} - R_o) / R_o$ versus $\omega / \omega_o$ , where $R_{max}$ is the maximum value of the radius during a steady state oscillation at frequency $\omega$ . The cases considered are the following:

case 1 b = 0.128 w = 0.592

case 2 b = 0.019 w = 0.127

for several values of the pressure amplitude $\eta$ . If the liquid is water at 20 $^{o}$C , the two cases would correspond to a bubble of radius $10^{-4}$cm and $10^{-3}$cm respectively; for both the polytropic exponent is $\gamma = 1.33$.

Figs 9.1 and 9.2 refer to case 1 for $\eta = 0.5$. It should be noted however that, because of the high value of w, the "effective pressure amplitude" $\xi = (1 - w)\eta$ is much lower, $\xi = 0.204$. The agreement is seen to be extremely good, even near resonance where $X_m$ is large (Fig. 9.1). In Fig. 9.1 the dotted vertical segment on the curve of Lauterborn's results is the "jump" in the numerical solution which

appears at the point of vertical tangent of the lower branch. The analytical results do not show an unstable section. However, a more careful analysis shows that this case is on the borderline between the two possible configurations of the peak, so that this difference does not appear to be significant. Fig. 9.10 presents a plot of $R(t) / R_o$ and of $p(t) / p_\infty$ for the case of Fig. 9.1, with $\omega / \omega_o = 0.9$. The highly non-linear nature of the oscillations is quite evident, and it illustrates from another point of view the effectiveness of the asymptotic method in dealing with this problem.

In the following figure corresponding to a higher value of $\xi$ (Fig. 9.3, case 2, $\eta = 0.3$, $\xi = 0.262$) the agreement is somewhat less satisfactory. Nevertheless many of the characteristics of the response, such as a close estimate of the value of $X_m$, the location of the peaks and whether they exhibit an unstable section or not, are described quite well by the analytical solution. It should be noted that in the resonant and first harmonic peak the analytical result continues much higher than the numerical one. The reason for this is that apparently Lauterborn has obtained his results by integration in the direction of increasing values of $\omega / \omega_o$. In this way he was unable to compute the response curve in the region in which it has two (stable) branches. The unstable section of this curve as computed analytically is also indicated in the figure. The value of $\omega / \omega_o$ for which the tangent to it becomes vertical gives the point at which a numerical solution becomes unstable and would show a "jump". The agreement with the jump in Lauterborn's solution is very good for the first harmonic peak, but seems to be less so for the resonant one. However it is apparent that here the jump occurs long

before the tangent becomes vertical, probably as an effect of initial conditions. If the numerical curve is continued ideally beyond the discontinuity, the agreement appears to be good in this case too.

Figures 9.4 (case 1) and 9.5 (case 2) corrspond to very close values of $\xi$, $\xi = 0.367$ and $\xi = 0.369$. A comparison shows that the relation with the numerical results is very little influenced by the values of the damping parameter $b$ and the Weber number $w$, but depends essentially on the values of $\xi$ and $X_m$. Finally Fig. 9.6 presents the results for a very large value of $\xi$, $\xi = 0.531$. It can be seen here that, in spite of the large quantitative discrepancies, a qualitative agreement still remains.

In the case of the subharmonic region, which is shown in detail in Fig 9.7, 9.8 and 9.9 (case 2), the picture is essentially the same, but some features are worth noting. Again it is seen that for the lowest value of $\xi$ (Fig. 9.7) the agreement is good, but that it gets worse as $\xi$ increases. It will be noticed, however, that the agreement remains excellent for all values of $\xi$ in the region in which the subharmonic mode is not present. The reason for this is obviously the fact that, far away from the resonance, the response is so small that the approximate analytical treatment is quite adequate. An interesting consequence of this is that the interval in which the purely harmonic solution is unstable (i.e., the interval in which the subharmonic mode will appear for any set of initial conditions) is predicted quite accurately for values of $\xi$ up to 1, as is apparent from the figures. As a confirmation of this we mention that in case 1 the subharmonic threshold as computed according to (6, 4.3) is $\eta_{th} = 1.54$, and that the numerical results do not show

any subharmonic peak for values of $\eta$ up to 1.5, whereas the subharmonic mode is present for $\eta = 1.6$. For case 2 the threshold value obtained by Lauterborn is $\sim 0.12$ [31], and the one computed according to (6.4.3) 0.1233. Fig. 9.11 presents an example of the curves $R(t)/R_o$ and $p(t)/p_\infty$ for the subharmonic case. Together with the subharmonic oscillation (curve a), also the (stable) purely harmonic one is plotted for comparison (curve b).

In summary, we may say that the comparison with Lauterborn's numerical results shows that:

(a) The asymptotic method used in this study gives very accurate results for pressure amplitudes of order 0.2. It should be stressed that this is a limit on the "effective pressure amplitude" $\xi$ defined by (3.6c):

$$\xi = 1 - \frac{2\sigma}{R_o p_o} \frac{p_{max}}{p_{average}}$$

rather than on $\eta = p_{max}/p_{av}$. For bubbles of small radius, $\eta$ can be much larger than $\xi$.

(b) This upper limit can be increased if the value of $X_m$ remains low, as would be the case for strong damping, the second harmonic, or values of $\omega/\omega_o$ greater than $\sim 1.2$, the regions of the subharmonics possibly excluded.

(c) As $\xi$ gets larger than $\sim 0.3$ the quantitative agreement gets less and less satisfactory, but the essential qualitative features are preserved in the approximate analytical results.

(d) The above picture is little affected by the values of the damping parameter b and of the Weber number w.

For values of $\omega / \omega_o < 0.25$ higher harmonics may cause small peaks. Since they are not given by the approximate treatment, this may be in error there. This discrepancy however is very small in the range of values of $\xi$ for which good agreement is found in other regions.

It has not been possible to find in the literature any numerical results for the second subharmonic region. Since the response falls off very rapidly as $\omega$ increases, it should be expected that, similarly to the first submarmonic, at least the thresholds are predicted quite accurately by the present treatment also for high values of $\xi$.

## 10. Concluding remarks

Direct experimental evidence with which to compare the results presented in this study unfortunately is not available because of several practical difficulties [20]. Some qualitative comparisons can nevertheless be made which substantiate several of our findings.

Vaughan [34] observed a linear increase of the subharmonic output with driving pressure from gassy liquids, such as fresh carbonated water. From (6.1.3) it can readily be seen that, well above threshold, the subharmonic amplitude increases with the driving pressure $\eta$ essentially like $(k_1 + k_2 \eta)^{\frac{1}{2}}$ for $\eta$ large enough. If the simultaneous emission from a large number of bubbles randomly located is measured, it is to be expected that the effects linear in $R - R_o$ will average out, leaving only the ones proportional to even powers. Thus, for large enough values of $\eta$, the observed linear relationship is obtained. A further confirmation is the acoustic output of a single bubble for increasing $\eta$ measured by Neppiras, which shows a behaviour compatible with $(k_1 + k_2 \eta)^{\frac{1}{2}}$ or $(k_1 + (k_2 \eta - k_3)^{\frac{1}{2}})^{\frac{1}{2}}$, (Ref. [19] Fig. 12 or Ref. [20],

Fig. 4), and certainly nonlinear. The experimental points, however, are too few to draw any definite conclusions.

For what concerns the threshold equation, Eq. (6. 1. 6), and its essentially linear dependence on viscosity, the fact may be noted that the same linear increase has been reported by Vaughan (Ref. [34], Fig. 14)(†).

The increase with excitation pressure in the acoustic output at the fundamental and first harmonic frequency has also been measured by Neppiras for single bubbles [19]. He found an approximately linear increase in the first case and an approximately quadratic one in the second. From formulae (8. 4) and (7. 1. 3) the same result can be obtained for small amplitudes.

We may also mention that Fig. 13 of Ref. [19] and Fig. 3(a) of [20] show that the subharmonic peak is inclined to the left on a frequency axis, in agreement with section 6. Finally we note that the second subharmonic discussed in Subsection 7. 3 has also been observed experimentally.

---

(†) Also Vaughan's results present the double-peak structure mentioned in Subsection 6. 5, so that it seems likely that the "threshold" referred to in Fig. 14 of the paper corresponds to the first peak. If Neppiras' interpretation of the peak structure is applicable here too (as is plausible, since Vaughan's liquids were not degassed), the threshold of the first peak is the one for emission by bubbles of subharmonic size, and hence (6. 1. 6) applies.

## Appendix

### Stability of harmonic solution in the subharmonic region

The purely harmonic solution ( i. e. Eq. (6. 10) with $C_o = 0$ ) is :

$$x_h = Q \cos \omega\tau + \epsilon ( P^2 c_1 + BPc_6 \sin \omega\tau + P^2 c_3 \cos 2\omega\tau ) \quad (A. 1)$$

let now:

$$x = x_h + \eta \quad (A. 2)$$

in the full equation (3. 11). It is assumed that $x_h$ given by (A. 1) is the exact solution of Eq. (3. 11) and $\eta$ a small perturbation about this exact solution. Linearizing Eq. (3. 9) about $x_h$ we get:

$$\ddot{\eta} + \epsilon [ 2B + f(x_h(\tau)) ] \dot{\eta} + [ \omega_o^2 + \epsilon g(x_h(\tau)) ] \eta = 0 \quad (A.3)$$

where the functions f, g are given by:

$$f = 3\dot{x}_h - 3\epsilon \dot{x}_h x_h - 4\epsilon B x_h \quad (A. 4)$$

$$g = -2a_1 x_h + P \cos \omega\tau + \epsilon (- \frac{3}{2} \dot{x}_h^2 + 3a_2 x_h^2 - 2x_h P \cos \omega\tau - 4B\dot{x}_h) \quad (A. 5)$$

by means of the transformation:

$$\eta = \exp \left( - \frac{\epsilon}{2} \int_o^\tau f ( x_h(\sigma) ) \, d\sigma \right) u(\tau) \quad (A. 6)$$

Eq. (A. 3) is put into the more convenient form:

$$\ddot{u} + 2\epsilon B\dot{u} + \left[ \omega_o^2 + \epsilon ( g - \frac{1}{2} \dot{f} ) - \epsilon^2 ( Bf + \frac{1}{4} f^2 ) \right] u \quad 0 \quad (A. 7)$$

Retaining only first and second order terms in $\epsilon$ in the last bracket, after substitution of (A. 1), (A. 4), (A. 5), this equation can be written more explicitly as:

$$\ddot{u} + 2\epsilon B\dot{u} + (\omega_o^2 + \epsilon^2 P^2 g_7 + 2\epsilon P\beta_1 \cos\omega\tau - $$

$$- 2\epsilon^2 BPg_8 \sin\omega\tau + \epsilon^2 P^2 g_9 \cos 2\omega\tau)\, u = 0 \qquad \text{(A. 8)}$$

here $g_7$, $g_8$ and $\beta_1$ are given by (6. 2. 6a), (6. 2. 6b) and (5. 8a) respectively, while $g_9$ is defined as follows:

$$g_9 = c_3(6\omega^2 - 2a_1) - \frac{1}{\omega_o^2 - \omega^2} + \frac{3}{2}\,\frac{a_2 + \frac{1}{4}\omega^2}{(\omega_o^2 - \omega^2)^2} \qquad \text{(A. 9)}$$

Since we are investigating the stability of the solution (A. 1) against the growth of a subharmonic component, we let

$$u = K(\tau)\cos\frac{\omega}{2}\tau + S(\tau)\sin\frac{\omega}{2}\tau \qquad \text{(A. 10)}$$

in (A. 8) and examine the conditions under which the (slowly varying) functions $K(\tau)$ and $S(\tau)$ remain bounded as $\tau \to \infty$. Imposing the additional requirement that:

$$\frac{1}{2}\omega\dot{K}\cos\frac{\omega}{2}\tau + \frac{1}{2}\omega\dot{S}\sin\frac{\omega}{2}\tau = 0 \qquad \text{(A. 11)}$$

(analogous to (4. 3)), a first order differential system is obtained for $K$ and $S$, to which the method of averaging can be applied obtaining:

$$- \omega \dot{K} - \frac{\omega^2}{4} S - \epsilon B \omega K + (\omega_o^2 + \epsilon^2 P^2 g_7) S -$$

$$- \epsilon \beta_1 PS - \epsilon^2 BP g_8 K = 0 \qquad \text{(A. 12a)}$$

$$- \omega \dot{S} - \frac{\omega^2}{4} K + \epsilon B \omega S + (\omega_o^2 + \epsilon^2 P^2 g_7) K +$$

$$+ \epsilon \beta_1 PK - \epsilon^2 BP g_8 S = 0 \qquad \text{(A. 12b)}$$

As is well known the condition that such a system be stable amounts to the requirement that the following polynomial has no positive roots:

$$\omega^2 \lambda^2 + 2 \epsilon B \omega^2 \lambda + \epsilon^2 B^2 \omega^2 - \epsilon^4 B^2 P^2 g_8^2 +$$

$$+ (\omega_o^2 - \frac{1}{4} \omega^2 + \epsilon^2 P^2 g_7)^2 - \epsilon^2 P^2 \beta_1^2 = 0 \qquad \text{(A. 13)}$$

Since $B > 0$ by hypothesis, this is equivalent to:

$$| \omega_o^2 - \frac{\omega^2}{4} + \xi^2 g_7 | > (\xi^2 (\beta_1^2 + b^2 g_8^2) - b^2 \omega^2)^{\frac{1}{2}} \qquad \text{(A. 14)}$$

where, as usual, $\xi = \epsilon P$, $b = \epsilon B$. From this equation the stability conditions (6. 2. 5) given in subsection 6. 2 follow immediately.

## References


1. M. Minnaert, On musical air-bubbles and the sounds of running water, Phil. Mag. 16, 235-248 (1933).

2. F. D. Smith, On the destructive mechanical effects of the gas bubbles liberated by the passage of intense sound through a liquid, Phil. Mag. 19, 1147-1151 (1935).

3. M. S. Plesset, D. Y. Hsieh, Theory of gas bubble dynamics in oscillating pressure fields, Phy. Fluids 3, 882-892 (1960).

4. C. Devin, Survey of thermal, radiation, and viscous damping of pulsating air bubbles in water, J. Acoust. Soc. Amer., 31, 1654-1667 (1953).

5. R. B. Chapman, M. S. Plesset, Thermal effects in the free oscillation of gas bubbles, J. Basic Eng. 93, 373-376 (1971).

6. H. G. Flynn, Physics of acoustic cavitation in liquids, in Physical Acoustics, pp. 57-172, Vol. 1, Part B, W. P. Mason, Ed., Academic Press (1964).

7. B. E. Noltingk, E. A. Neppiras, Cavitation produced by ultrasonics, Proc. Phys. Soc. (London) 63B, 674-685 (1950).

8. E. A. Neppiras, B. E. Noltingk, Cavitation produced by ultrasonics: Theoretical conditions for the onset of cavitation, Proc. Phys. Soc. (London) 64B, 1032-1038 (1951).

9. R. B. Robinson, R. H. Buchanan, Undamped free pulsations of an ideal bubble, Proc. Phys. Soc. (London) 69B, 893-900 (1956).

10. M. I. Borotnikova, R. I. Soloukhin, A calculation of the pulsations of gas bubbles in an incompressible liquid subject to a periodically varying pressure, Sov. Phis. Acoustics 10, 28-32 (1964).

11. L. P. Solomon, L. L. Evans, Generation of subharmonics of order 1/2. A continuation, J. Acoust. Soc. Amer. 45, 339 (A) (1969).

12. L. P. Solomon, L. L. Evans, Subharmonics of the bubble equation addenda. J. Acoust. Soc. Amer. 47, 92(A) (1970).

13. O. A. Kapustina, Gas bubble in a small amplitude sound field, Sov. Phys. Acoustics 15, 427 (1970).

14. W. Lauterborn, Eigenfrequenzen von gasblasen in Flussigkeiten, Acustica 20, 14-20 (1968).

15. W. Lauterborn, Resonanzkurven von gasblasen in Flussigkeiten, Acustica, 23, 73-81 (1970).

16. W. Lauterborn, Subharmonische schwingungen von gasblasen in wasser, Acustica 22, 238-239 (1969-1970).

17. W. Guth, Nichtlineare schwingungen von luftblasen in wasser, Acustica 6, 532-538 (1956).

18. A. Eller, H. G. Flynn, Generation of subharmonics of order one-half by bubbles in a sound field, J. Acoust. Soc. Amer. 46, 722-727 (1969).

19. E. A. Neppiras, Subharmonic and other low-frequency emission from bubbles in sound-irradiated liquids, J. Acoust. Soc. Amer., 46, 587-601 (1969).

20. E. A. Neppiras, Subharmonic and other low-frequency signals from sound-irradiated liquids, J. Sound Vib. 10, 176-186 (1969).

21. See e. g. M. S. Plesset, Cavitating Flows, in Topics in Ocean Engineering, Vol. 1, pp. 85-95, C. I. Bretschneider Ed., Gulf Publishing Co. (1969), or D. Y. Hsieh, Some analytical aspects of bubble dynamics, J. Basic Eng. 87, 991-1005 (1965).

22. M. S. Plesset, Bubble dynamics, in Cavitation in Real Liquids, pp. 1-18, R. Davies Ed., Elsevier Publishing Co. (1964).

23. R. M. Cole, Underwater Explosions, Dover (1965), p. 307.

24. N. N. Bogolyubov, N. M. Krylov, Introduction to nonlinear mechanics, Princeton University Press (1943).

25. N. N. Bogolyubov, Y. A. Mitropolsky, Asymptotic methods in the theory of non-linear oscillations, Hindustan Publishing Corp. (1961).

26. J. D. Cole, Perturbation methods in applied mathematics, Chapter 3, Blaisdell Publishing Co. (1968).

27. J. Kevorkian, The two variable-expansion procedure for the approximate solution of certain non-linear differential equations, in Space Mathematics, Part III, pp. 206-275, Lectures in Applied Mathematics, Vol. 7, Amer. Math. Soc., Providence, R. I. (1966).

28. J. A. Morrison, Comparison of the modified method of averaging and the two-variable expansion procedure, S. I. A. M. Review 8, 66-85, (1966).

29. D. Y. Hsieh, M. S. Plesset, Theory of rectified diffusion of mass into gas bubbles, J. Acoust. Soc. Amer. 33, 206-215 (1961).

30. L. A. Skinner, Acoustically induced gas bubble growth, J. Acoust. Soc. Amer. 51, 378-382 (1972).

31. W. Lauterborn, Numerical investigation of non-linear oscillations of gas bubbles in liquids. I. Free oscillations and frequency response curves, to be published.

32. R. Esche, Untersuchung der schwingungskavitation in Flussigkeiten, Acustica 2, 208-218 (1952).

33. P. DeSantis, D. Sette, F. Wanderlingh, Cavitation detection: The use of the subharmonics, J. Acoust. Soc. Amer. 42, 514-516 (1967).

34. P. W. Vaughan, Investigation of acoustic cavitation thresholds by observation of the first subharmonic, J. Sound Vib. 7, 236-246, (1968).

35. See Part II of this thesis, p. 114.

36. L. Bohn, Schalldruckverlauf und Spektrum bei der schwingungskavitation, Acustica 7, 201-216 (1957).

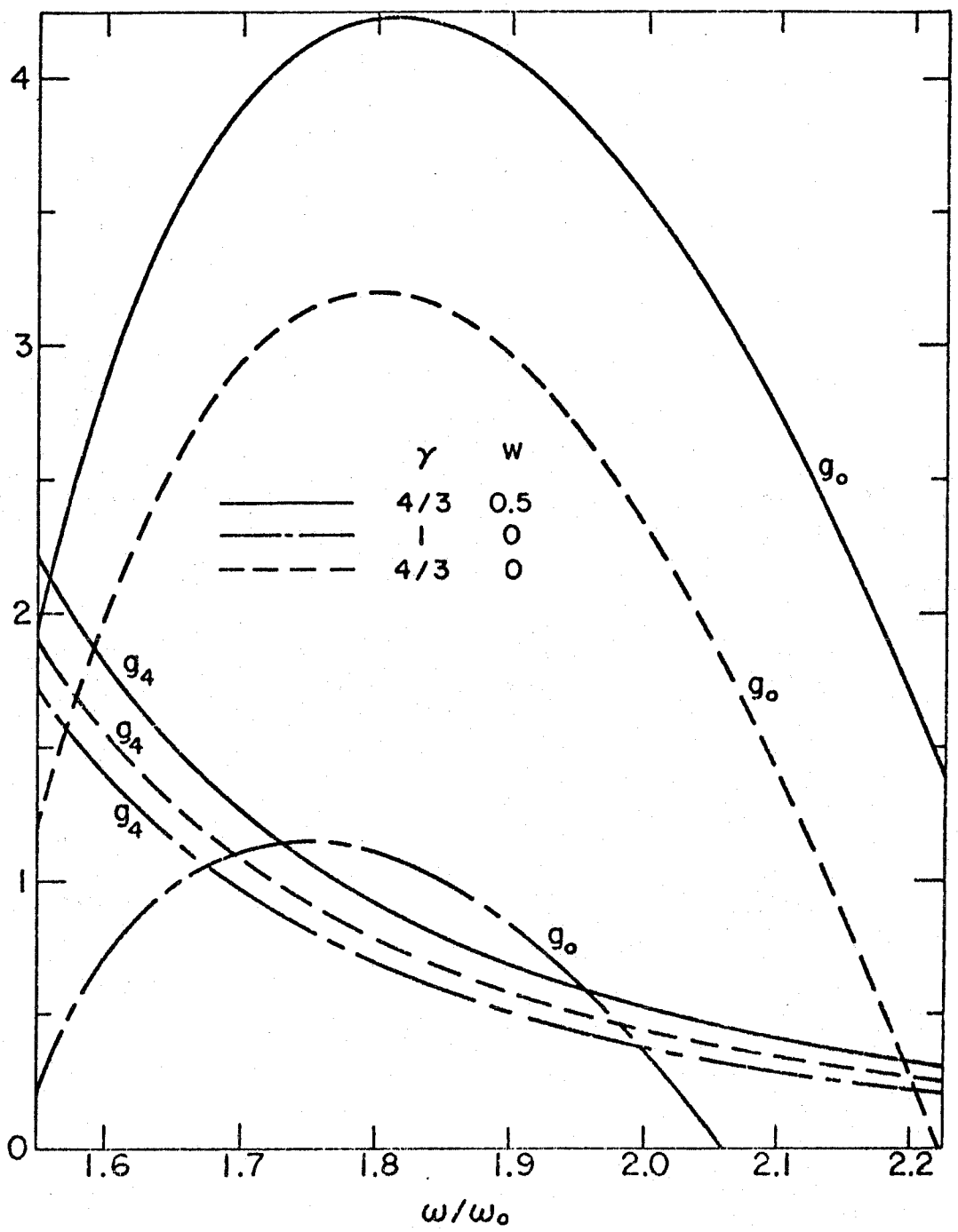


Fig. 5.1 - The functions $g_o$ and $g_4$ defined by (5.10a), (5.10e) in the first subharmonic region.

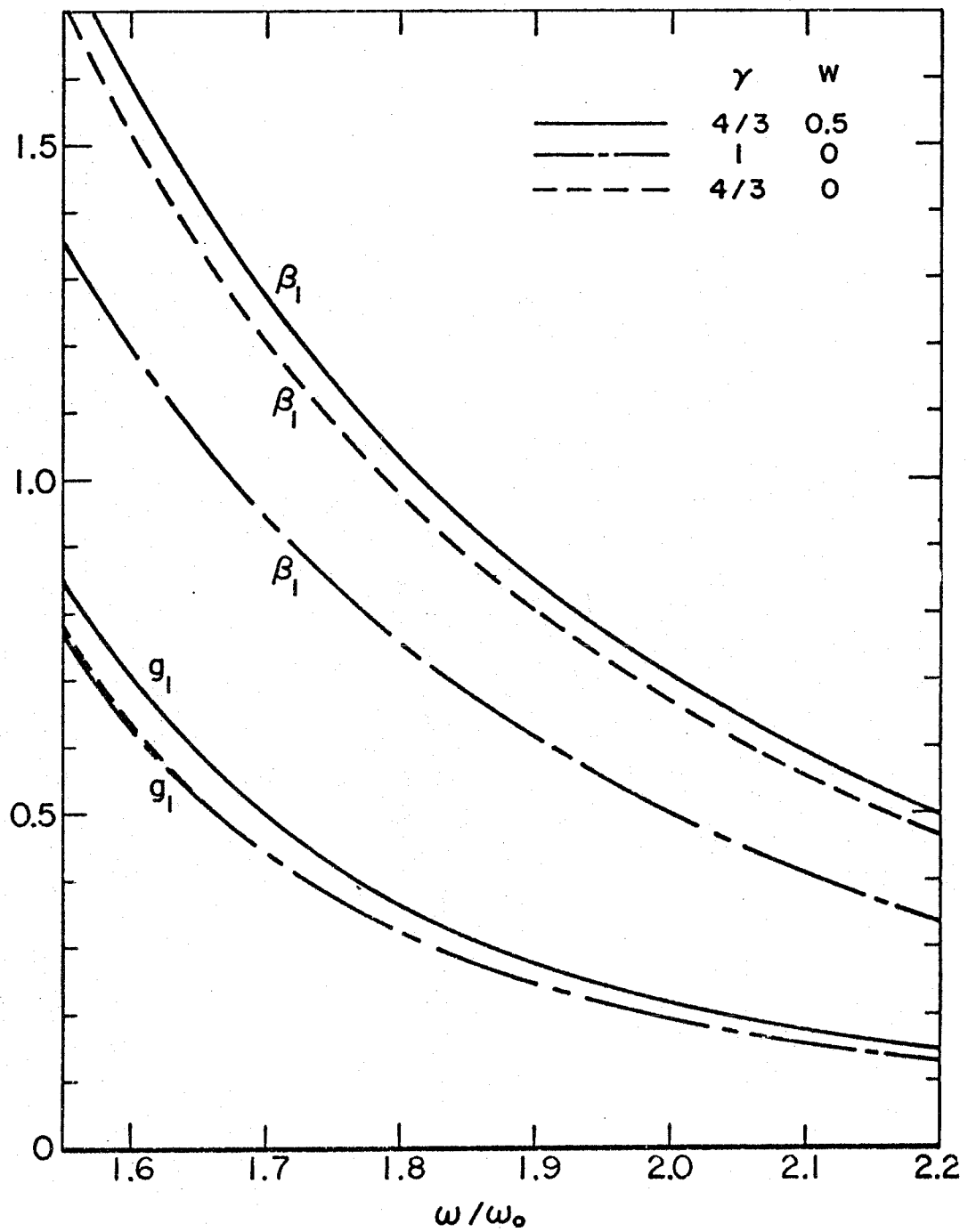


Fig. 5. 2 - The functions $\beta_1$ and $g_1$ defined by (5. 8a), (5. 10b) in the first subharmonic region.

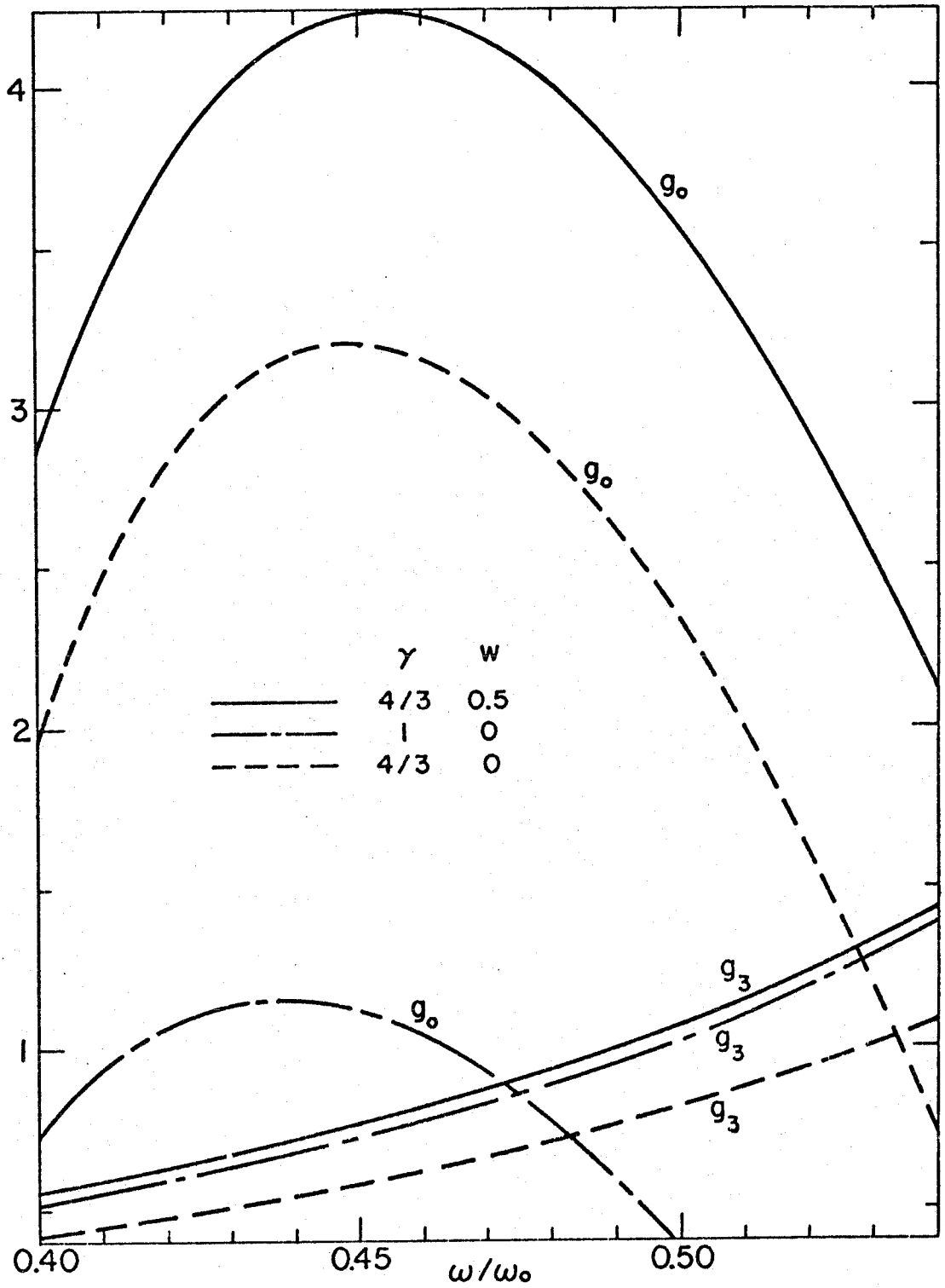


Fig. 5.3 - The functions $g_o$ and $g_3$ defined by (5.10a), (5.10d) in the first harmonic region.

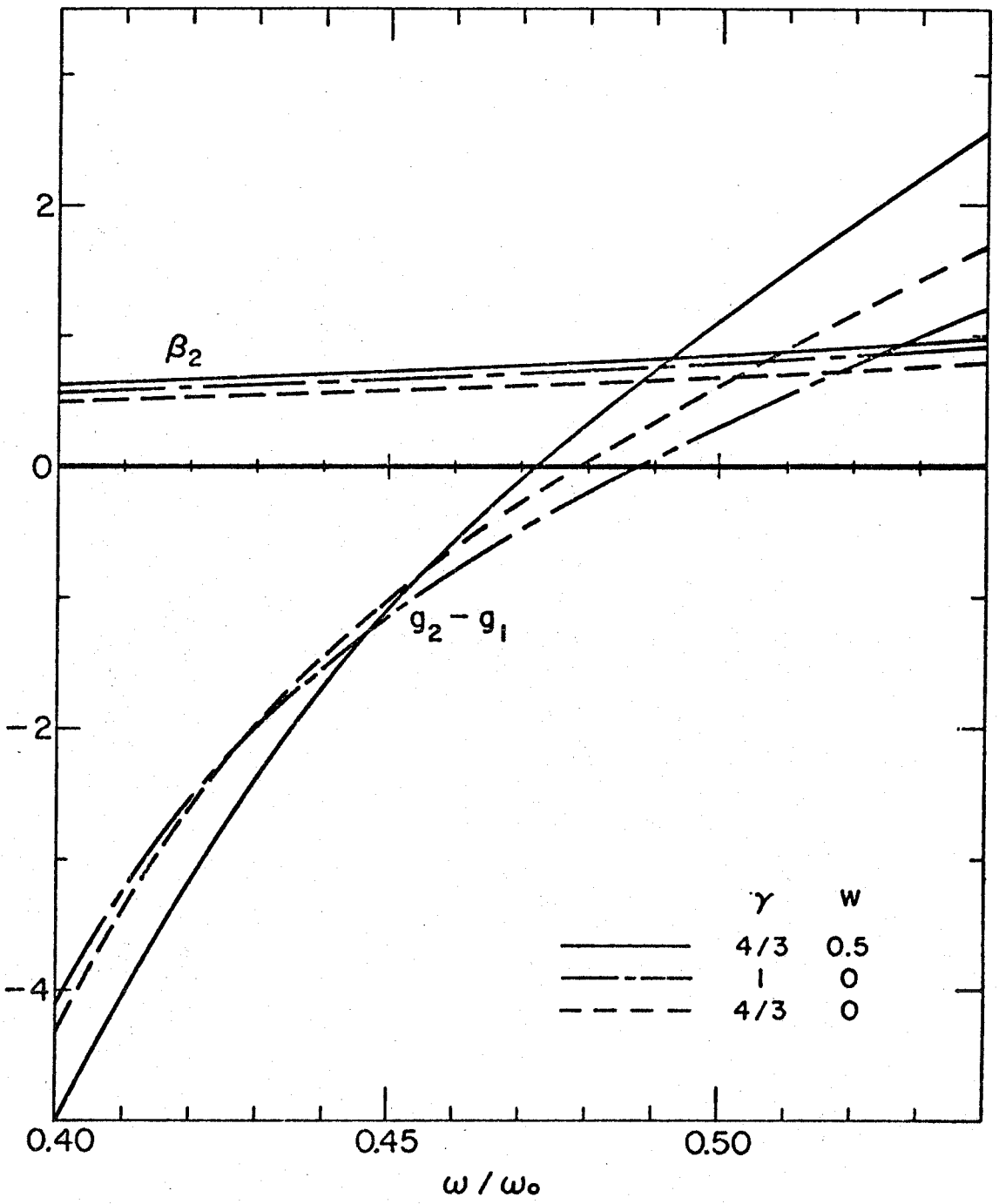


Fig. 5.4 - The functions $\beta_2$, $g_2 - g_1$ defined by (5.8b), (5.10b, c) in the first harmonic region.

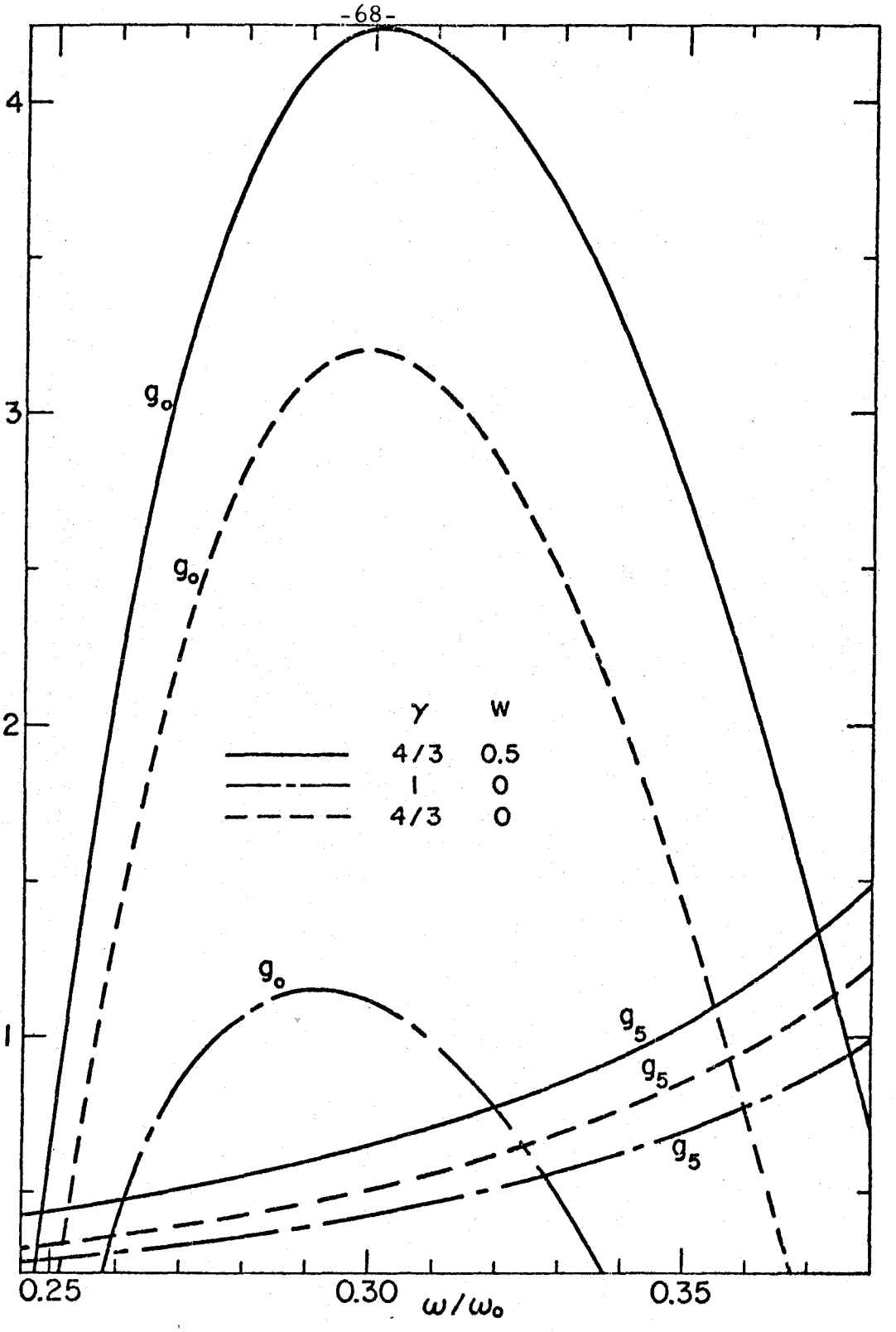


Fig. 5.5 - The function $g_o$ and $g_5$ defined by (5.10a), (5.10f) in the second harmonic region.

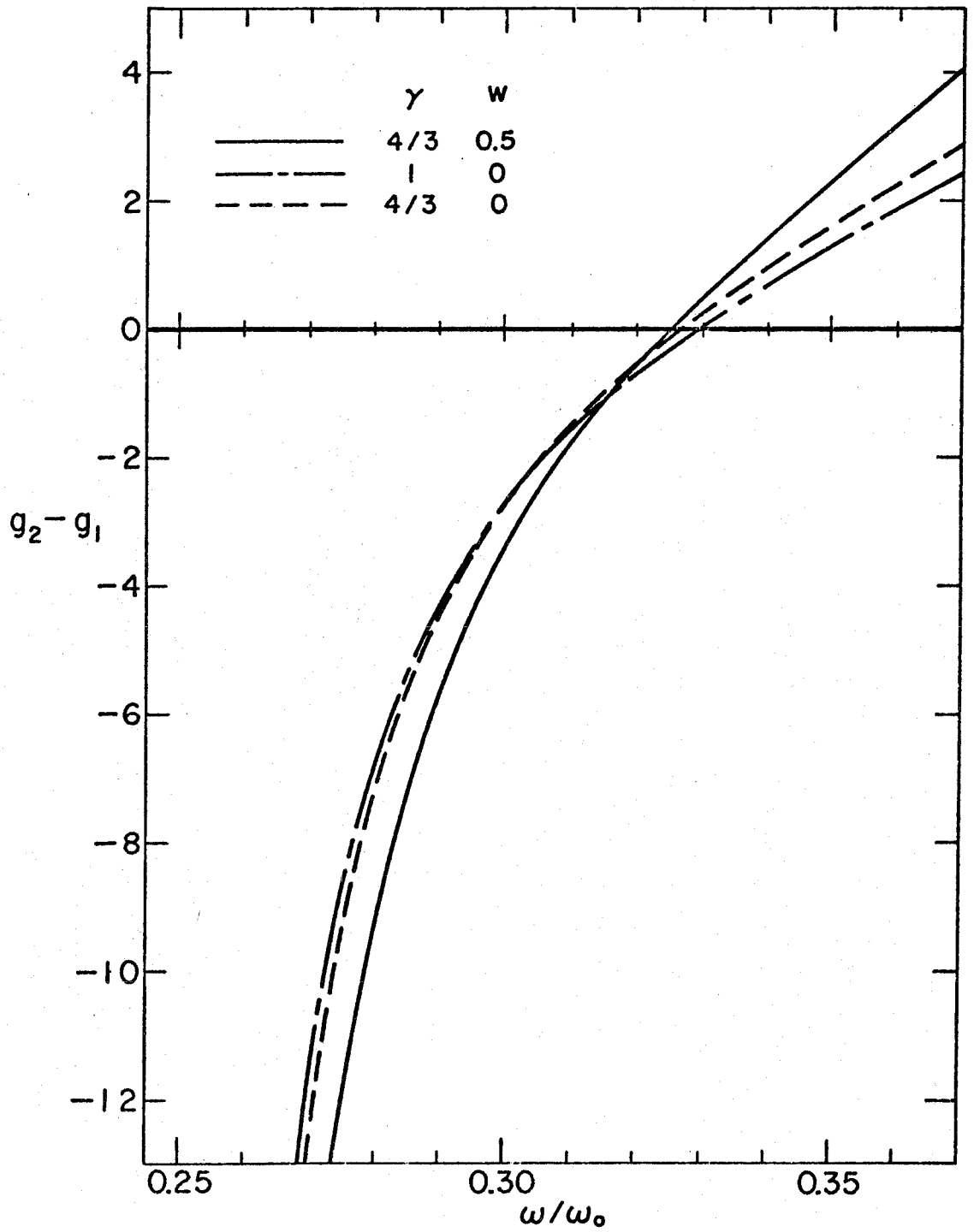


Fig. 5.6 - The function $g_2 - g_1$ defined by (5.10b, c) in the second harmonic region.

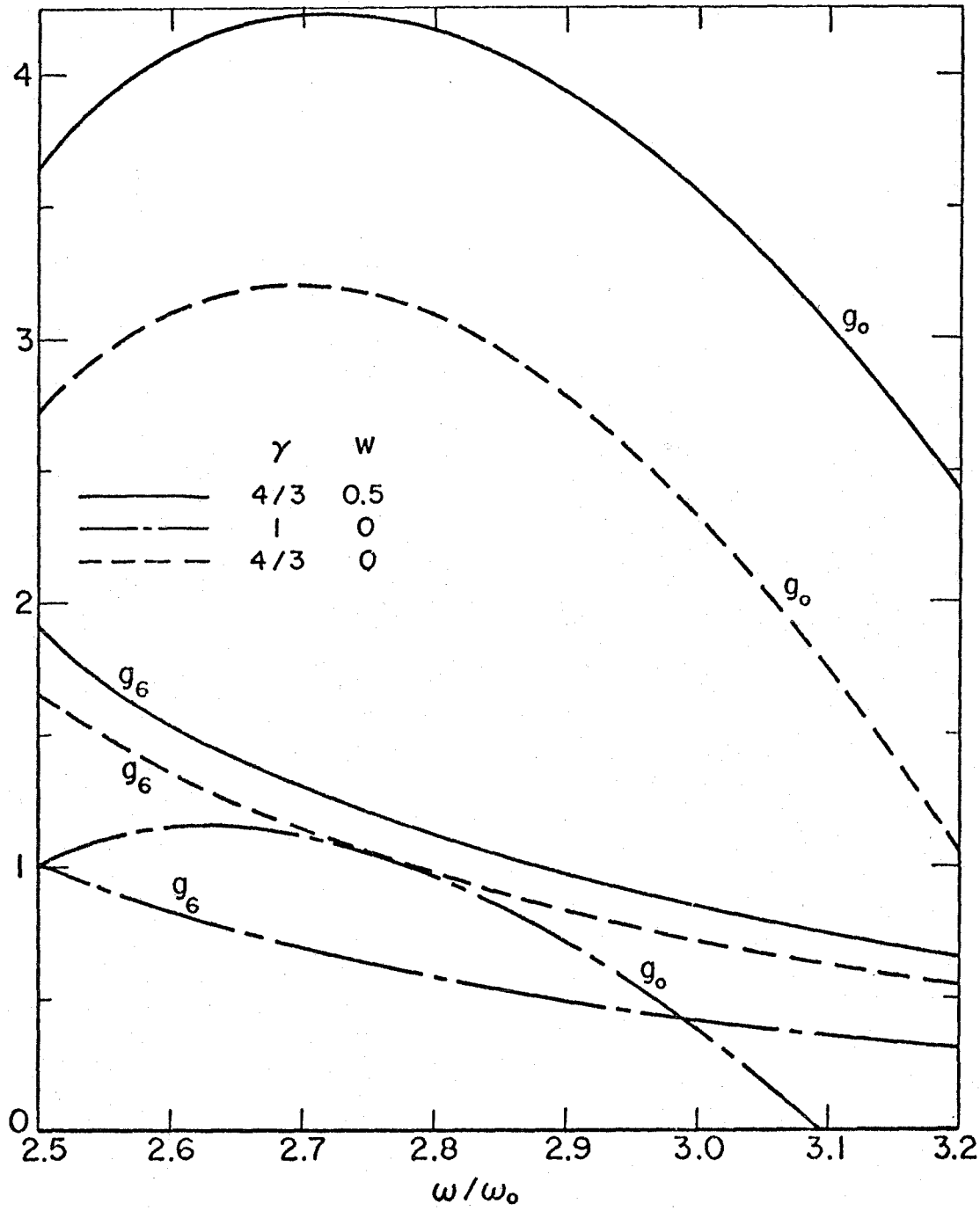


Fig. 5.7 - The functions $g_o$ and $g_6$ defined by (5.10a), (5.10g) in the second subharmonic region.

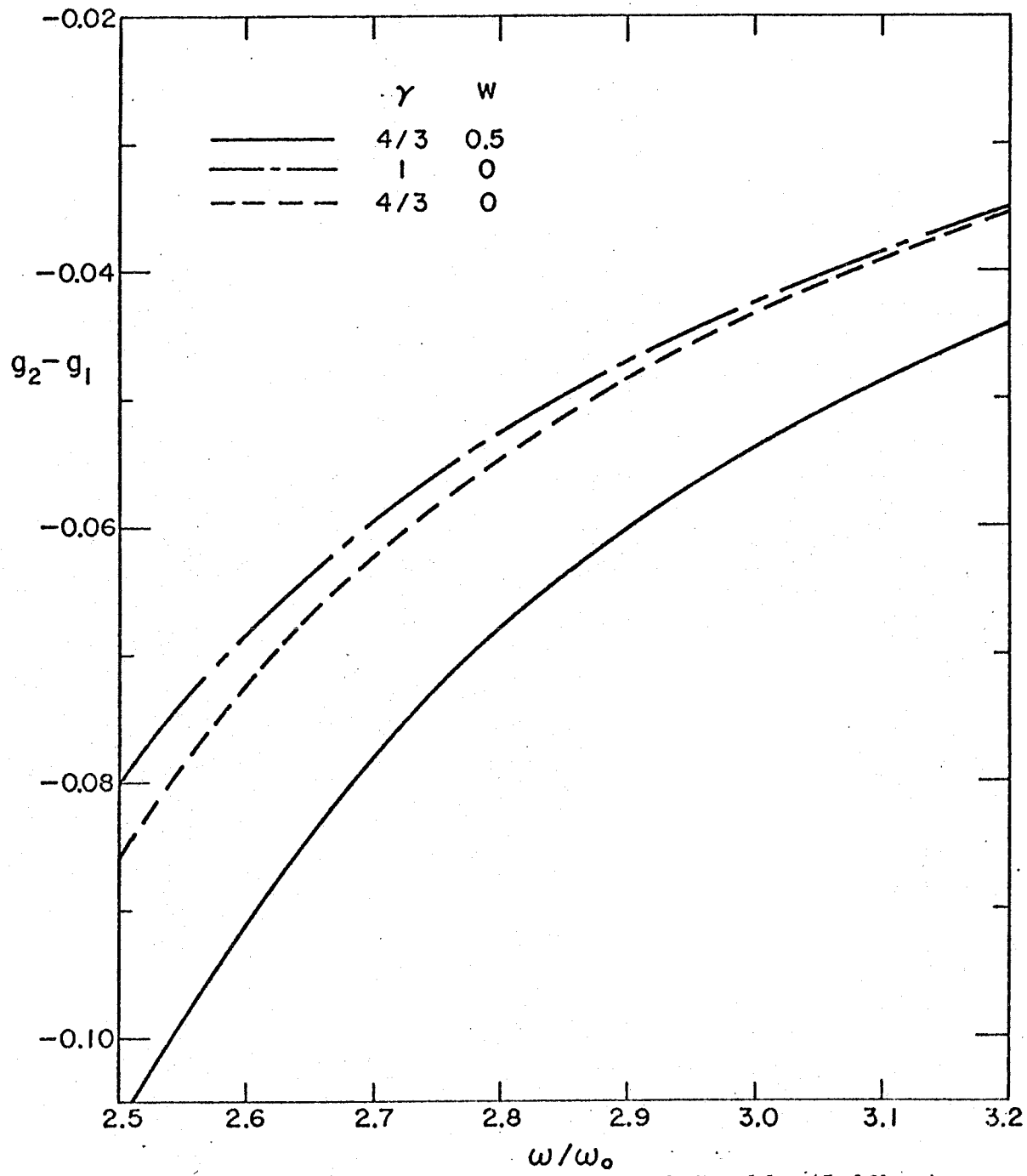


Fig. 5.8 - The function $g_2 - g_1$ defined by (5.10b, c) in the second subharmonic region.

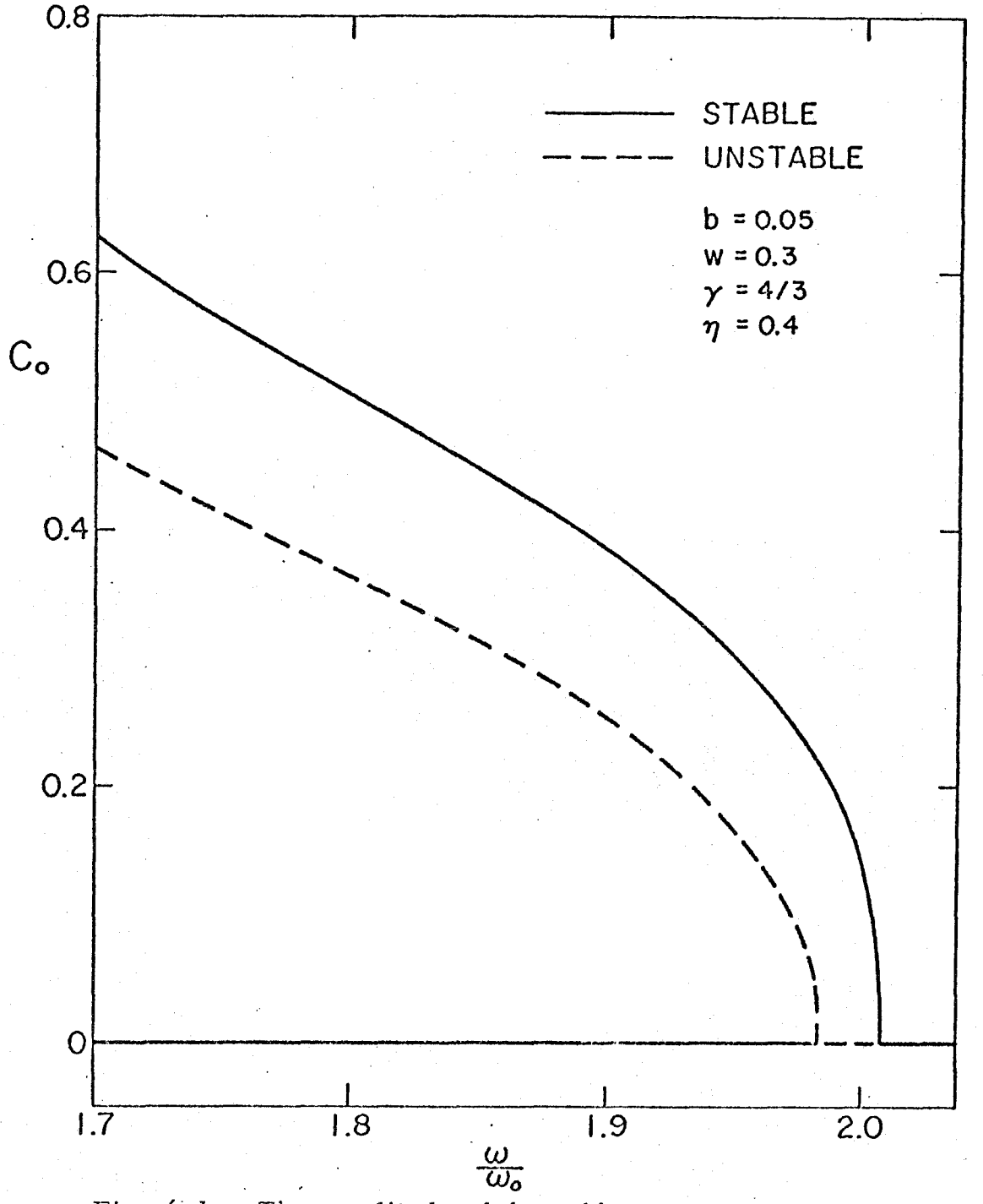


Fig. 6.1 - The amplitude of the subharmonic component determined by Eq. (6.1.3) as a function of $\omega/\omega_o$, for $\eta = 0.4$. In the interval of instability of the purely harmonic solution ($C_o = 0$) a subharmonic component sets in for any initial conditions.

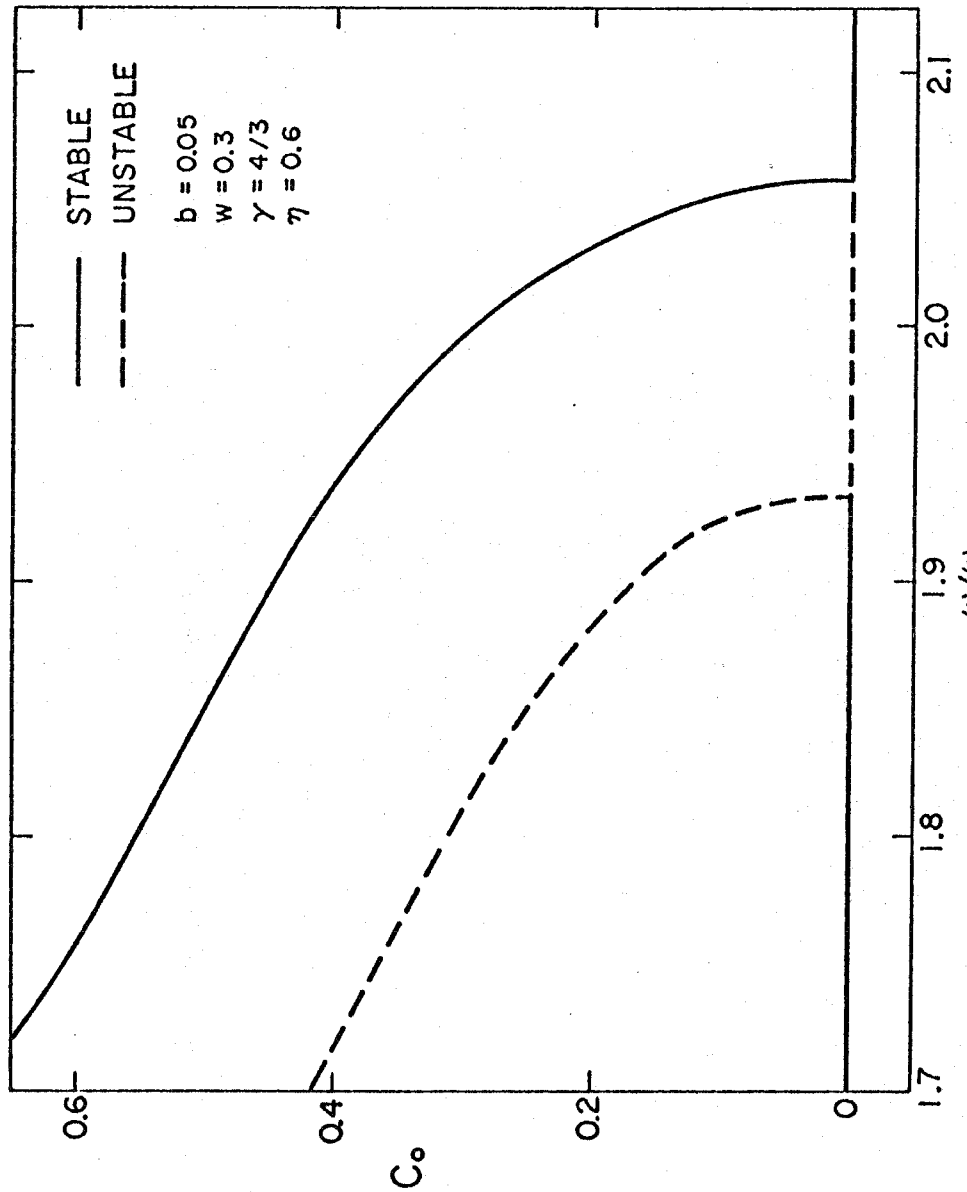


Fig. 6.2 - The amplitude of the subharmonic component determined by Eq. (6.1.3) as a function of $\omega/\omega_o$, for $\eta = 0.6$. In the interval of instability of the purely harmonic solution ($C_o = 0$) a subharmonic component sets in for any initial conditions.

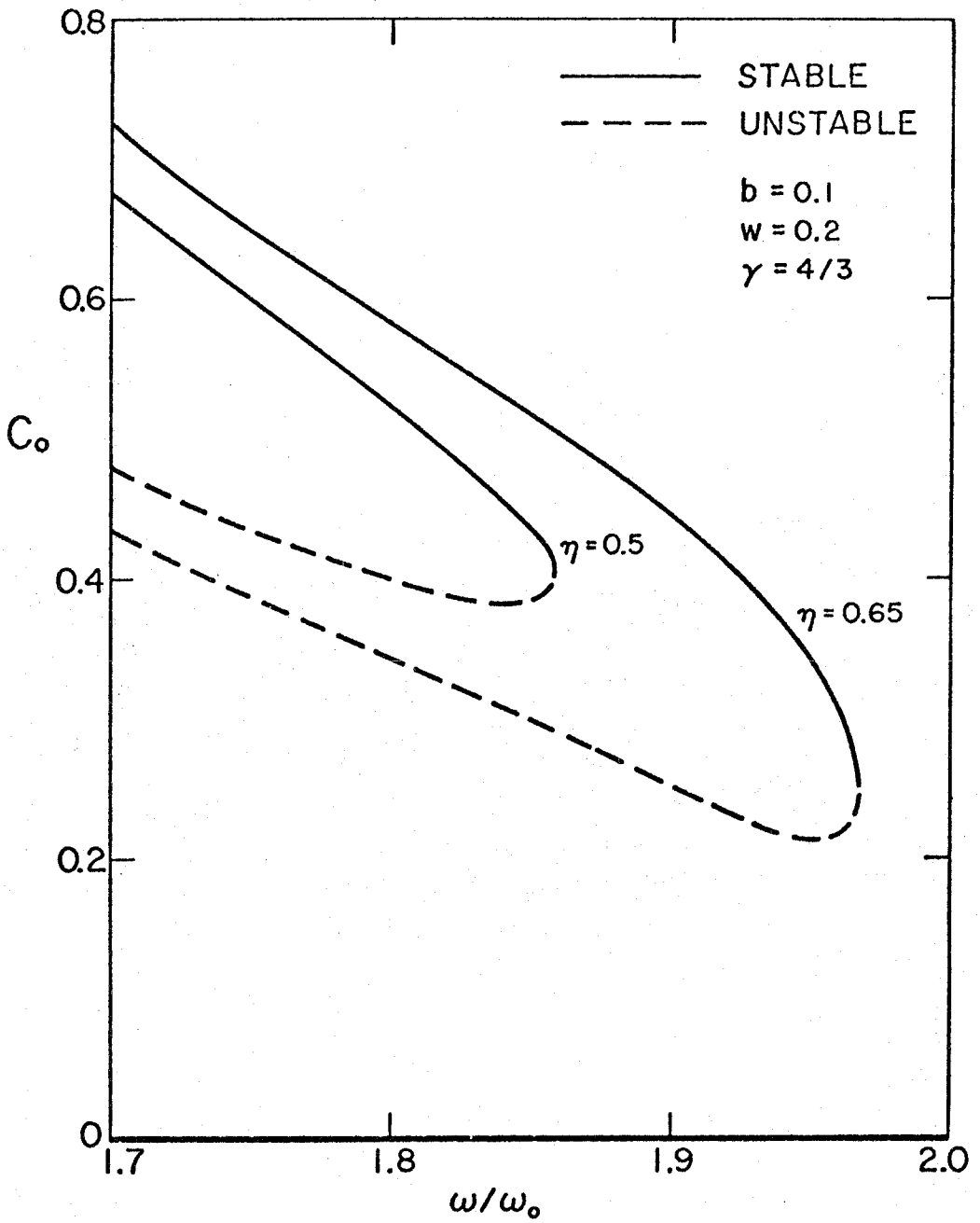


Fig. 6.3 - The amplitude of the subharmonic component determined by (6.1.3) as a function of $\omega/\omega_o$. In these instances the purely harmonic solution ($C_o = 0$) is always stable, and a subharmonic mode can set in only if appropriate initial conditions are chosen.

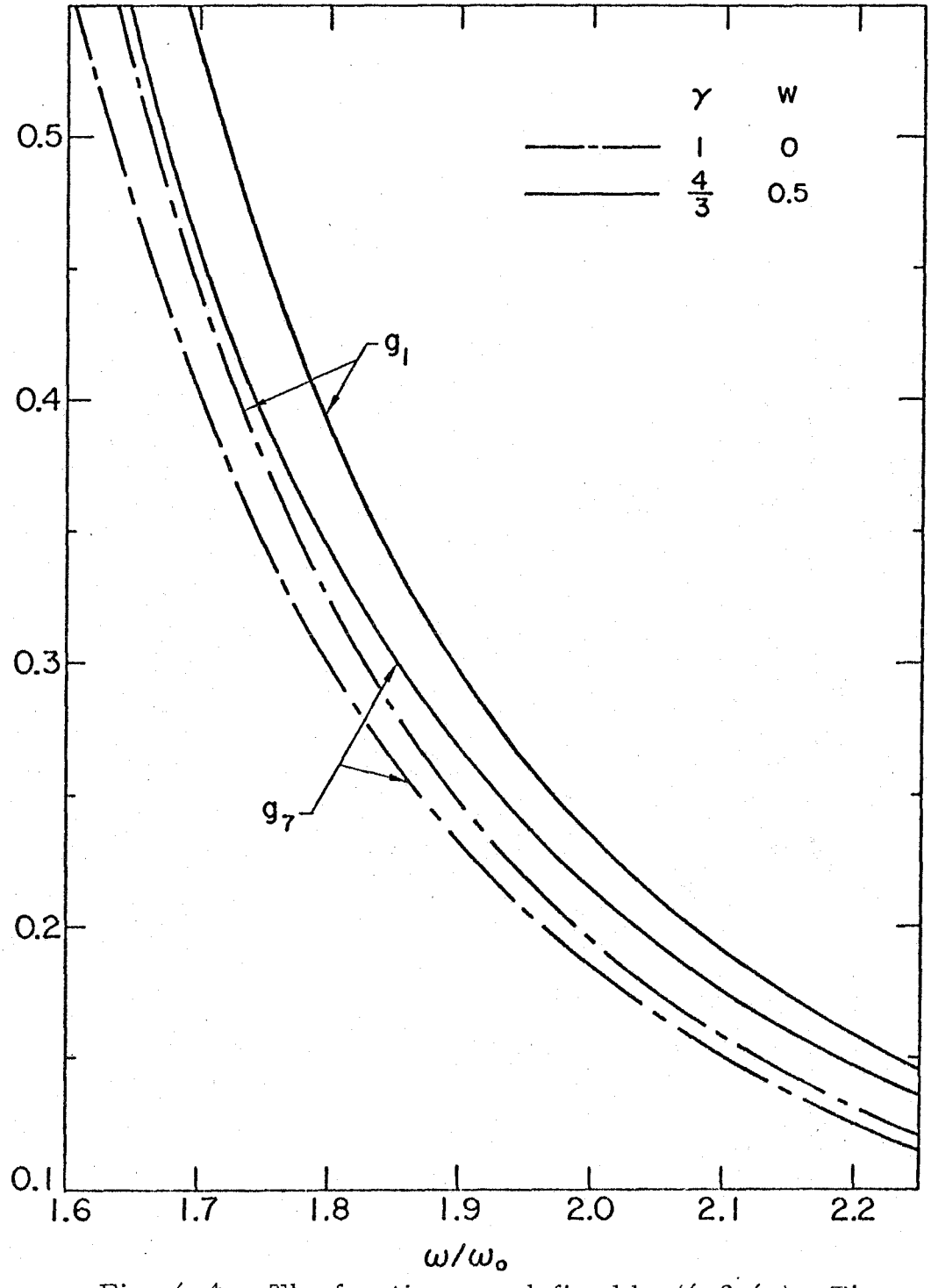


Fig. 6.4 - The function $g_7$ defined by (6.2.6a). The function $g_1$ given by (5.10.b) is shown for comparison.

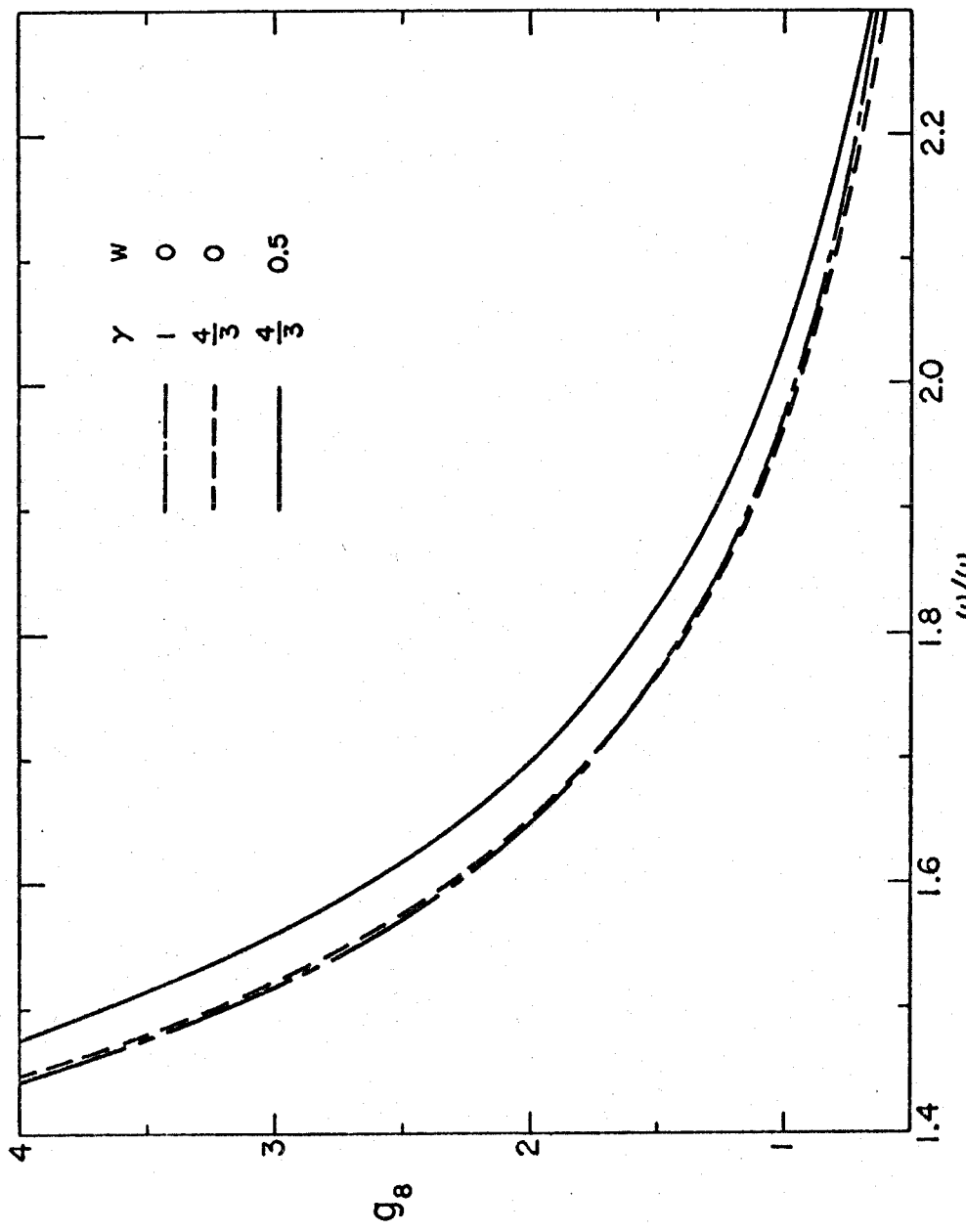


Fig. 6.5 - The function $g_8$ defined by Eq. (6.2.6b).

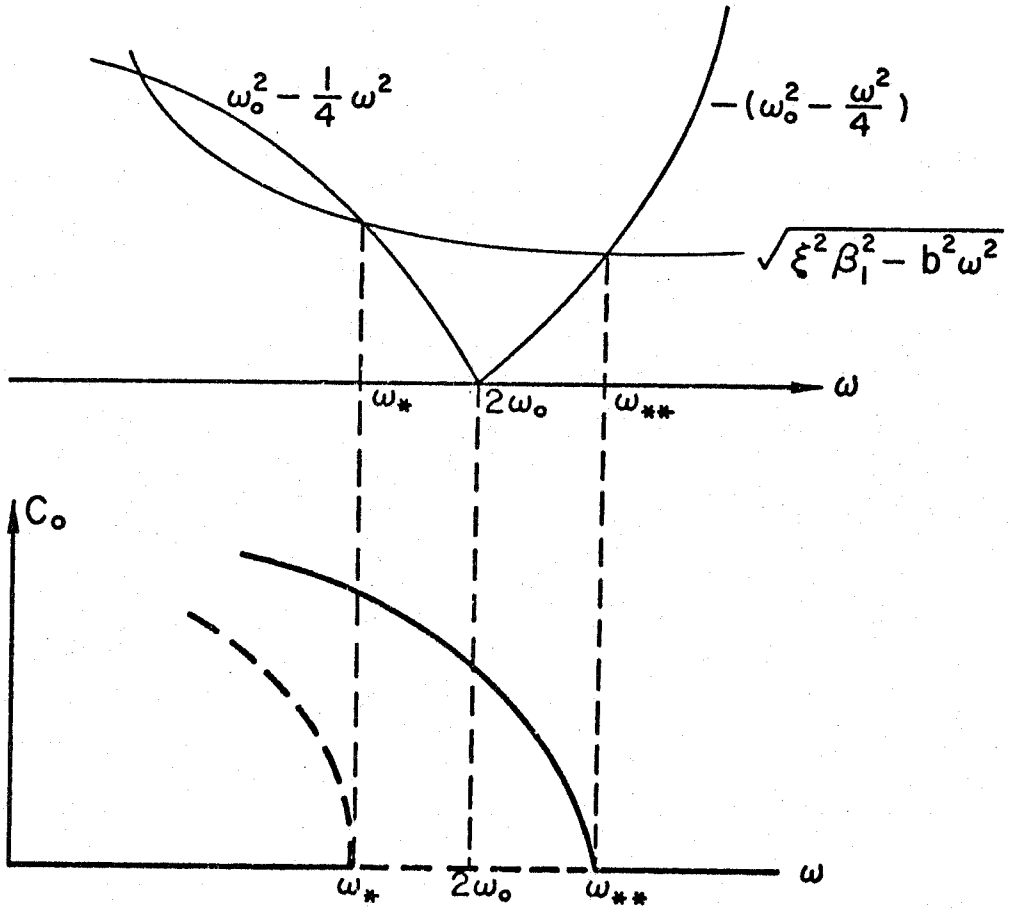


Fig. 6.6 - Illustration of the conditions of stability of the purely harmonic solution, for which $C_o = 0$.

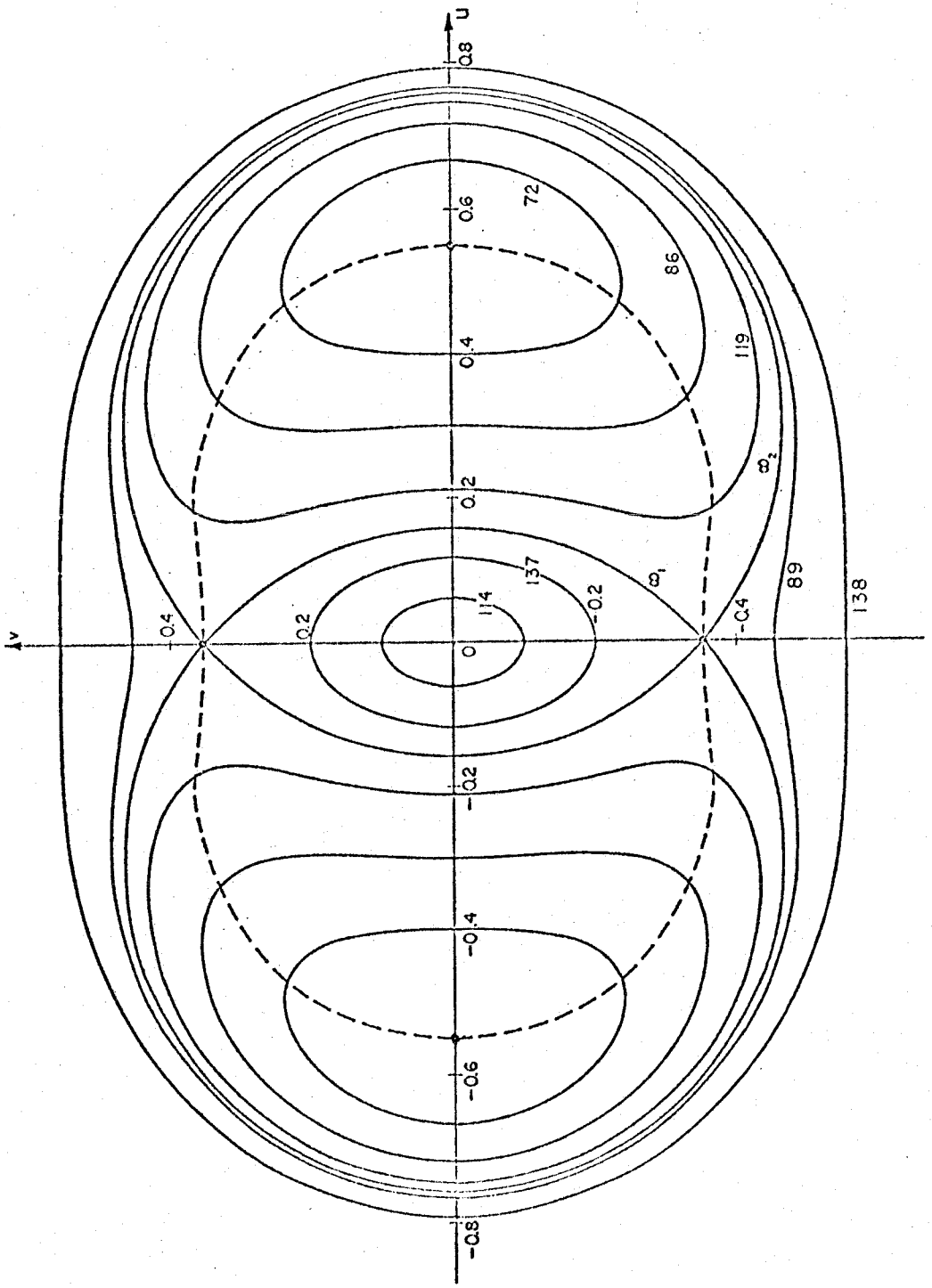


Fig. 6.7 - Solution curves of system (6.2) in the undamped case. Here $u = C \cos \varphi$, $v = C \sin \varphi$. C and $\varphi$ (the subharmonic amplitude and phase) are periodic functions of time. The numbers labeling the different curves denote the period in units of $\omega\tau$. The large dots indicate the position of the critical points given by (6.3.3). The dashed curve is the locus H = 0.

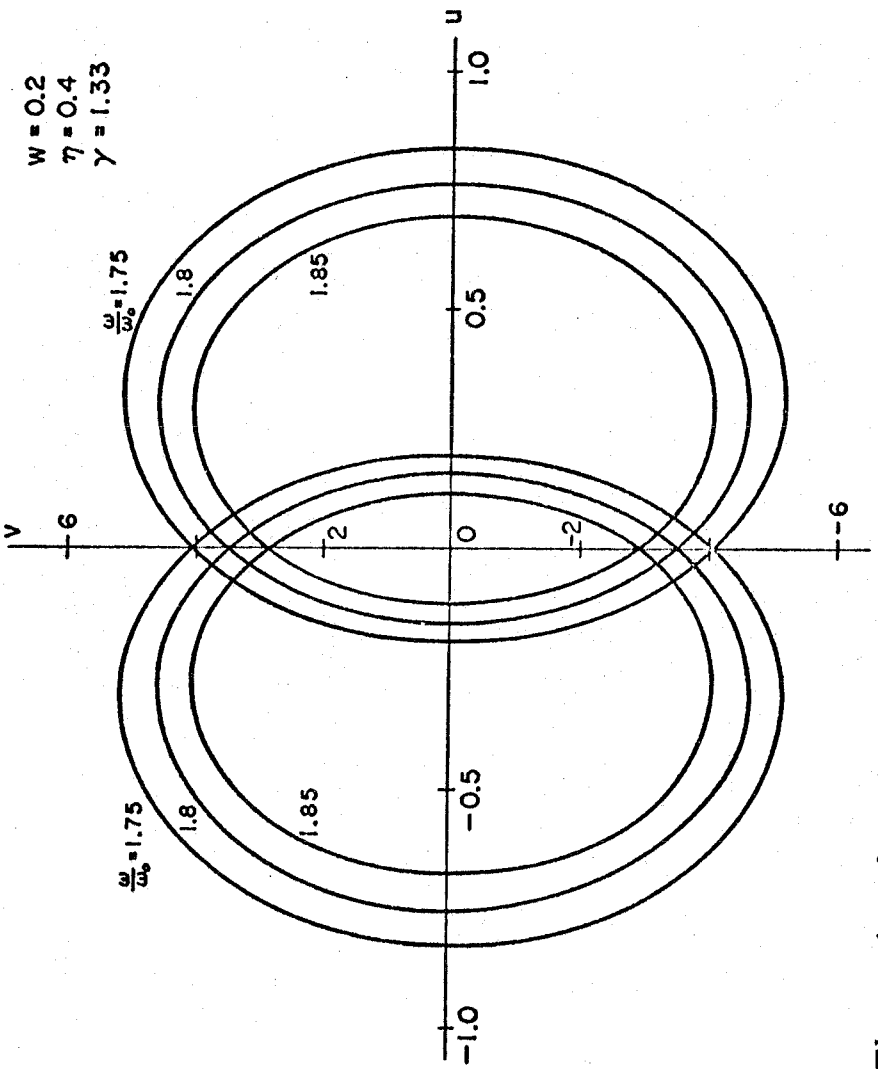


Fig. 6.8 - The regions bounded by the separatrices for fixed $\eta$ and different values of $\omega/\omega_o$ in the undamped case. As the forcing frequency gets closer to $2\omega_o$, the domain of influence of the purely harmonic solution (central region) gets smaller. Here $u = C\cos\varphi$, $v = C\sin\varphi$, with C and $\varphi$ the subharmonic amplitude and phase.

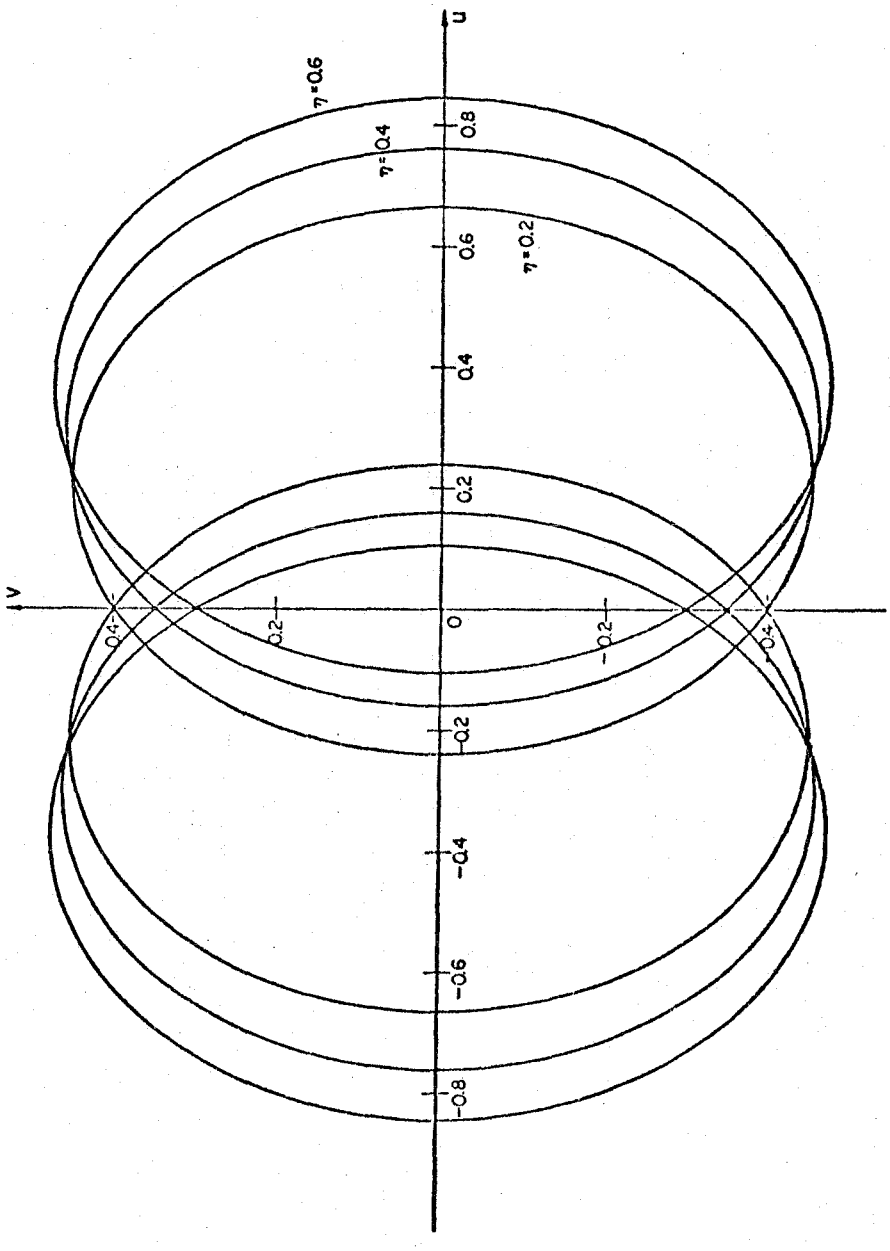


Fig. 6.9 - The regions bounded by the separatrices for fixed $\omega/\omega_o = 1.8$ and different values of $\eta$; $u = C\cos\varphi$, $v = C\sin\varphi$, with $C$ and $\varphi$ the subharmonic amplitude and phase.

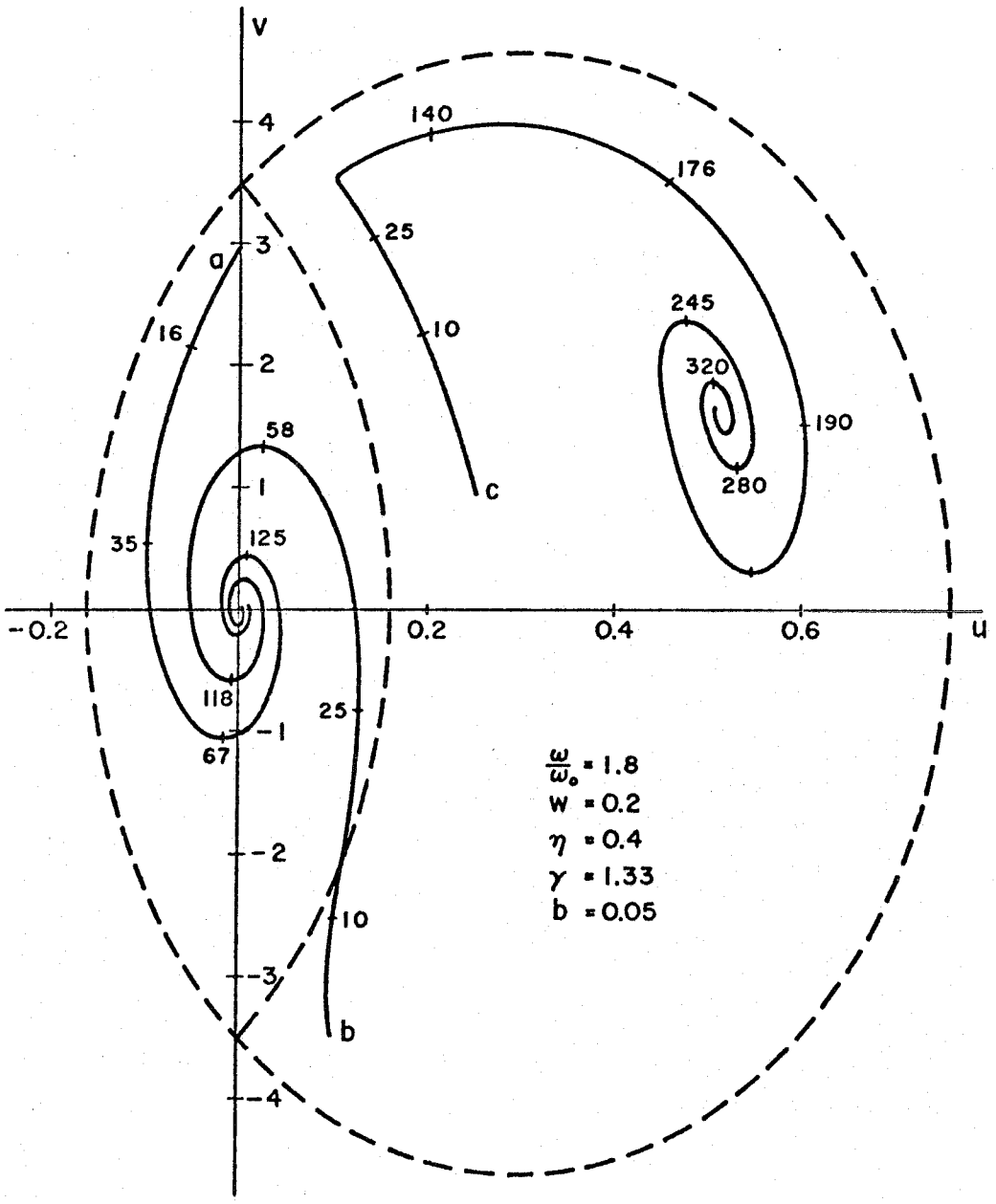


Fig. 6.10 - Solution curves of the system (6.2) in the damped case, showing the influence of the initial data on the steady-state subharmonic component. This will be absent in cases a and b, but not in case c. The dashed curves are the inner and the right half of the undamped separatrices. The numbers along the curves denote time in units of $\omega\tau$.

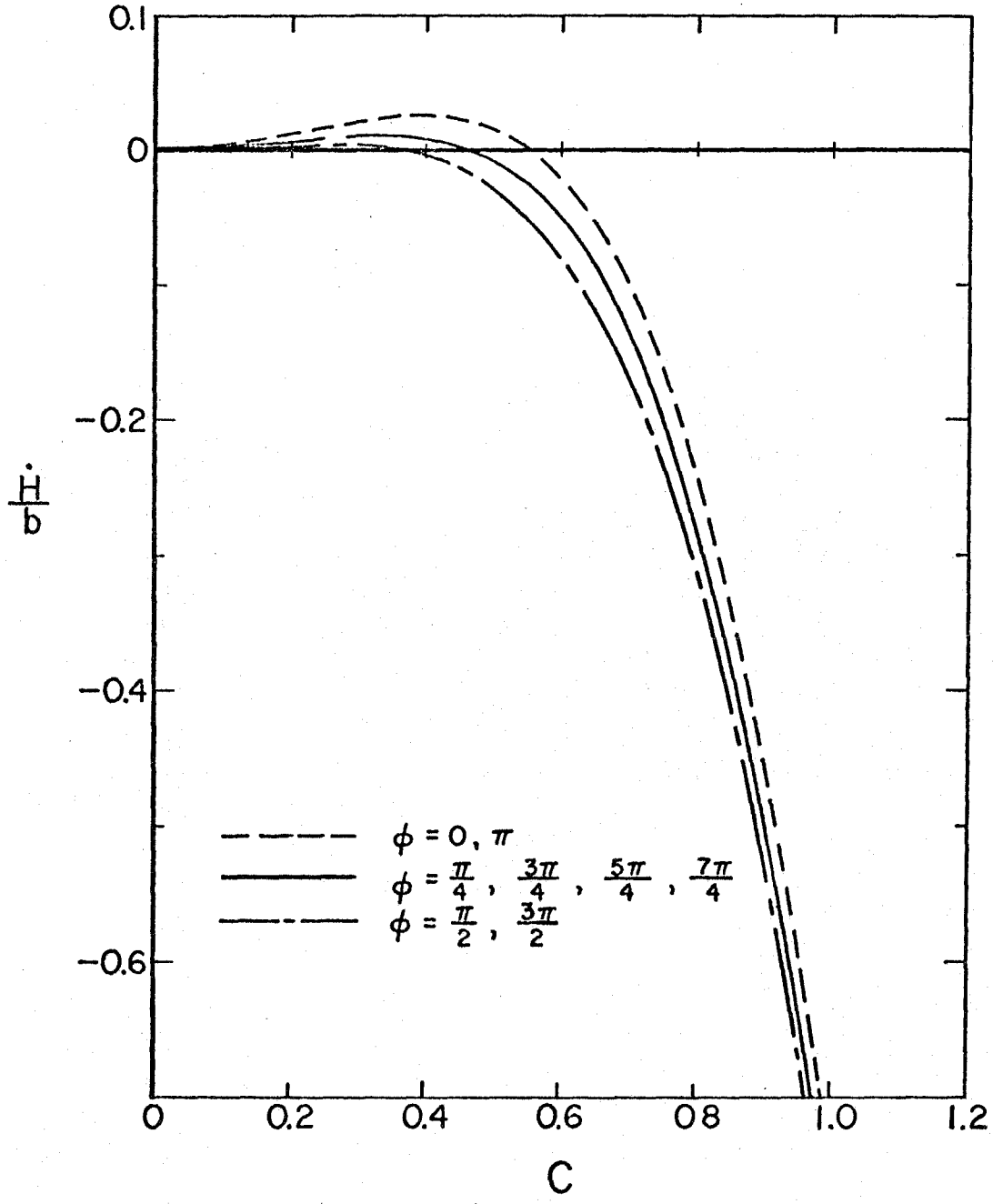


Fig. 6.11 - Graph of $(dH/d\tau)/b$ in the damped case along different "rays" $\varphi$ = const. in the phase plane. The very steep descent of the curves indicates that the "domain of influence" of the origin extends very little beyond the region bounded by the inner separatrix.

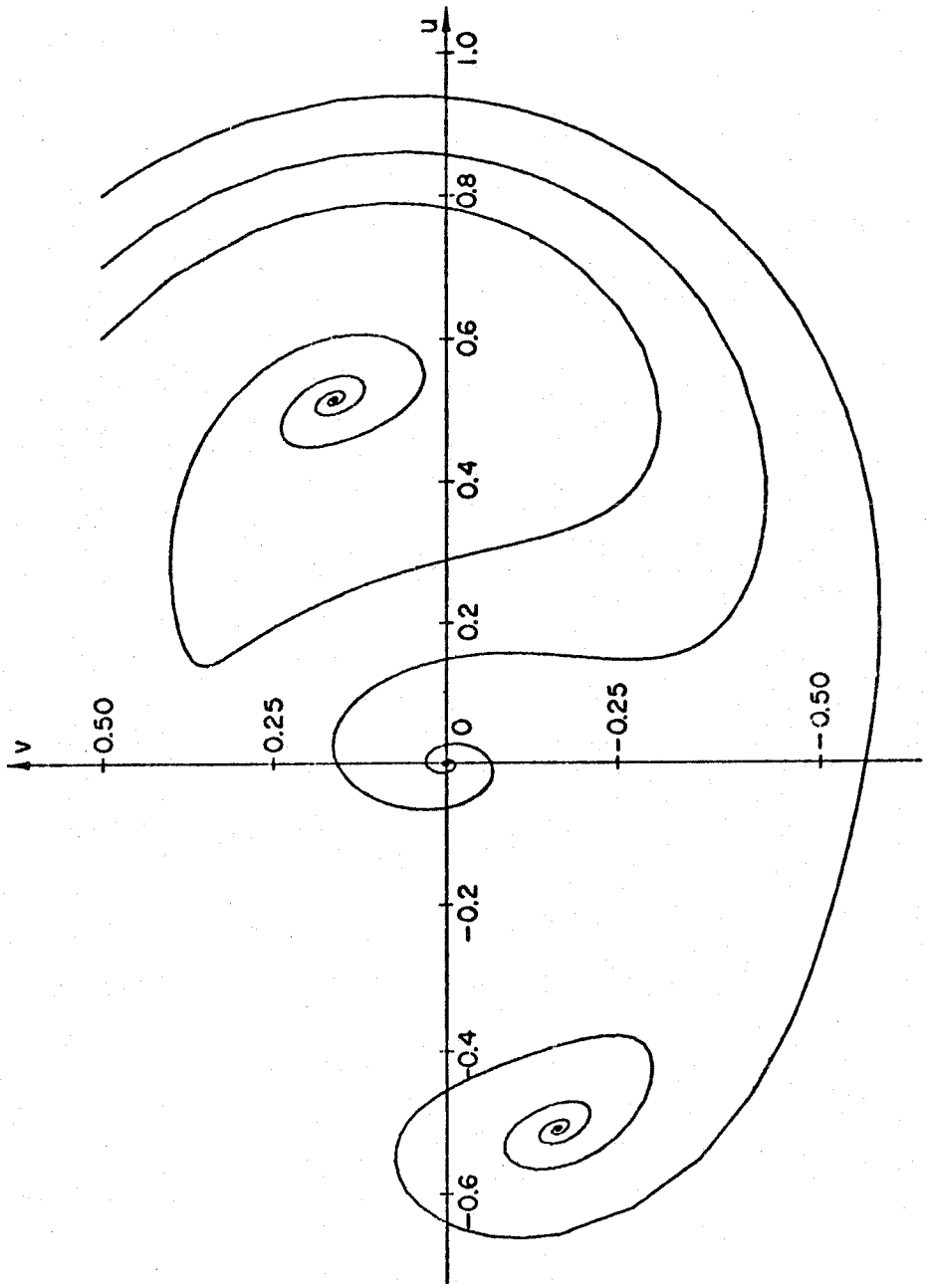


Fig. 6.12 - Solution curves of the system (6.2) in the damped case, when the initial data lies outside the region bourded by the separatrices.

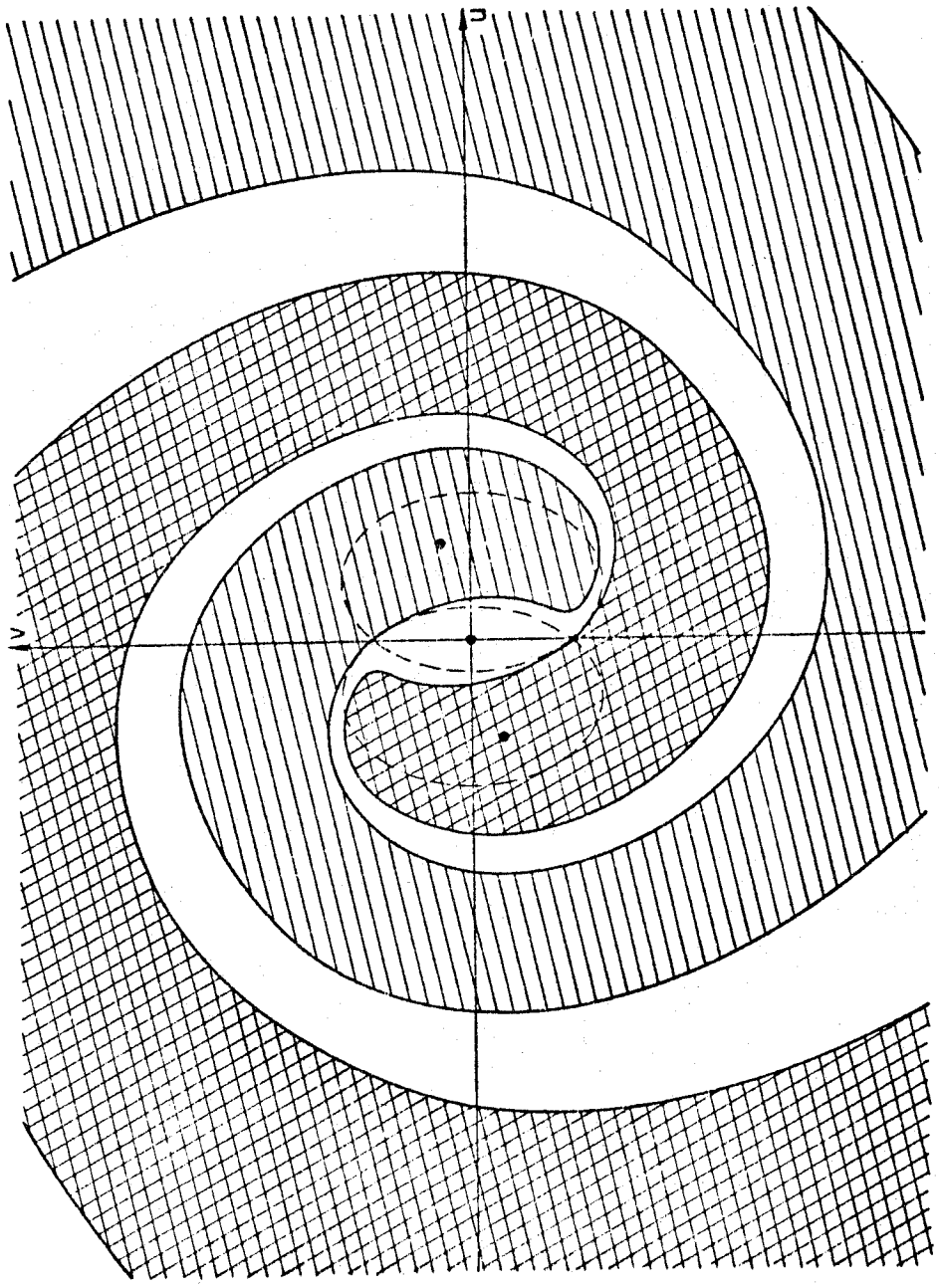


Fig. 6.13 - Qualitative sketch of the structure of the "domains of influence" of the three singular points (denoted by the heavy dots). Each domain of influence is made up of all trajectories spiraling into the same singular point as $\tau \to \infty$. The separatrices of the undamped case are indicated by dashed lines.

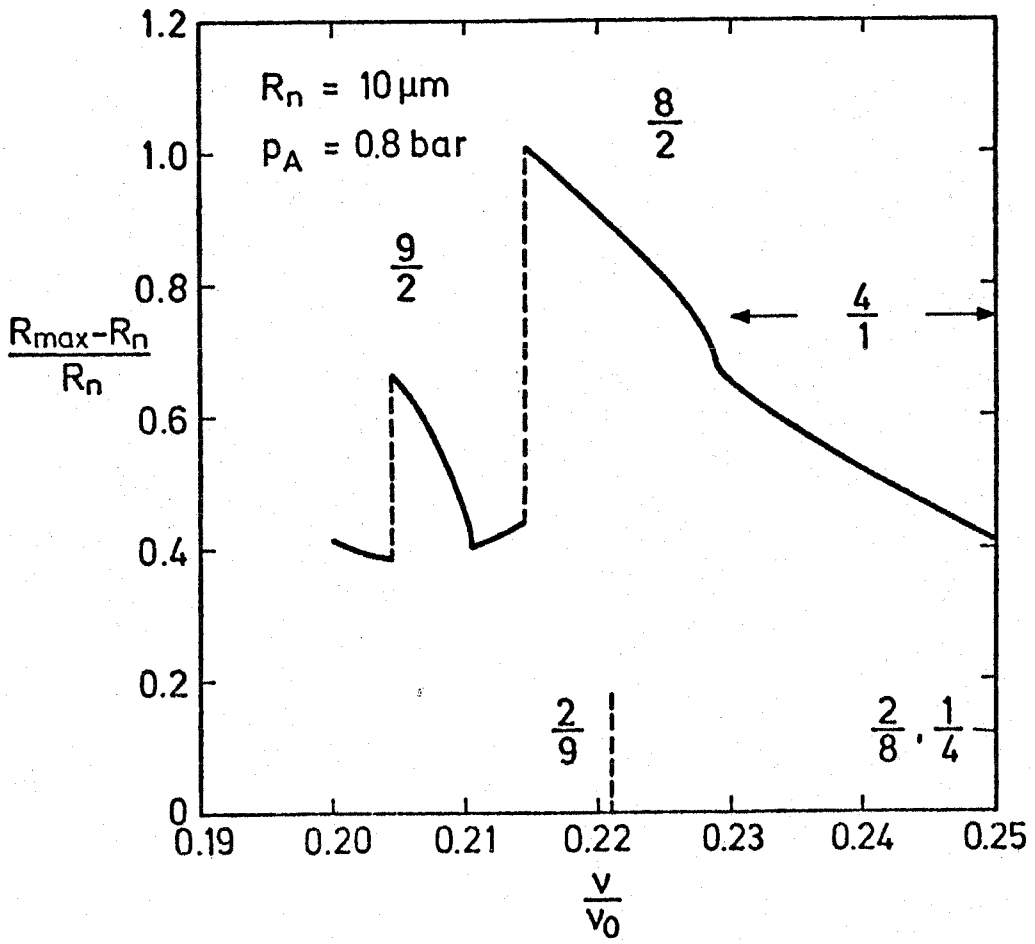


Fig. 6.14 - The numerically computed response curve in the region of the third harmonic, $\omega/\omega_o \simeq \frac{1}{4}$ (from Ref. [31]). The notation has the following relation with that employed in the present study: $R_n = R_o$, $\eta = 0.8$, $\nu/\nu_o = \omega/\omega_o$. The peak labeled as 9/2 corresponds to $\omega/\omega_o \simeq 2/9$ etc.

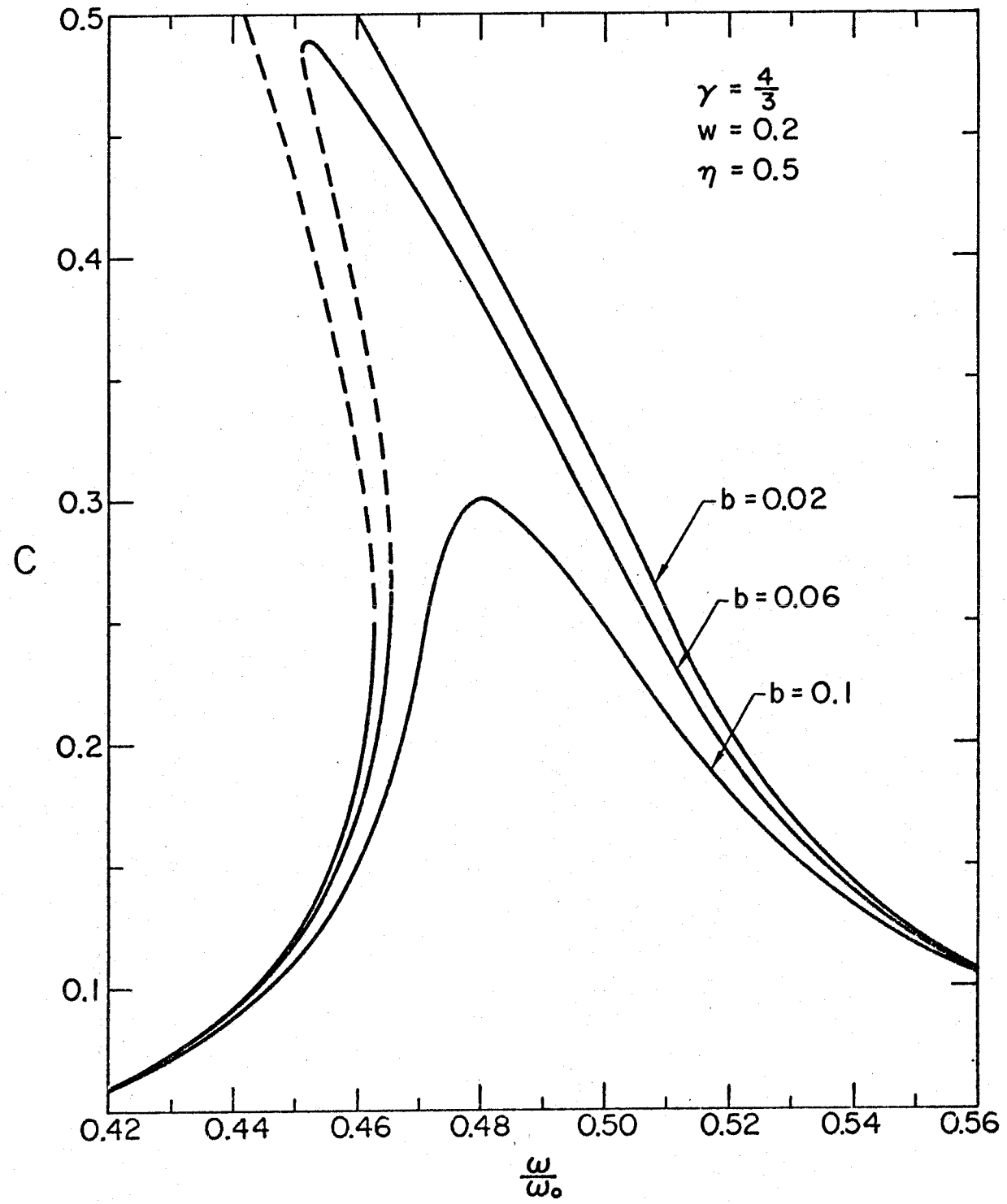


Fig. 7.1 - The amplitude of the first harmonic component for several values of the damping parameter, b. For low damping the peak is bent over to the left and exhibits an unstable section (dashed line) between the points of vertical tangency.

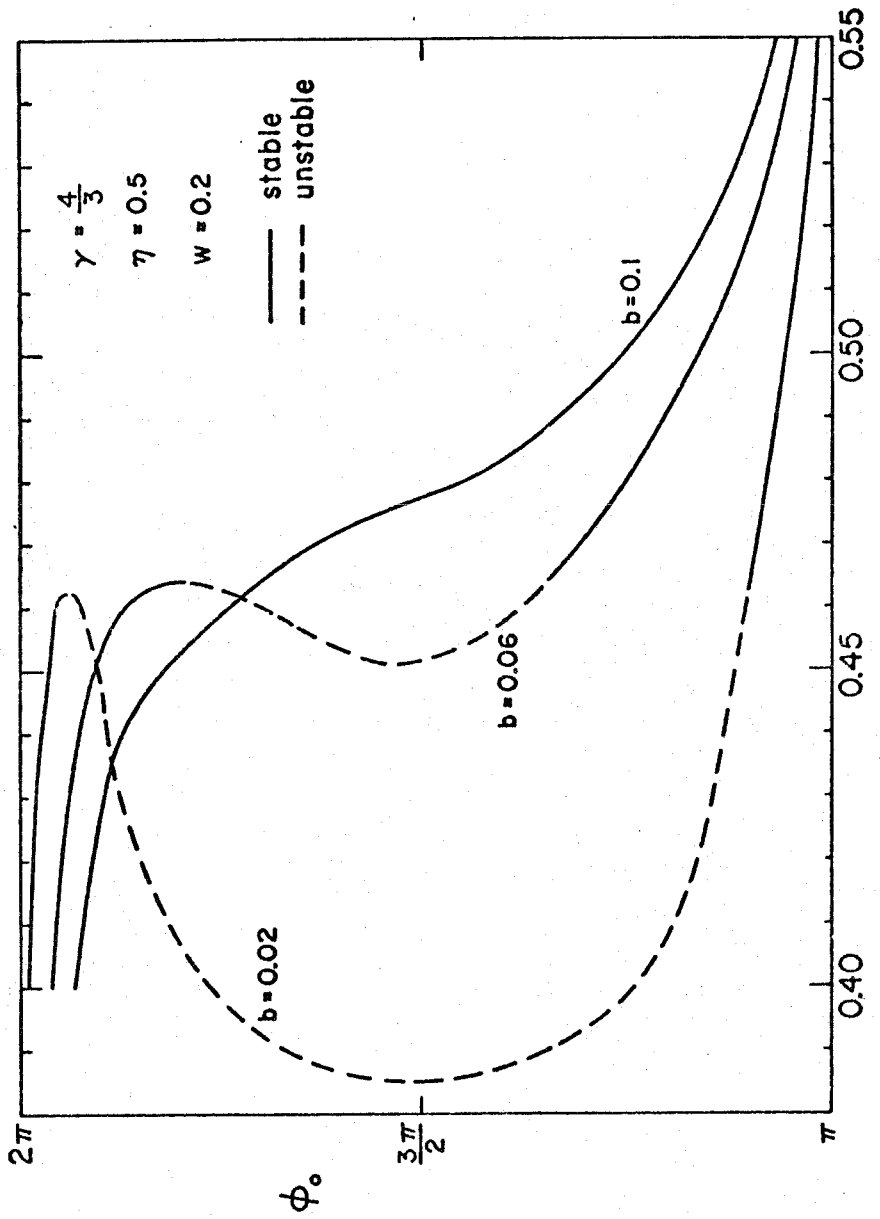


Fig. 7.2 - Phase of the first harmonic component, the amplitude of which is shown in Fig. 7.1. The dashed parts of the lines correspond to the unstable sections of the peak.

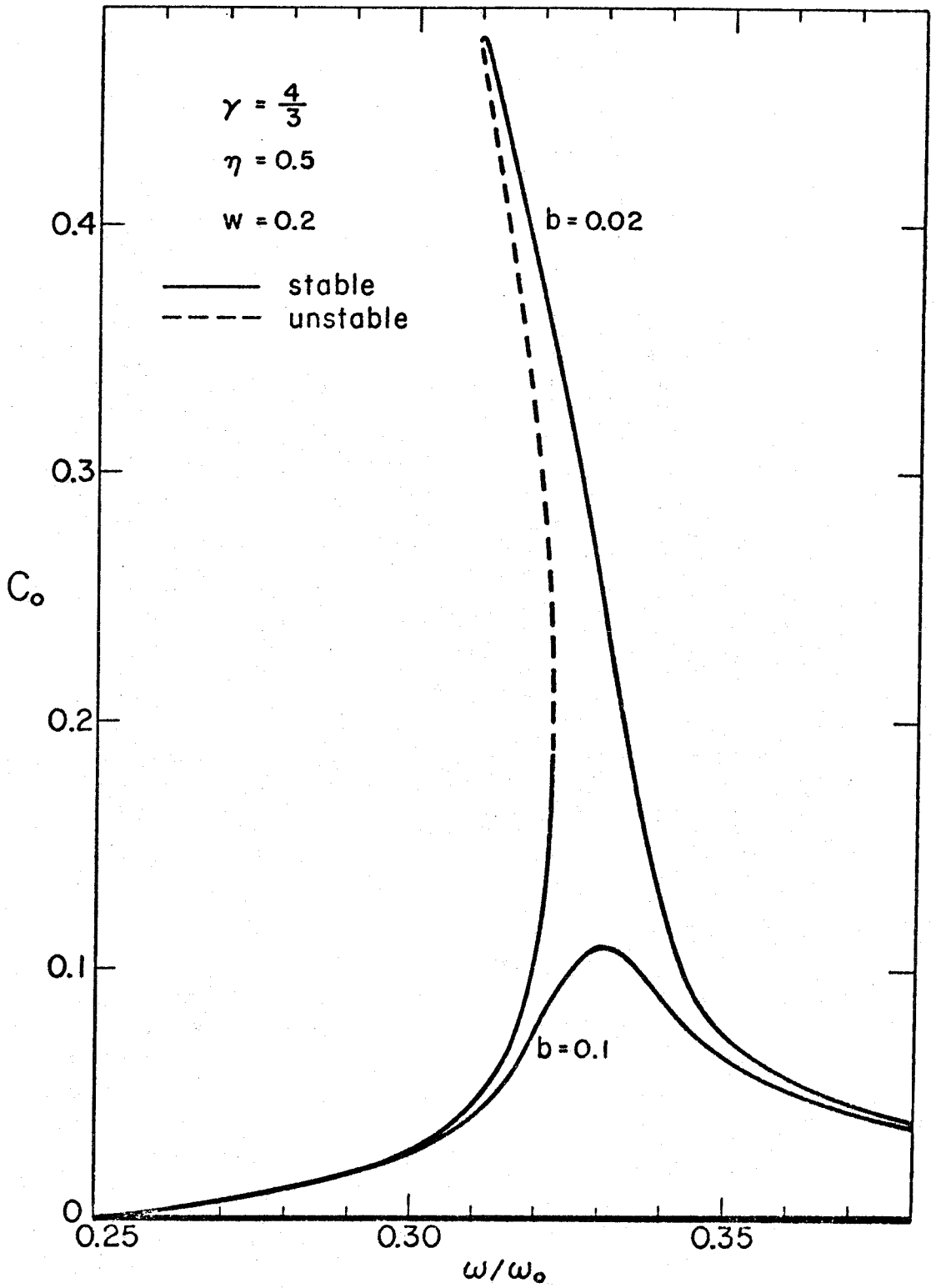


Fig. 7.3 - The amplitude of the second harmonic component for two values of the damping parameter.

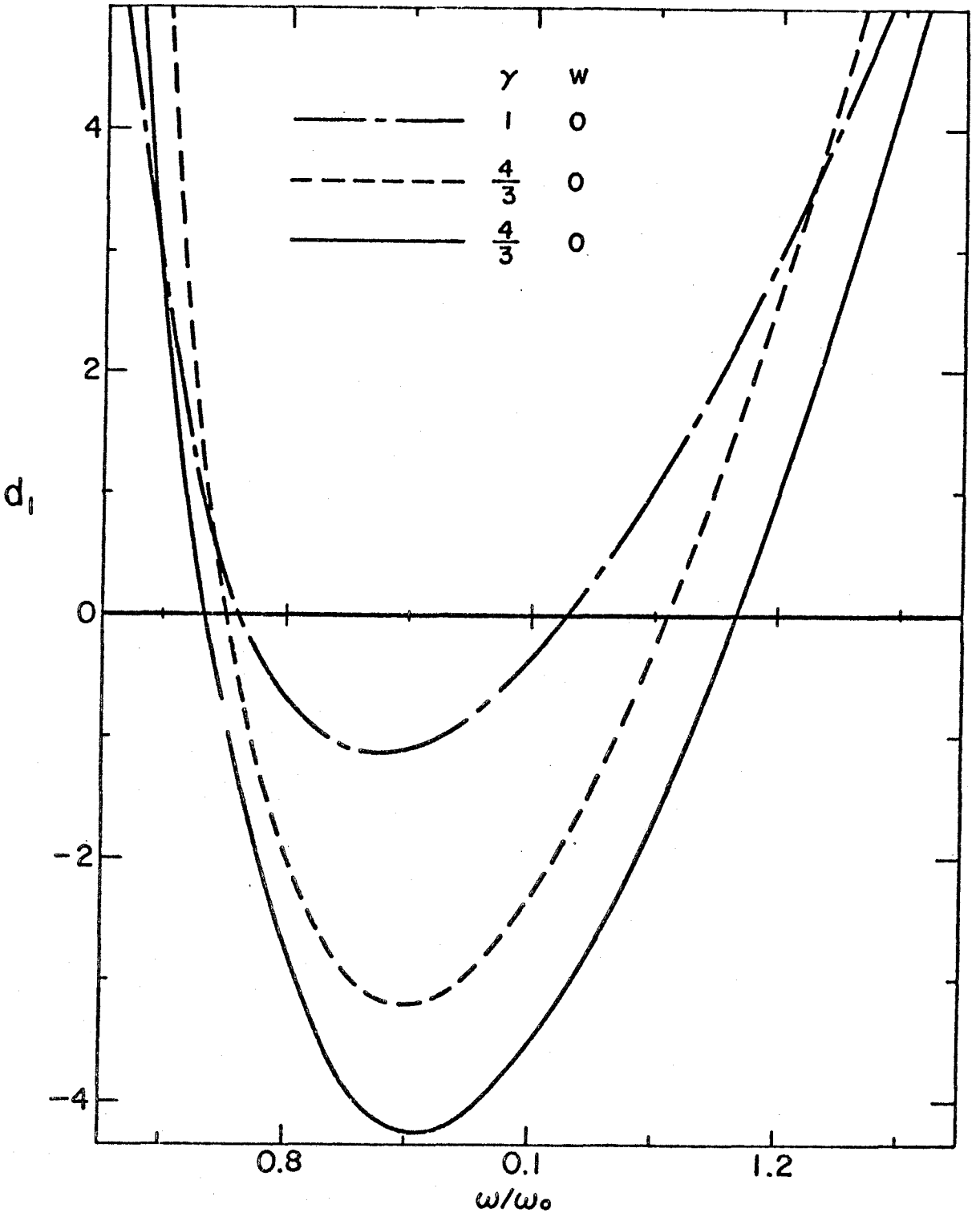


Fig. 8.1 - The function $d_1$ defined by (8.6a).

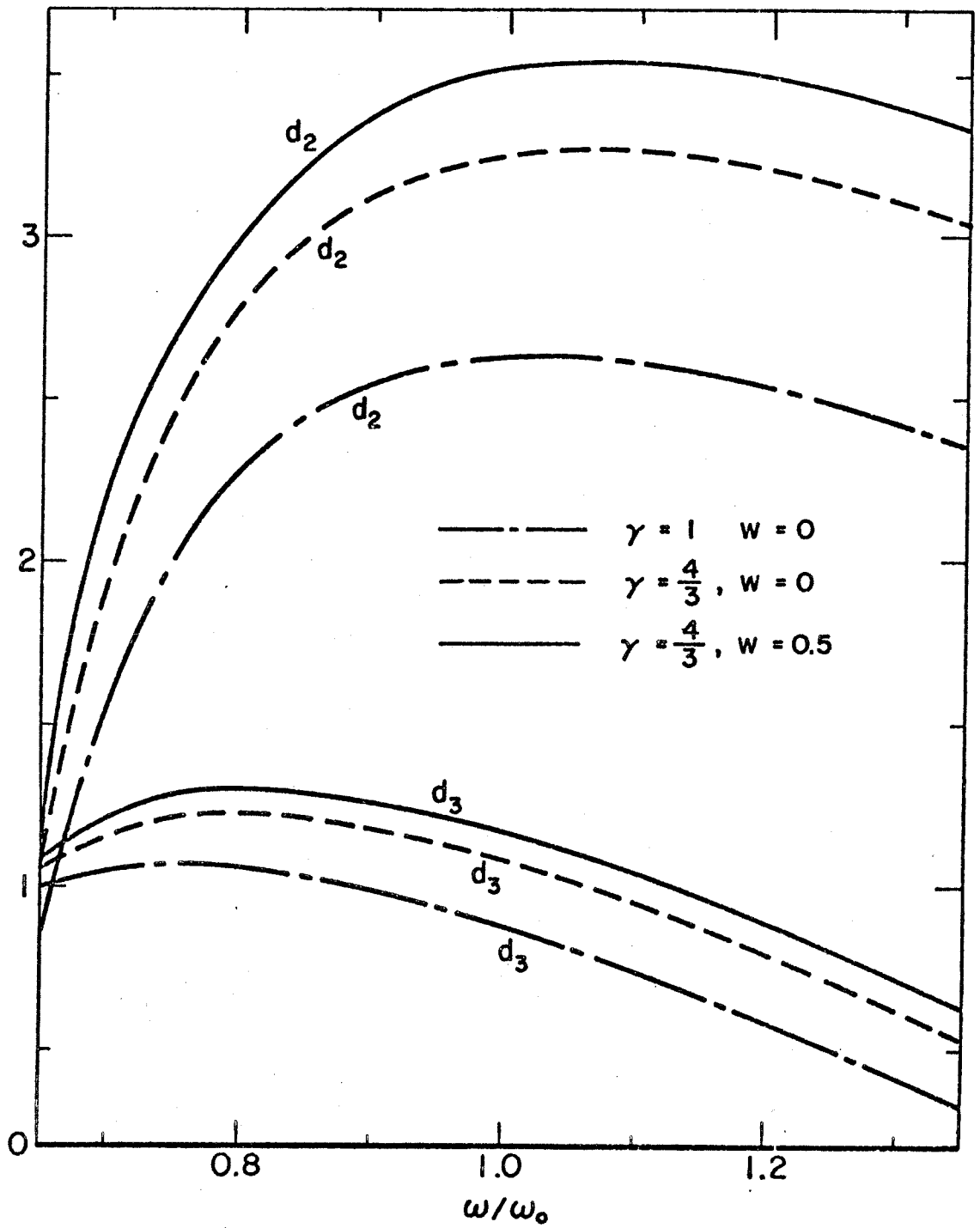


Fig. 8.2 - The functions $d_2$ and $d_3$ defined by (8.6b, c).

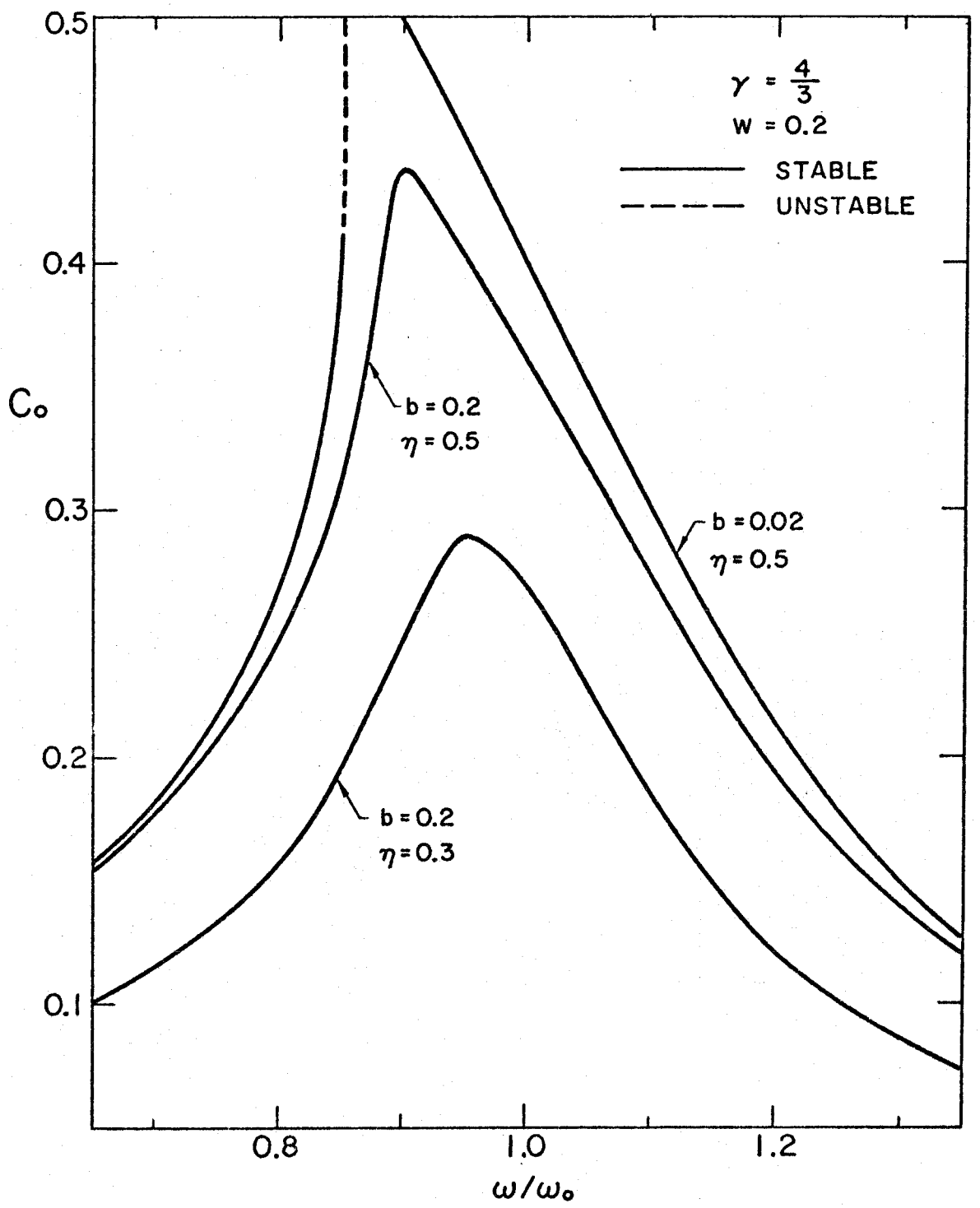


Fig. 8.3 - The amplitude of the resonant component for different values of the excitation $\eta$ and damping parameter b.

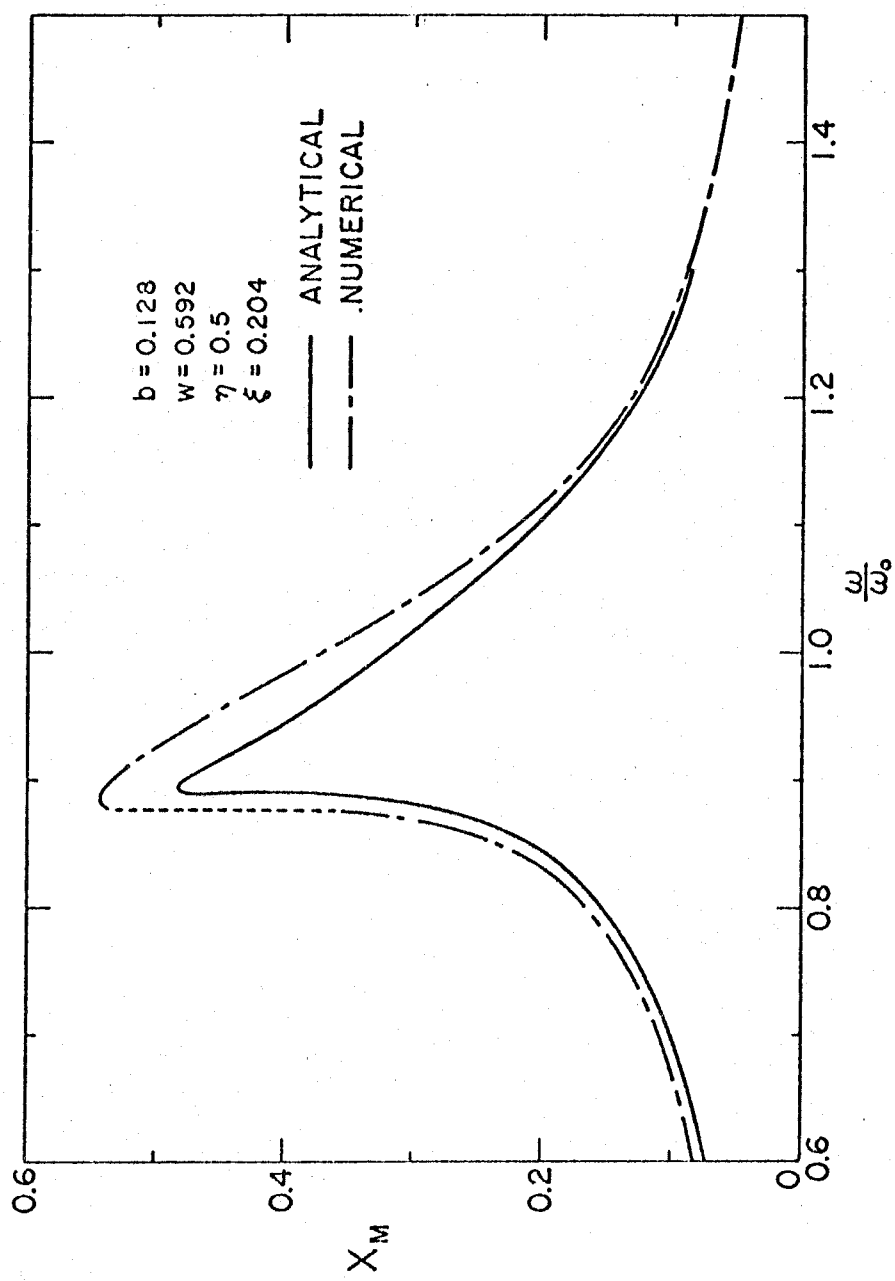


Fig. 9.1 - Comparison between Lauterborn's numerical results[31] and the present analytic oñes in the resonant region; $X_M = (R_{max} - R_o)/R_o$.

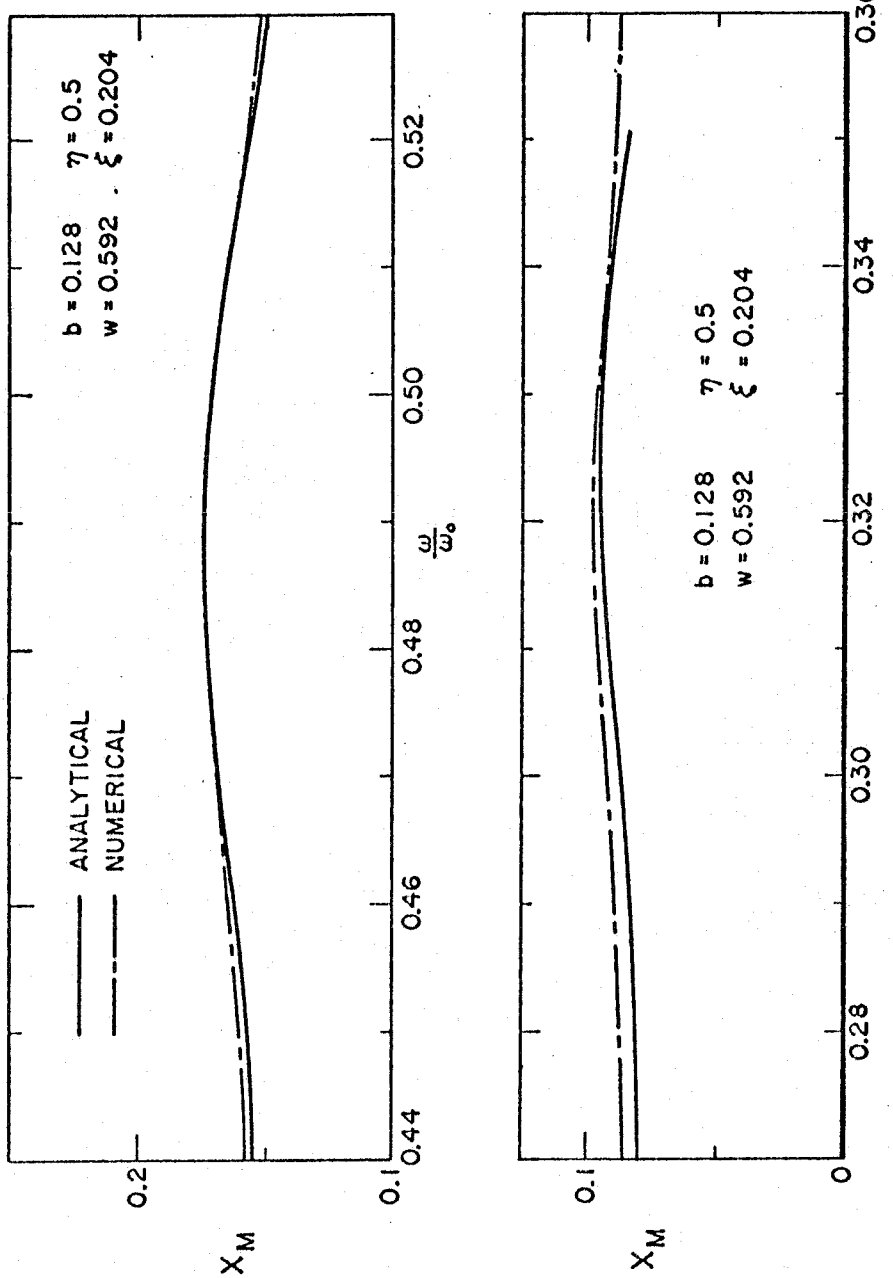


Fig. 9.2 - Comparison between Lauterborn's numerical results[31] and the present analytic ones in the first (upper) and second (lower) harmonic regions. $X_M = (R_{max} - R_o)/R_o$.

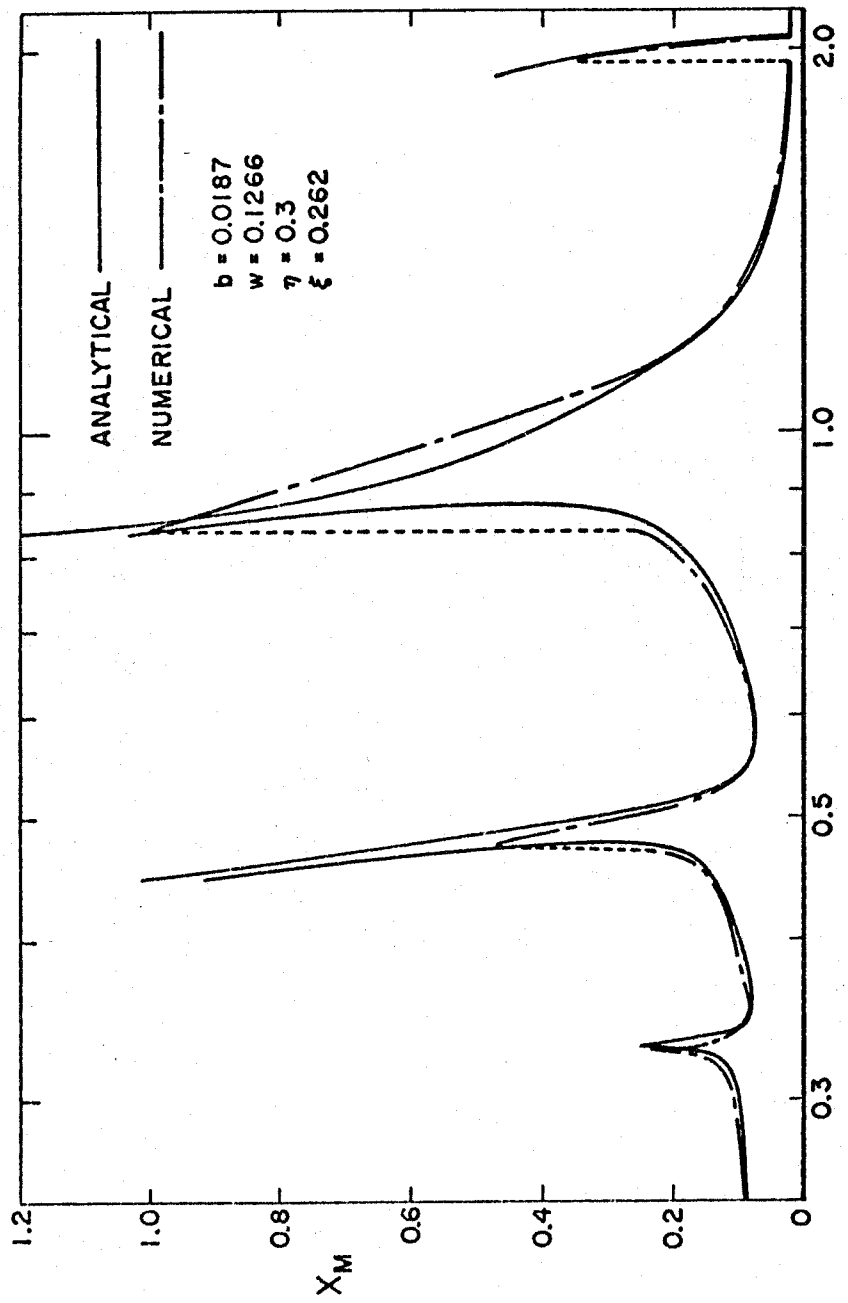


Fig. 9.3 - Comparison between Lauterborn's numerical results[31] and the present analytic ones. $X_M = (R_{max} - R_o)/R_o$.

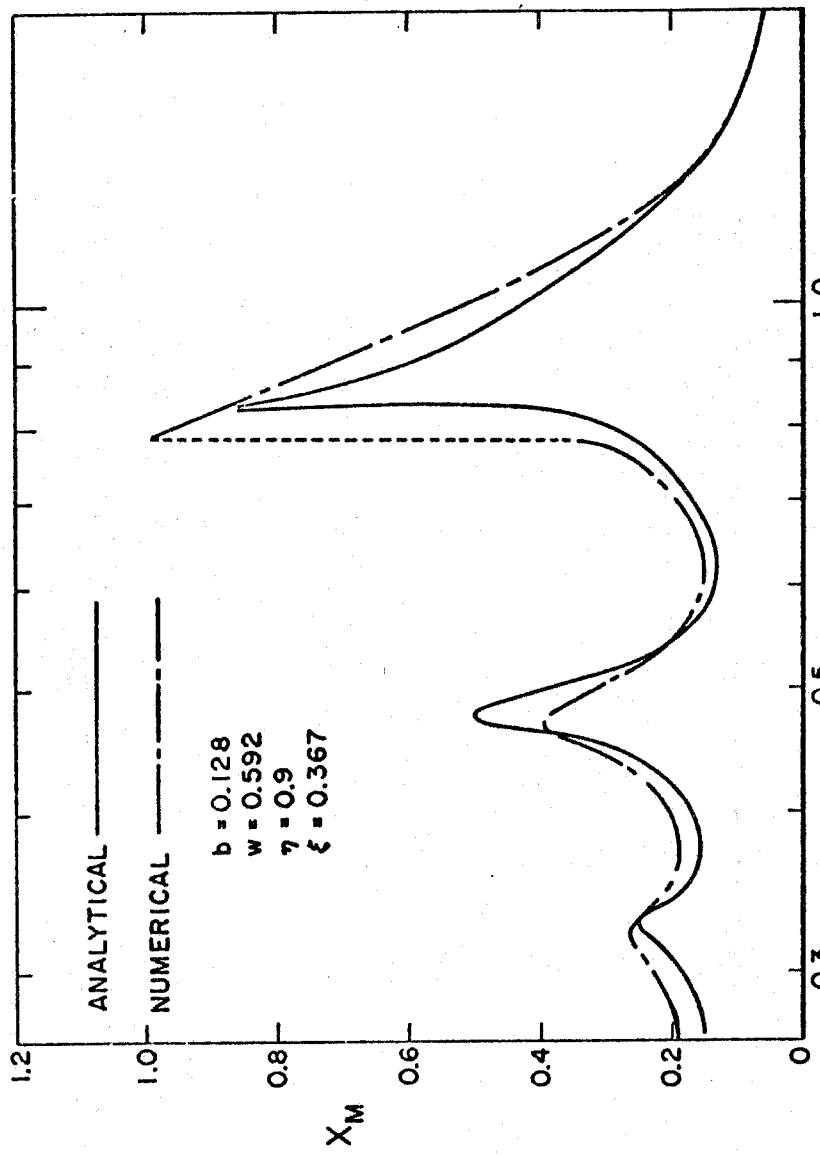


Fig. 9.4 - Comparison between Lauterborn's numerical results[31] and the present analytic ones. $X_M = (R_{max}-R_o)/R_o$.

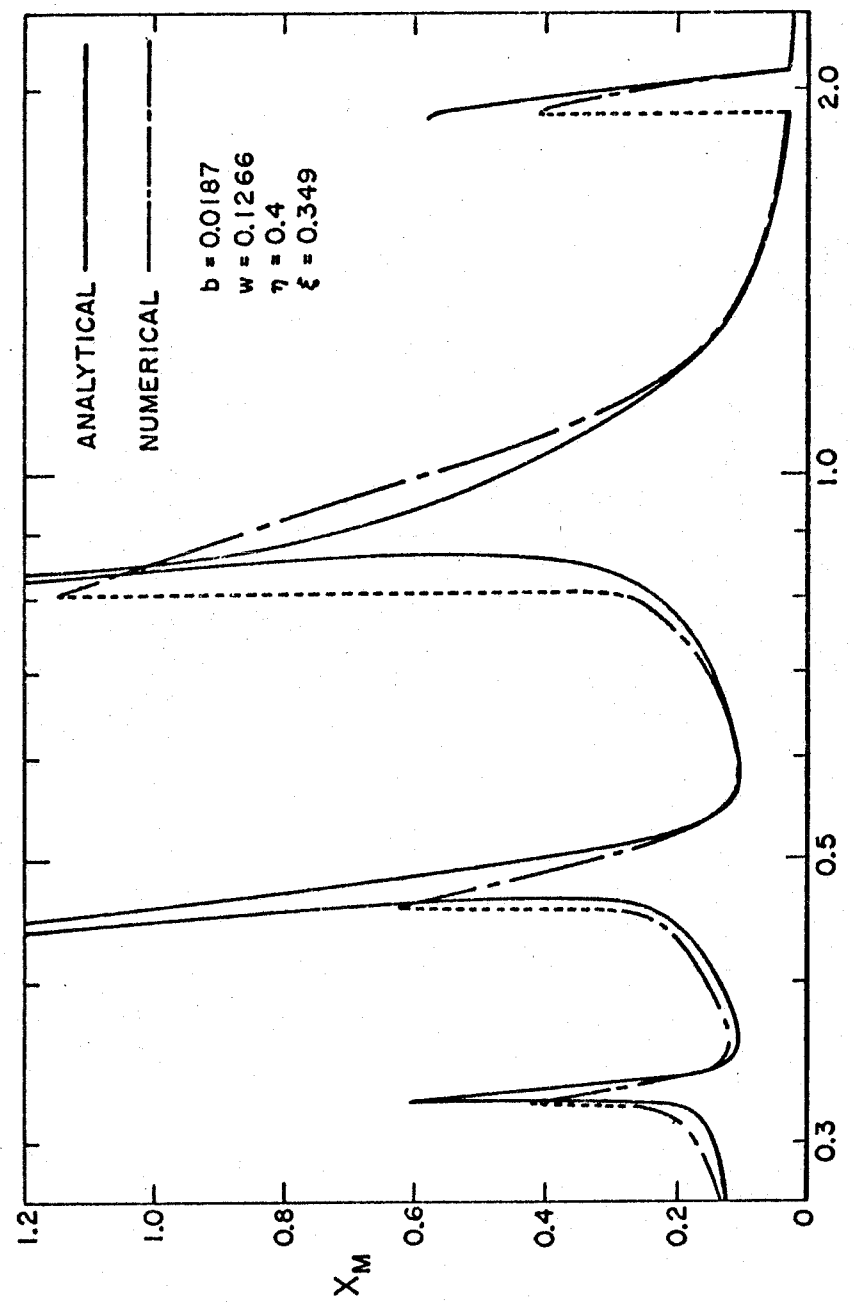


Fig. 9.5 - Comparison between Lauterborn's numerical results[31] and the present analytic ones. $X_M = (R_{max}-R_o)/R_o$.

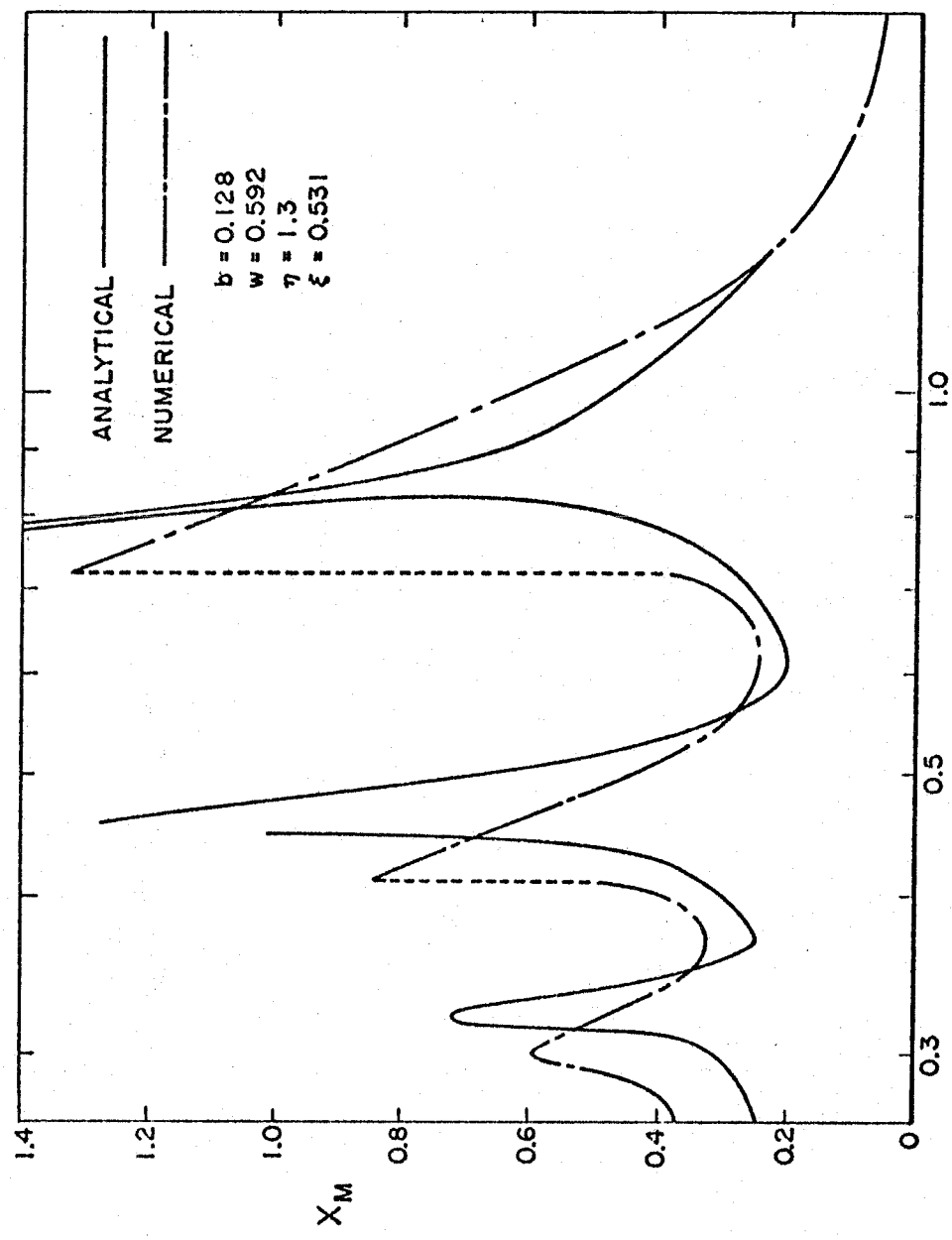


Fig. 9.6 - Comparison between Lauterborn's numerical results[31] and the present analytic ones for a very high value of the sound pressure $\eta$. $X_M = (R_{max} - R_o)/R_o$.

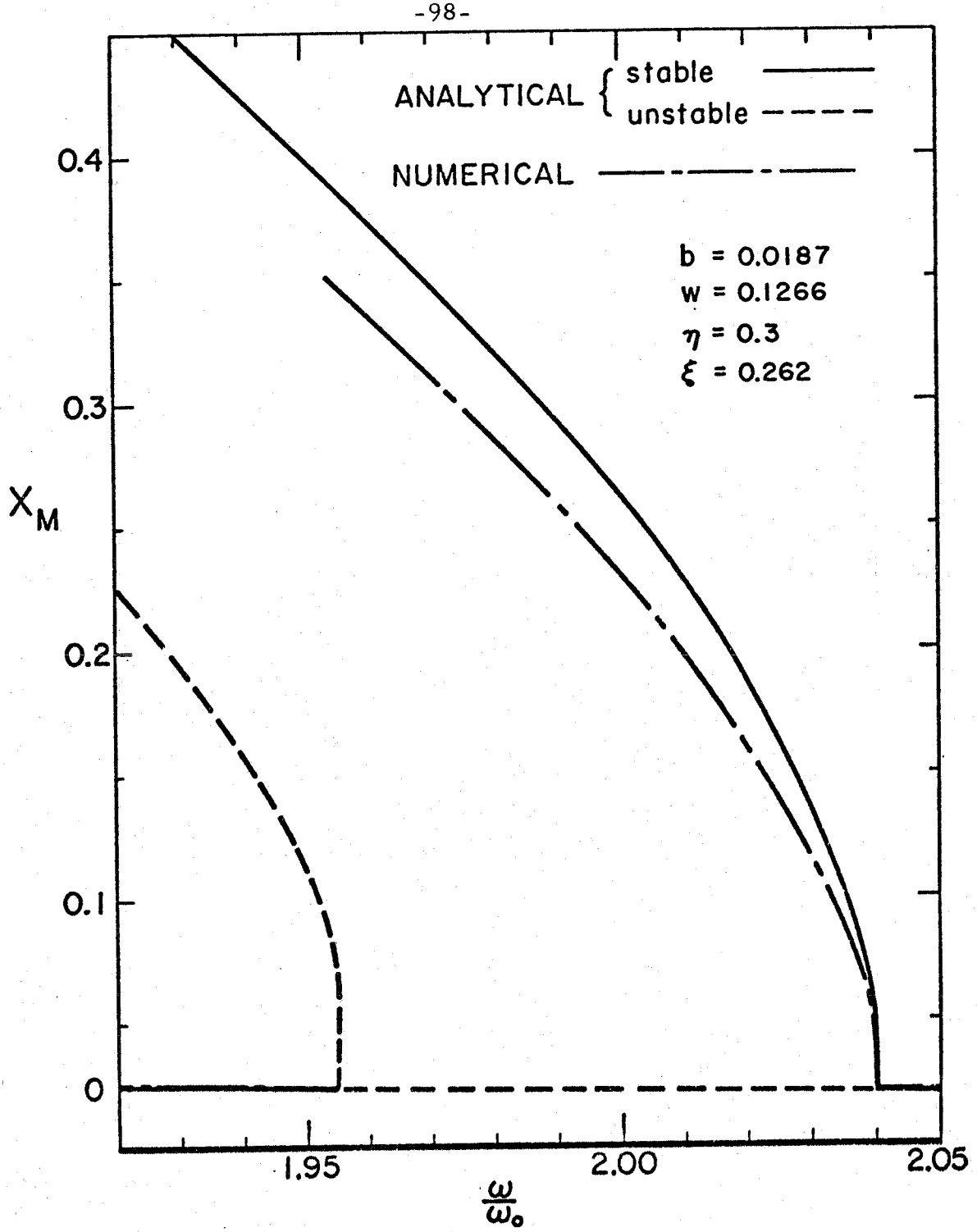


Fig. 9.7 - Comparison between Lauterborn's numerical results[31] and the present analytic ones in the subharmonic region.

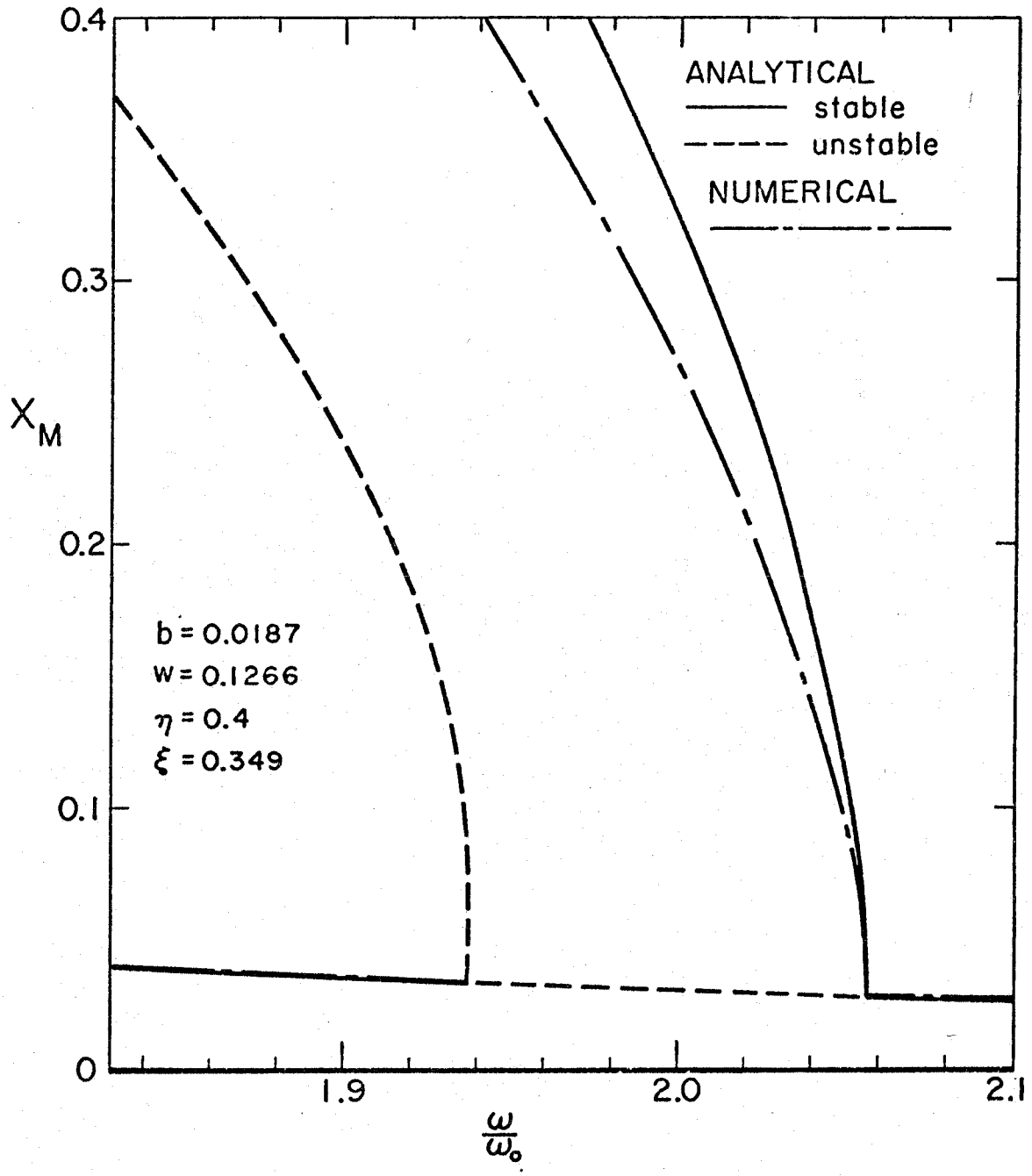


Fig. 9.8 - Comparison between Lauterborn's numerical results[31] and the present analytic ones in the subharmonic region.

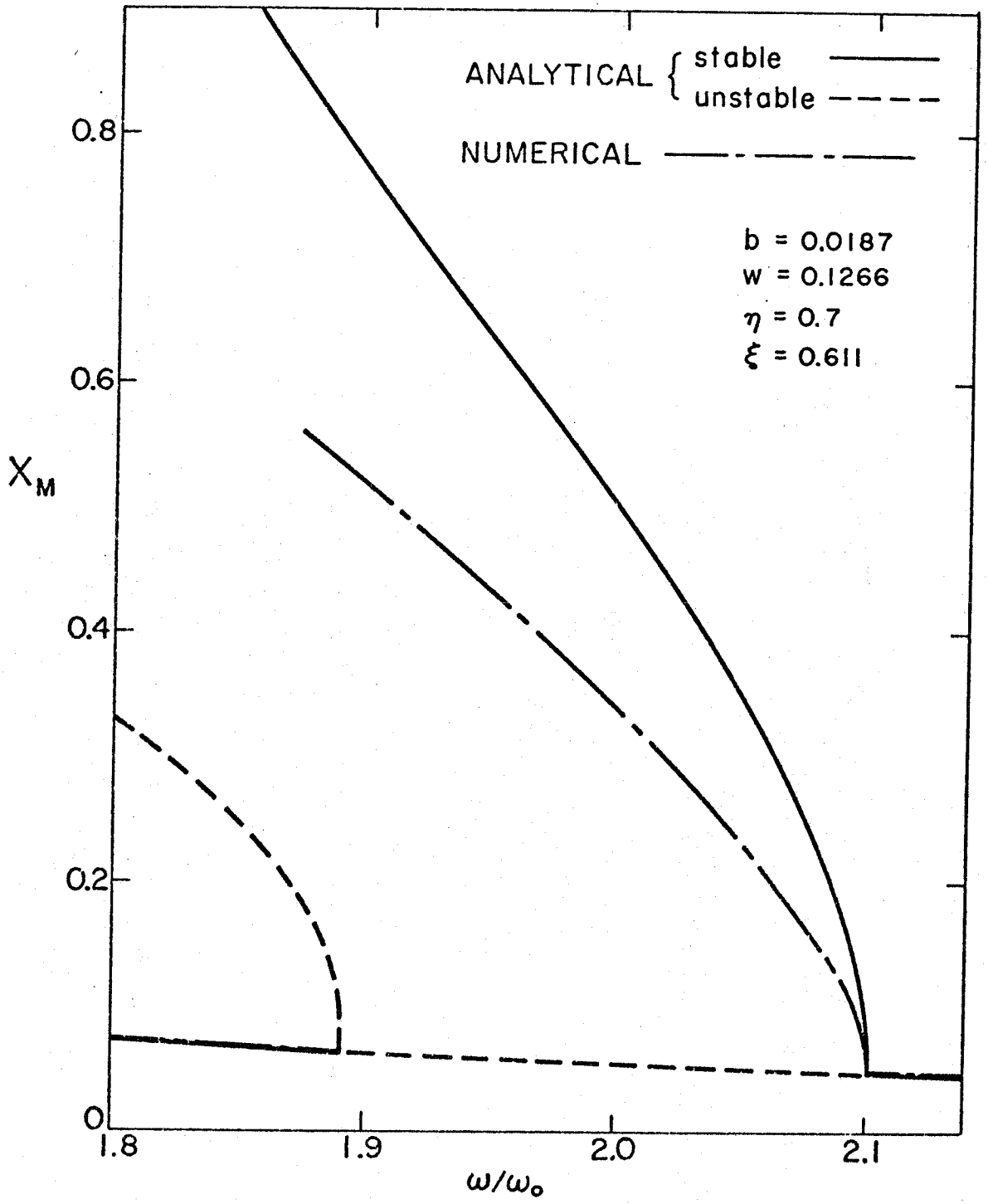


Fig. 9.9 - Comparison between Lauterborn's numerical results[31] and the present analytic ones in the subharmonic region.

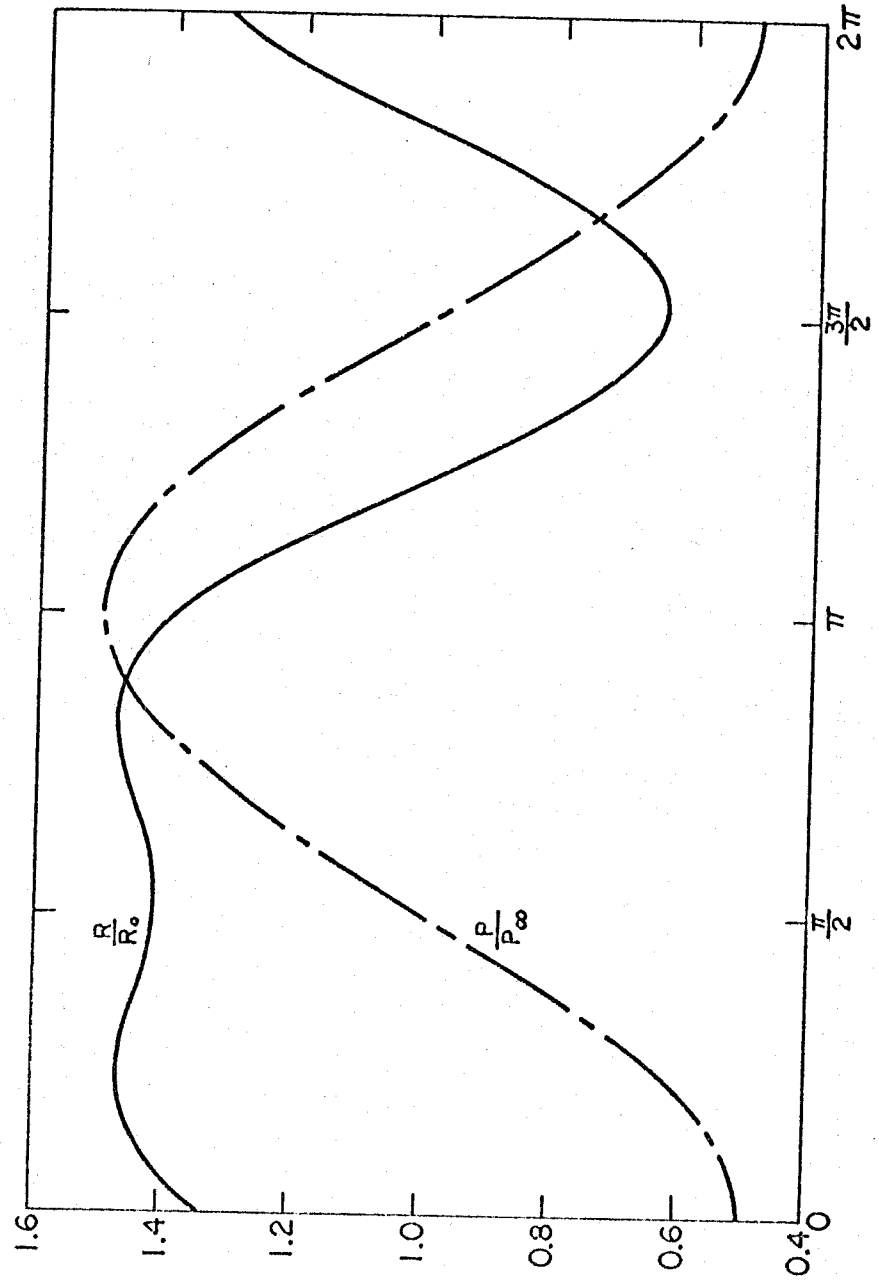


Fig. 9.10 - Normalized radius and pressure oscillations near resonance for the case of Fig. 9.1 in units of $\omega\tau$. The value of $\omega/\omega_o$ is 0.9.

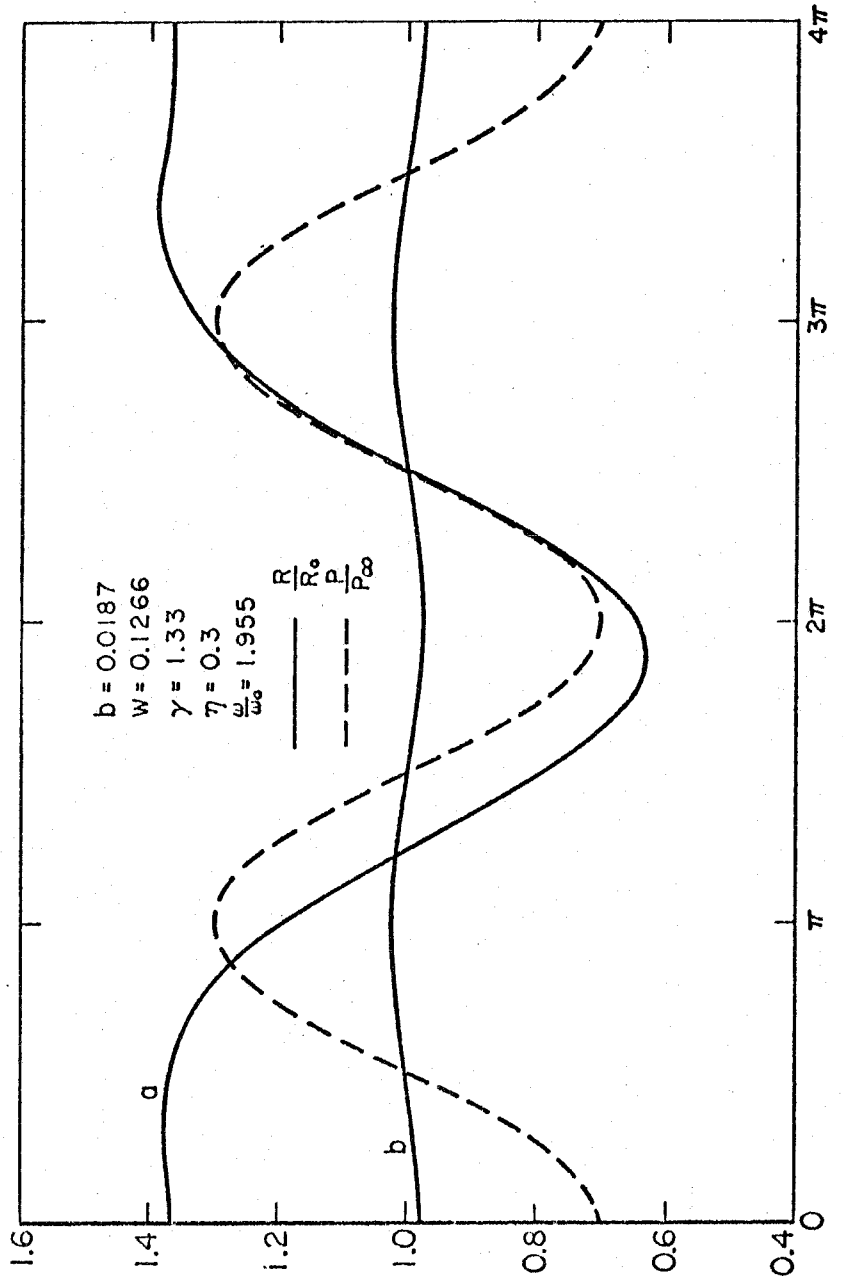


Fig. 9.11 - Normalized radius and pressure oscillations in the subharmonic region ($\omega/\omega_o$ = 1.955) for the case of Fig. 9.7.

Curve a shows the subharmonic oscilations, curve b the (stable) purely harmonic ones.

# PART II

# SUBHARMONICS AND ULTRAHARMONICS IN THE FORCED OSCILLATIONS OF NONLINEAR SYSTEMS

## 1. INTRODUCTION

Some degree of nonlinearity is present virtually in every practical problem involving oscillations. Sometimes this complication can be ignored and a linearized treatment is adequate, but in very many cases the interest lies in the very nonlinear aspects of the oscillations. In view of the large number of applications to electronic circuits, control theory, mechanical vibrations, and other branches of physics, it appears desirable to develop a simple and direct understanding of the essential characteristics of such processes. The advantage would be twofold, making possible an intuitive appraisal of the effect of nonlinearities in specific circumstances, and allowing the introduction of such topics at an earlier stage in the educational curriculum. The present paper is intended as a step in this direction.

We discuss the forced, steady state oscillations of weakly nonlinear systems, with particular emphasis on ultraharmonic and subharmonic modes and their differences. Duffing's equation is used as a model for the discussion, which however is conducted in such a way as to allow immediate generalization to other nonlinear equations.

The central part of this paper is constituted by Sections 3 and 5. In the first one a simple method for identifying the resonance frequencies of weakly nonlinear systems is given, in the second one the physical reasons for the differences exhibited by ultraharmonic and subharmonic oscillations are explained. Section 2 deals with some aspects of linear oscillations relevant for the following dis-

cussion, Section 4 contains a succint presentation of some of the salient features of nonlinear oscillations, and Section 6 deals with the principal resonance in the case of weak excitation. Finally, Section 7 presents a method for the higher order perturbation analysis of weakly nonlinear systems in steady state regime.

The amount of literature on nonlinear oscillations is so extensive that no attempt has been made to give exhaustive bibliographical indications. Some standard books and articles are listed in Refs. 1 through 10.

For the sake of brevity, physical examples of nonlinear systems have only been considered in a footnote. In this connection a series of papers by Ludeke [11] is recommended.

## 2. LINEAR OSCILLATIONS

Consider the equation describing the motion of a damped harmonic oscillator under the action of a sinusoidal forcing function:

$$\ddot{x} + 2b\dot{x} + \omega_o^2 x = P\cos\omega t \quad , \tag{1}$$

where dots denote differentiation with respect to time and $\omega_o$ is the natural frequency of the system. The general solution of (1) consists of damped oscillations at frequency $(\omega_o^2 - b^2)^{\frac{1}{2}}$, plus oscillations at the impressed frequency $\omega$:

$$x(t) = a_o e^{-bt}\cos[(\omega_o^2 - b^2)^{\frac{1}{2}}t + \psi_o] + Q(\omega, b)\cos(\omega t + \varphi) \quad , \tag{2}$$

where $a_o$, $\psi_o$ are two constants determined by the initial conditions and $Q(\omega, b)$, $\varphi$ are given by:

$$Q(\omega, b) = P\,[(\omega_o^2 - \omega^2)^2 + 4b^2\omega^2]^{-\frac{1}{2}} \quad , \tag{3a}$$

$$\varphi = \tan^{-1}[2b\omega/(\omega^2 - \omega_o^2)] \quad . \tag{3b}$$

The quantity $Q(\omega, b)$ is the response function of the linear oscillator, and it presents the familiar resonance structure with a sharp maximum at $\omega^2 = \omega_o^2 - 2b^2$ (Fig. 1).

It is evident from (2) that, as time gets large in comparison with $b^{-1}$, the first term (and with it the influence of the initial conditions) disappears so that in the limit $t \to \infty$ we obtain the steady state solution of (1) as:

$$x_o = Q(\omega, b)\cos(\omega t + \varphi) \quad .$$

The disappearence of the oscillations at frequency $(\omega_o^2 - b^2)^{\frac{1}{2}}$ is a consequence of the fact that in a linear system there is no mechanism of energy transfer between different modes, so that only the mode corresponding to the driving frequency can sustain itself in the presence of dissipative forces.

In view of later considerations we should like to note here that the resonance structure of the response allows an amplification of the excitation amplitude, so that even a weak driving force (of order $\epsilon$, say, with $|\epsilon| \ll 1$) can produce a response of order one if the damping is sufficiently small (of order $\epsilon$). Indeed, if we let $P = \epsilon P'$ , $b = \epsilon\beta$, with $P', \beta$ quantities of order one, we get from (3a):

$$Q(\omega, \epsilon\beta) \simeq P'/2\beta\omega_o \qquad \text{for} \quad \omega \simeq \omega_o$$

which is of order one.

## 3. NONLINEAR OSCILLATIONS

To illustrate some general features of nonlinear systems, let us now consider a particular nonlinear oscillator described by the well-known Duffing equation [12]:

$$\ddot{x} + 2\epsilon\beta\dot{x} + \omega_o^2 x = P\cos\omega t + \epsilon x^3 \quad , \tag{4}$$

where $|\epsilon| \ll 1$ [13]. It may be expected that the steady state solution of this equation will be related to the solution of the linear equation obtained as $\epsilon \to 0$, i.e. Eq.(1), so that it is natural to introduce a new unknown y through :

$$x = x_o + y = Q\cos(\omega t+\varphi) + y \quad , \tag{5}$$

with Q and $\varphi$ given by Eqs.(3). Upon substitution into (4) we are led to the following equation for y :

$$\ddot{y} + 2\epsilon\beta\dot{y} + \omega_o^2 y = \epsilon\left[\tfrac{1}{4} Q^3(\cos 3\omega t + 3\cos\omega t) + \tfrac{3}{2} Q^2 y(1+\cos 2\omega t) + 3Q y^2\cos\omega t + y^3\right] \quad . \tag{6}$$

For simplicity of writing, the time origin has been shifted by $\varphi/\omega$, so that $\cos(\omega t+\varphi) \to \cos\omega t$, and elementary trigonometric relations have been used to express $\cos^2\omega t$, $\cos^3\omega t$ in terms of the multiple angles $2\omega t$, $3\omega t$. It is easy to see that, in spite of the small quantity $\epsilon$ multiplying the "forcing function" in the RHS of this equation, the response y is not necessarily small, because of the amplification effects mentioned in Section 2. For instance, the first term

in the RHS would cause a response of order one when $3\omega \sim \omega_o$. Notice that the appearence of the new frequency $3\omega$ is an effect of the nonlinearity $x^3$, which causes a coupling of the first term of (5), $x_o$, with itself. We may now suspect that other resonating frequencies are present in the RHS of (6), arising from the coupling of y with $x_o$, and of y with itself. They can be determined without actually solving the equation by the following simple reasoning.

Suppose that we had the correct expression for the y appearing in the RHS of (6), $y_R$, say, and that we are then left to solve the resulting linear equation for the y appearing in the LHS, $y_L$. Of course this should be done in such a way that, in the end, $y_R = y_L$. Suppose also that we are interested only in terms of order one, neglecting all terms of order $\epsilon$ and smaller. The discussion of Section 2 shows that, in order to produce a component of order one in $y_L$, a term in the bracket in the RHS of (6) should satisfy two requirements:

(i) it should have a frequency close to $\omega_o$;

(ii) it should have an amplitude of order one.

It follows from (i) that the only term of order one in $y_L$ will have a frequency close to $\omega_o$. However, since $y_L$ must equal $y_R$, it also follows from (ii) that this same term is the only one present in $y_R$ that we should consider to determine the resonant frequencies to lowest order in $\epsilon$. We therefore let $y \propto \cos\omega_o t$ in the RHS of (6) and compute the new frequencies introduced by the nonlinearity by means of the trigonometric relation $2\cos\alpha\cos\beta = \cos(\alpha+\beta)+\cos(\alpha-\beta)$.

Whenever one of these frequencies is close to $\omega_o$, the corresponding term will produce a response of order one. In this way we get the results shown in Table I.

We shall not be concerned here with the more complex case of strong excitation of the fundamental resonance, $\omega \sim \omega_o$, but only with the ultraharmonic and subharmonic resonances occurring when $3\omega \sim \omega_o$ and $\omega \sim 3\omega_o$ respectively. The reason for the naming is that in the first case the strong response at $\sim \omega_o$ is at three times the exciting frequency $\omega$, while in the second case it is at one-third of $\omega$.

## 4. ULTRAHARMONICS AND SUBHARMONICS

In the ultraharmonic region, $\omega \sim \frac{1}{3}\omega_o$, neglecting terms that cannot produce resonance, we get from (6):

$$\ddot{y} + 2\epsilon\beta\dot{y} + (\omega_o^2 - \tfrac{3}{2}\epsilon\Omega^2)y = \tfrac{1}{4}\epsilon\Omega^3\cos 3\omega t + \epsilon y^3 \quad . \tag{7}$$

This equation is very similar to the original one, except that the order of magnitude of the driving amplitude has been lowered from one to $\epsilon$. In agreement with the discussion in the previous Section, to determine the solution of (7) to order one we now let:

$$y = C_3 \cos(3\omega t + \varphi_3) + O(\epsilon)$$

and retain only terms oscillating with frequency $3\omega$. The result is:

$$[(\omega_o^2 - 9\omega^2 - \tfrac{3}{2}\epsilon\Omega^2)C_3 - \tfrac{3}{4}\epsilon C_3^3 - \tfrac{1}{4}\epsilon\Omega^3\cos\varphi_3]\cos(3\omega t+\varphi_3)$$

$$- [6\epsilon\omega\beta C_3 + \tfrac{1}{4}\epsilon\Omega^3\sin\varphi_3]\sin(3\omega t+\varphi_3) = O(\epsilon) \simeq 0 \quad ,$$

from which:

$$(\omega_o^2 - 9\omega^2 - \tfrac{3}{2}\epsilon Q^2)\, C_3 - \tfrac{3}{4}\epsilon C_3^3 = \tfrac{1}{4}\epsilon Q^3 \cos\varphi_3 \qquad (8a)$$

$$-6\,\epsilon\,\beta\,\omega C_3 = \tfrac{1}{4}\epsilon Q^3 \sin\varphi_3 \quad . \qquad (8b)$$

The amplitude $C_3$ determined by these equations is plotted as a function of $3\omega/\omega_o$ in Fig. 2 for two values of the damping parameter $\beta$. In the undamped case, $\beta=0$, the phase $\varphi_3$ can be either 0 or $\pi$, so that the first equation becomes:

$$(3\omega/\omega_o)^2 = 1 - \tfrac{3}{2}\epsilon\omega_o^{-2}Q^2 - \tfrac{3}{4}\epsilon\omega_o^{-2}C_3^2 \pm \tfrac{1}{4}\epsilon\omega_o^{-2}C_3^{-1}Q^3$$

It is clear from this equation that, as $C_3$ increases, the two branches tend asymptotically to the curve:

$$(3\omega/\omega_o)^2 = 1 - \tfrac{3}{2}\epsilon\omega_o^{-2}Q^2 - \tfrac{3}{4}\epsilon\omega_o^{-2}C_3^2 \qquad (9)$$

also shown in Fig. 2. If $\beta>0$, the two branches join together across this curve and the amplitude has a maximum. On the other hand, as $|3\omega - \omega_o|$ increases, the corresponding value of $C_3$ decreases. The situation is therefore very similar to the resonance phenomenon in the linear case (Fig. 1), the only substantial difference being the fact that the asymptotic curve is not a vertical straight line, but is bent to the right or to the left according as $\epsilon<0$ or $\epsilon>0$.[14] The bending of the resonance peak has the important consequence (typical of nonlinear oscillations) that the function $C_3(\omega)$ is multi-valued in a certain frequency range. A stability analysis shows that the intermediate value of $C_3$ corresponds to an unstable state[15] which therefore cannot be observed because any infinitesimal dis-

turbance will grow leading the amplitude towards one of the other two (stable) values. The appearence of one or the other of these values in the steady state oscillations is determined by the initial conditions of the motion. In contrast with the linear case, therefore, the steady state nonlinear oscillations retain some memory of the initial values of displacement and velocity.

To discuss the subharmonic oscillations, when $\omega \sim 3\omega_o$, we start again from (6) retaining only the terms capable of producing resonance according to Table I:

$$\ddot{y} + 2\epsilon\beta\dot{y} + (\omega_o^2 - \tfrac{3}{2}\epsilon Q^2)\, y = \tfrac{3}{2}\epsilon Q y^2 \cos\omega t + \epsilon y^3 \quad . \tag{10}$$

The structure of this equation is very different from (7) because all terms of the RHS contain y: this circumstance causes very profound differences between ultraharmonic and subharmonic oscillations. If we let:

$$y = C_{1/3} \cos(\tfrac{1}{3}\omega t + \varphi_{1/3})$$

in (10) and retain only terms oscillating with frequency $\frac{1}{3}\omega$ we get, in place of (8):

$$(\omega_o^2 - \tfrac{1}{9}\omega^2 - \tfrac{3}{2}\epsilon Q^2)\, C_{1/3} - \tfrac{3}{4}\epsilon C_{1/3}^3 = \tfrac{3}{4}\epsilon Q C_{1/3}^2 \cos 3\varphi_{1/3} \tag{11a}$$

$$-\tfrac{2}{3}\epsilon\omega\beta C_{1/3} = \tfrac{3}{4}\epsilon Q C_{1/3}^2 \sin 3\varphi_{1/3} \tag{11b}$$

Two examples of the response curves determined by these equations are plotted for the case $\epsilon < 0$ in Fig. 3.

The first important remark to be made about Eqs. (11) is that $C_{1/3}=0$ is a solution for any value of $\varphi_{1/3}$. Therefore, for any

value of $\omega$ and P, the steady state oscillations ordinarily will not contain a subharmonic component, which however will be present if the initial values of displacement and velocity lie in suitable ranges. For this to happen, however, it is usually necessary that the equilibrium state (or a preexisting steady, purely harmonic oscillation) be perturbed quite substantially (shock excitation of the subharmonic). Another possibility for the appearence of the subharmonic at a particular frequency is when the purely harmonic, $C_{1/3}=0$, oscillations are unstable. Although this does not occur in the case of Duffing's equation, it is nevertheless commonly found to happen in other nonlinear systems. An example is shown in Fig. 4, where the subharmonic response of order $\frac{1}{2}$ (i.e. occurring for $\omega \sim 2\omega_o$) exhibited by the radial oscillations of a spherical gas bubble in an incompressible liquid [16] is shown. In the dashed frequency interval on the abscissa axis, only the subharmonic oscillations correspond to a stable mode.

Another striking characteristic of the subharmonic response is obtained by considering the reality conditions for $C_{1/3}$. It is a simple matter to show from Eqs.(11) that no subharmonic component can be present unless the following threshold condition for the driving amplitude is fulfilled:

$$Q^2 > \frac{8}{21}\epsilon^{-1}\{\omega_o^2 - \tfrac{1}{9}\omega^2 - [(\omega_o^2 - \tfrac{1}{9}\omega^2)^2 - \tfrac{28}{9}\epsilon^2\beta^2\omega^2]^{\frac{1}{2}}\}$$

It will be noticed that the RHS of this equation reduces to zero if no damping is present.

In Fig. 3 the dotted line shows the function $Q(\omega, \epsilon\beta)$ in the subharmonic region for $P=1$. This quantity would be the total amplitude of the response if no subharmonic were present. Its comparison with the subharmonic response gives an idea of the violence of subharmonic oscillations, which is an important reason for their practical importance[17].

## 5. DISCUSSION

It has been shown that in a particular nonlinear system large amplitude oscillations can occur at a frequency different from the driving frequency provided that there exists a mechanism capable of transferring efficiently (i. e. via resonance) the energy introduced at frequency $\omega$ into a mode close to the natural frequency of the system. Obviously this result holds true also for more general nonlinearities of the form $\epsilon x^m \dot{x}^n$, with m, n integers such that $m+n > 1$. In this case too we let:

$$x = x_o + y = Q\cos(\omega t + \varphi) + y \qquad (12)$$

where the first term is the steady solution of the linearized equation. Since the ultraharmonic oscillations occur at a frequency higher than the driving frequency $\omega$, it is obvious that the term $x_o$ in (12) is by itself sufficient to feed energy into such modes. Indeed, upon substitution into $\epsilon x^m \dot{x}^n$, it will give rise to a term of the form

$\epsilon Q^{m+n} \cos^m(\omega t+\varphi) \sin^n(\omega t+\varphi)$ which, when expressed in terms of multiple angle functions, will contain frequencies $k\omega$ capable of inducing large responses whenever $k\omega \sim \omega_o$. Under suitable conditions, also the coupling between $x_o$ and y caused by the nonlinearity can introduce additional "channels" through which energy can be transmitted to a particular ultraharmonic mode, but even if these couplings were absent, the mode in question would still be capable of sustaining itself. In this respect the ultraharmonic oscillations behave basically like ordinary linear forced oscillations, and they will occur whenever the frequency is in an appropriate range, just as resonance occurs in the linear case when $|\omega - \omega_o|$ is not too large. Their amplitude can always adjust itself in such a way that the energy dissipated by the viscous forces equals the energy input by the driving force because the dissipation, $-2\epsilon\beta\dot{y}^2$, is proportional to $C_j^2$ (where $C_j$ is the amplitude of the j-th ultraharmonic), while the energy intake, $x_o^k \dot{y}$, is proportional to $Q^k C_j$ (plus possibly terms containing the second and higher powers of $C_j$).

For the subharmonic oscillations the situation is fundamentally different. Since they occur at a frequency lower than the driving frequency, a mechanism for frequency demultiplication of the energy input is required. Mathematically, this mechanism is furnished by the couplings $x_o^i y^j$ through the second term in the trigonometric identities $2\cos\alpha\cos\beta = \cos(\alpha+\beta)+\cos(\alpha-\beta)$ etc. It follows that the energy input term is now of the form $(x_o^i y^j)\dot{y}$, and is no longer proportional to the first power of the amplitude, but to the second or higher, while the characteristics of the energy dissipation are

unchanged. It may happen therefore that, for a given driving amplitude, the resulting subharmonic amplitude is too low for the system to absorb energy at a rate sufficient to balance the dissipation. These considerations explain why subharmonic oscillations usually exhibit a threshold effect, which however disappears as the damping is reduced to zero.

## 6. THE PRINCIPAL HARMONIC

An exhaustive treatment of the principal harmonic for $\omega \sim \omega_o$ in the case of strong excitation is beyond the scope of the present considerations. Nevertheless the case in which the driving force is weak (of order $\epsilon$) can easily be discussed. Consider therefore the equation:

$$\ddot{x} + 2\epsilon\beta\dot{x} + \omega_o^2 x = \epsilon P\cos\omega t + \epsilon x^3 \quad , \tag{13}$$

for the case when $\omega \sim \omega_o$. Following a line of reasoning similar to the one adopted in Section 3 we may let:

$$x = C_1\cos(\omega t + \varphi_1) \quad ,$$

disregarding other harmonics which give no contribution to zero order in $\epsilon$. Upon substitution into (13) the following two equations are obtained:

$$(\omega_o^2 - \omega^2 - \tfrac{3}{4}\epsilon C_1^2) C_1 = \epsilon P\cos\varphi_1 \quad , \tag{14a}$$

$$-2\epsilon\beta\omega C_1 = \epsilon P\sin\varphi_1 \quad . \tag{14b}$$

It is interesting to note the similarity of these equations with Eqs. (8) for the ultraharmonic case. This analogy illustrates from another point of view the affinity between ultraharmonic and ordinary resonance. The shape of the peak is similar to the one shown in Fig. 2, and can readily be computed from (14).

## 7. HIGHER ORDER APPROXIMATIONS

It is not difficult to extend the considerations of Section 3 to obtain steady state solutions of a higher accuracy. To this end we begin by letting:

$$y = y_o + \epsilon x_1 = C_i \cos(i\omega + \varphi_i) + \epsilon x_1$$

in (6), where $i = \frac{1}{3}$ in the subharmonic case and $i=3$ in the ultraharmonic one; the amplitude $C_i$ and phase $\varphi_i$ are given by Eqs. (11) and Eqs. (8) respectively. As an example of the procedure, let us consider the subharmonic case here. The following equation for $x_1$ is obtained:

$$\ddot{x}_1 + 2\epsilon\beta\dot{x}_1 + \omega_o^2 x_1 = \tfrac{1}{4}Q^3(\cos 3\omega t + 3\cos\omega t) + \tfrac{3}{4}Q^2C\left[\cos\left(\tfrac{7}{3}\omega t+\varphi\right)+\cos\left(\tfrac{5}{3}\omega t+\varphi\right)\right]$$

$$+\tfrac{3}{2}QC^2\left[\cos\omega t+\tfrac{1}{2}\cos\left(\tfrac{5}{3}\omega t+\varphi\right)\right] + \tfrac{1}{4}C^3\cos(\omega t+3\varphi)$$

$$+\epsilon\left\{\left[\tfrac{3}{2}Q^2(1+\cos 2\omega t)+3QC\left|\cos\left(\tfrac{4}{3}\omega t+\varphi\right)+\cos\left(\tfrac{2}{3}\omega t-\varphi\right)\right|\right.\right.$$

$$\left.\left.+\tfrac{3}{2}C^2\left(1+\cos\left(\tfrac{2}{3}\omega t+2\varphi\right)\right)\right]x_1 + 3\epsilon\left[Q\cos\omega t+C\cos\left(\tfrac{1}{3}\omega t+\varphi\right)\right]x_1^2 + \epsilon^2 x_1^3\right\}$$

where for convenience of writing the subscript $\frac{1}{3}$ has been omitted.

This is now a nonlinear equation for $x_1$, which can be dealt with in the same way indicated in Section 3. We therefore let:

$$x_1 = x_1^o + y_1 \quad ,$$

where $x_1^o$ is the solution of the equation obtained by neglecting the terms in the curly brackets, and $y_1$ the correction of order one introduced by the terms in the curly brackets oscillating with frequency close to $\omega_o$. This procedure can clearly be continued, and an asymptotic expansion of the solution in the form:

$$x = x_o + y_o + \epsilon(x_1^o + y_1^o) + \epsilon^2(x_2^o + y_2^o) + \ldots$$

can be obtained. It should be noted that all the terms $y_k^o$ in this expansion oscillate with frequency close to the natural frequency $\omega_o$.

To obtain a solution in a frequency region different from the principal harmonic, ultraharmonic or subharmonic domains already considered, it is sufficient to omit the term $y_o$ and to start by letting:

$$x = Q\cos(\omega t+\varphi) + \epsilon x_1$$

in Eq. (4). The following equation for $x_1$ is then obtained:

$$\ddot{x}_1 + 2\epsilon\beta\dot{x}_1 + \omega_o^2 x_1 = \tfrac{1}{4}Q^3(\cos 3\omega t + 3\cos\omega t)$$

$$+ \epsilon\left[\tfrac{3}{2}Q^2(1+\cos 2\omega t)\, x_1 + 3\epsilon Q\cos\omega t\, x_1^2 + \epsilon^2 x_1^3\right] .$$

(In writing this equation the time origin has again been shifted by $\varphi/\omega$). By the same method used for the construction of Table I it is easily found that, aside from the resonance regions already

considered, no other resonating frequency is introduced by the terms in brackets to this order[18].

The procedure outlined in this Section essentially amounts to an algorithm for the iterative solution of the system of equations that would be obtained by expanding $x$ in a truncated Fourier series.

## REFERENCES AND FOOTNOTES


1. J.J. Stoker, Nonlinear Vibrations in Mechanical and Electrical Systems (Interscience Publishers Inc., New York 1950).
2. N. N. Bogoliubov and N. Kryloff, Introduction to Nonlinear Mechanics (Princeton University Press, Princeton, 1943); N. N. Bogolibov and Y. A. Mitropolsky, Asymptotic Methods in the Theory of Nonlinear Oscillations (Hindustan Publishing Co., New Delhi, 1961).
3. N. W. McLachlan, Ordinary Nonlinear Differential Equations in Engineering and Science (Clarendon Press, Oxford, 1956).
4. N. Minorski, Nonlinear Oscillations (Van Nostrand Co., Princeton and New York, 1962).
5. R. A. Struble, Nonlinear Differential Equations (McGraw Hill, New York, 1962) Chapters 7, 8.
6. J. K. Hale, Oscillations in Nonlinear Systems (McGraw Hill, New York, 1963); Ordinary Differential Equations (Wiley- Interscience, New York, 1969) Chapters IV-VI.
7. C. Hayashi, Nonlinear Oscillations in Physical Systems (Mc Graw Hill, New York, 1964).
8. A. A. Andronov, A.A. Vitt, and S. E. Khaikin, Theory of Oscillators (Pergamon Press, Oxford and New York, 1966).
9. J. Kevorkian, in Lectures in Applied Mathematics (American Mathematical Society, Providence, 1966) Vol. 7, Space Mathematics, Part III; J. D. Cole, Perturbation Methods in Applied Mathematics (Blaisdell Publishing Co., Waltham, 1968).

10. L. A. Pipes and L. R. Harvill, Applied Mathematics for Engineers and Physicists (McGraw Hill, New York, 1970), Third Ed., Chapter 15.

11. C. A. Ludeke, J. Appl. Phys. 13, 418 (1942); 17, 603 (1946); 20, 600 (1949); 22, 1321 (1951); Trans. ASME 79, 439 (1957); Am. J. Phys. 16, 430 (1948); with W. Pong, J. Appl. Phys. 24, 96 (1953); with J. D. Blades, J. Appl. Phys. 28, 1326 (1957).

12. G. Duffing, Erzwungene Schwingungen bei veränderlicher Eigenfrequenz (F. Vieweg u. Sohn, Braunschweig, 1918).

13. This equation describes for instance the forced oscillations of a pendulum of moderate amplitude; in this case the cubic term is introduced by the series expansion of $\sin\theta$. Another example is furnished by an oscillatory circuit with a nonlinear inductor described by $i=L^{-1}\Phi+b\,\Phi^3$, where i is the current, $\Phi$ the magnetic flux, L the inductance and b a constant characterizing the amount of nonlinearity. The forced oscillations of a body on top of an elastic bar, the constitutive law of which contains a cubic term is a third example.

14. In the first case the restoring force, $-\omega_o^2 x+\epsilon x^3$, increases with displacement ("hardening spring"), so that on the average it is larger than its linear part, $-\omega_o^2 x$. This circumstance causes an increase in the "average" natural frequency $\bar{\omega}_o$ which, clearly, becomes amplitude dependent: $\bar{\omega}_o^2=1-\frac{3}{2}\epsilon\omega_o^{-2}Q^2-\frac{3}{4}\epsilon\omega_o^{-2}C_3^2$. It is evident that this fact is responsible for the bending of the peak, which would be vertical if the scale of the abscissa axis were in terms of $3\omega/\bar{\omega}_o$ instead of $3\omega/\omega_o$. Similarly, for

$\epsilon>0$ ("softening spring"), the average value of the natural frequency decreases and the peak leans to the left.

15. The stability analysis can be carried out in several ways. See e.g. Ref. 4, pp. 375-380.

16. A. Prosperetti, "Nonlinear Oscillations of Gas Bubbles in Liquids. Steady State Solutions", J. Acoust. Soc. Amer., in press.

17. Since resonance is responsible for the transfer of energy from the mode at $\omega$ to the mode at $\sim\omega_o$, $\omega_o$ should not be too different from the appropriate multiple or submultiple of $\omega$ for the present method to apply. Indeed, the assumption that $|3\omega - \omega_o|$ or $|\omega - 3\omega_o|$ is of order $\epsilon$ is implicit in all our results.

18. It can be shown, however, that Duffing's equation has an infinity of resonant frequencies. See e.g. M. E. Levenson, J. Appl. Phys. 20, 1045 (1949). These frequencies could be found by carrying the present method to higher orders in $\epsilon$.

TABLE I

The new frequencies $\omega_k$ introduced to first order by the nonlinearity in the RHS of Eq. (6)

| Term | $\omega_k$ | Condition for resonance |
|---|---|---|
| $\frac{1}{4}\Omega^3 \cos^3 \omega t$ | $3\omega$ | $\omega \sim \frac{1}{3}\omega_o$ |
| | $\omega$ | $\omega \sim \omega_o$ |
| $\frac{3}{2}\Omega^2(1+\cos 2\omega t)\, y$ | $\omega_o$ | none |
| | $2\omega + \omega_o$ | impossible |
| | $2\omega - \omega_o$ | $\omega \sim \omega_o$ |
| $3\Omega y^2 \cos \omega t$ | $\omega$ | $\omega \sim \omega_o$ |
| | $2\omega_o + \omega$ | impossible |
| | $2\omega_o - \omega$ | $\omega \sim 3\omega_o$ |
| $y^3$ | $\omega_o$ | none |
| | $3\omega_o$ | impossible |

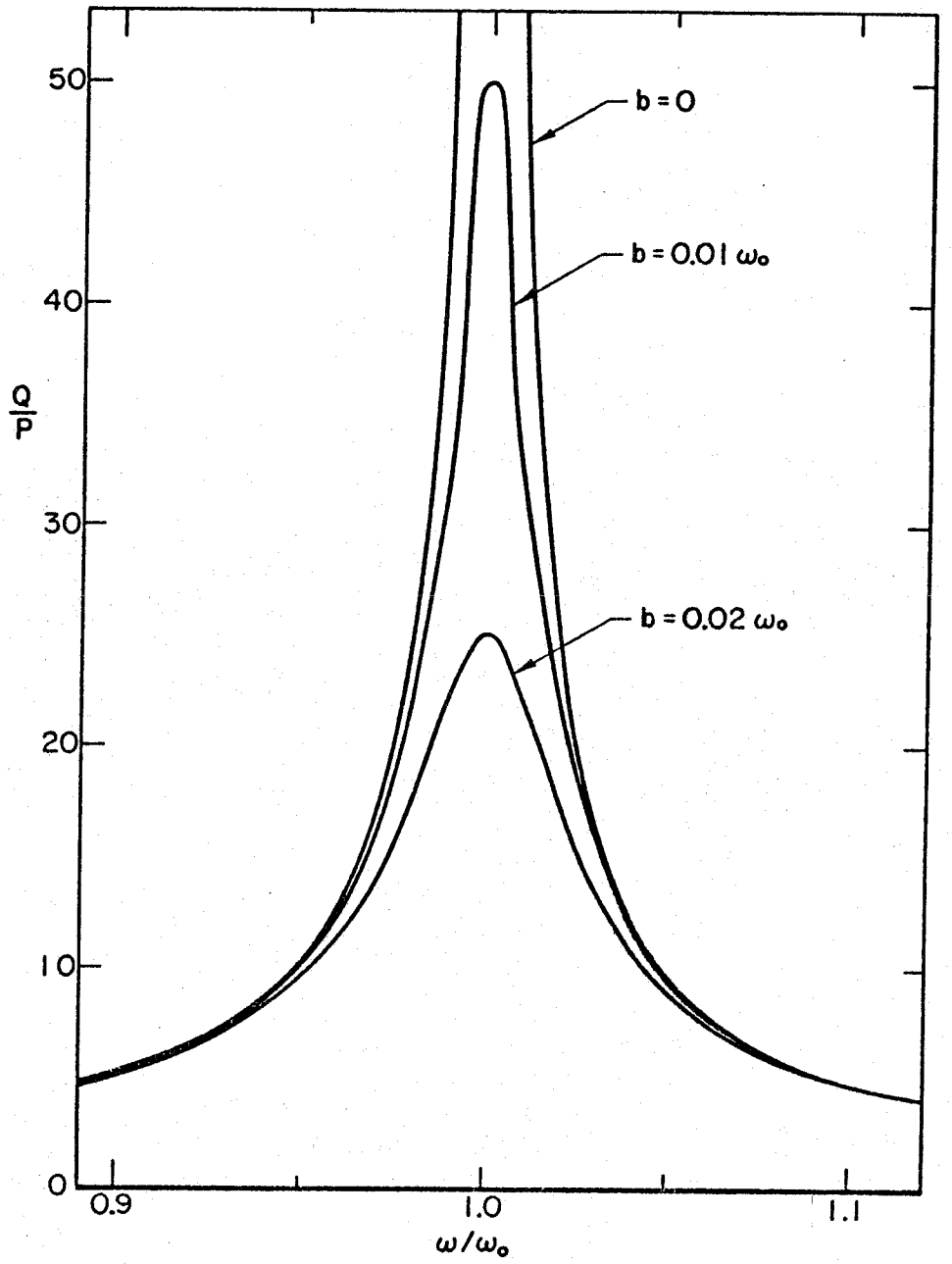


Fig. 1. The response function $Q(\omega, b)$ of the linear oscillator for various values of the damping parameter b (Eq. 3a).

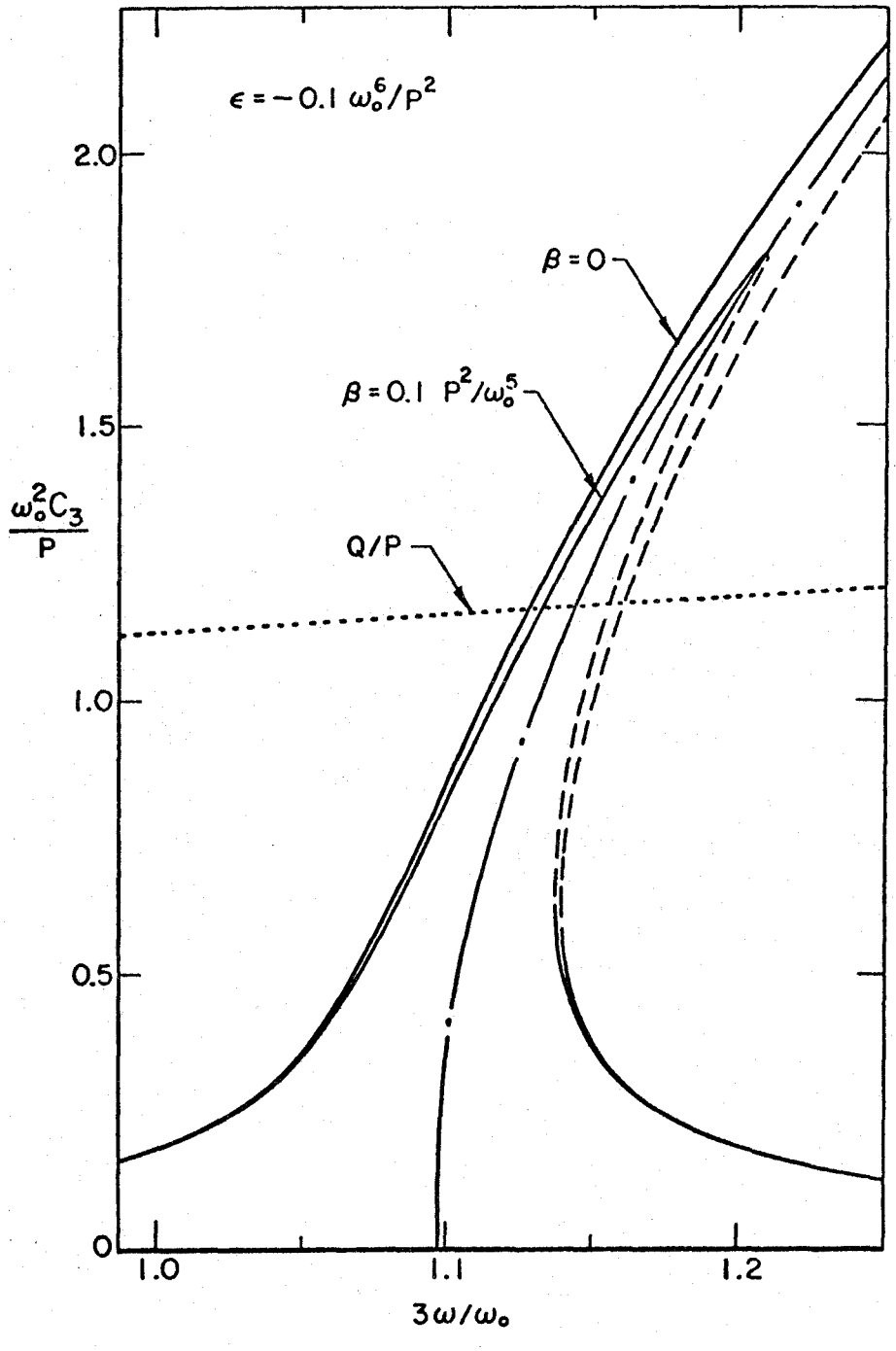


Fig. 2. Amplitude of the ultraharmonic, $C_3$, as a function of $3\omega/\omega_o$, as determined by Eqs. (8). The dashed portions of the curves correspond to unstable oscillations. The dash-and-dot line is the "backbone curve", Eq. (9), and the dotted line $Q(\omega, 0)$, Eq. (3a).

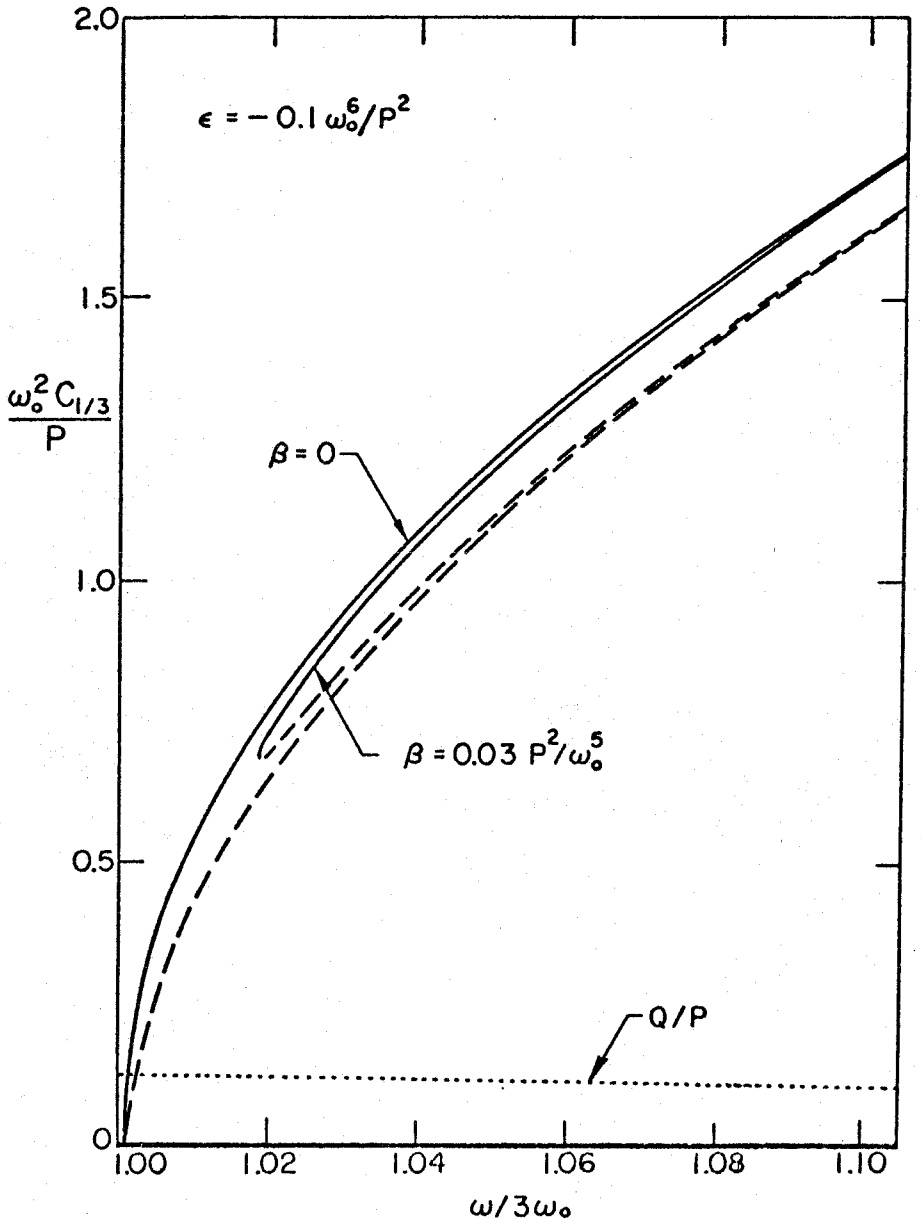


Fig. 3. Amplitude of the subharmonic, $C_{1/3}$, as a function of $\omega/3\omega_o$, as determined by Eqs. (11). The dashed portions of the curves correspond to unstable oscillations. The dotted line represents $Q(\omega, 0)$, Eq. (3a), which, to zero order in $\epsilon$, is the total amplitude of the response in the absence of the subharmonic.

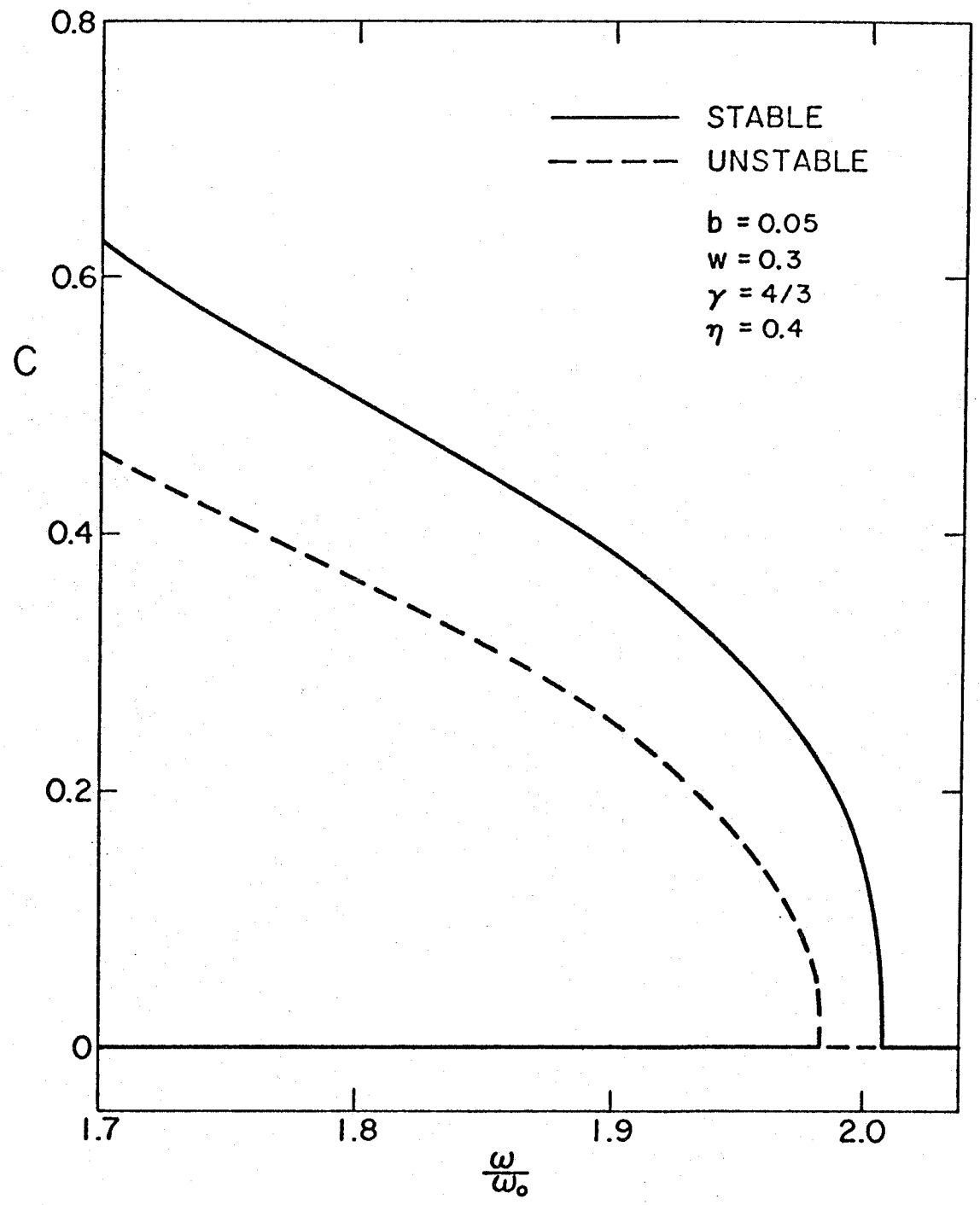


Fig. 4. Amplitude of the subharmonic response of order $\frac{1}{2}$ (i.e. for $\omega \sim 2\omega_o$) for the oscillations of a spherical gas bubble in an incompressible, viscous liquid (from Ref. 16, Fig. 1).

# PART III

# ON VISCOUS FLOWS WITH PERTURBED SPHERICAL SYMMETRY AND THE FREE OSCILLATIONS OF LIQUID DROPS

## 1. Introduction

Several inviscid flows with perturbed spherical symmetry, such as the oscillations of liquid globes (Thomson, 1890), drops (Rayleigh, 1896) and bubbles (Lamb, 1932, p. 475), are classic problems in fluid mechanics. More recent developments include the analysis of the spherical analogue of the Rayleigh-Taylor instability performed by Plesset (1954) and Birkhoff (1954, 1956), and its application to the growth and collapse of bubbles (Plesset and Mitchell, 1956).

The effect of viscosity on such flows, however, has not been fully investigated. Lamb (1932, p. 640) obtained simple approximate results for the damping of oscillating drops and bubbles by computing the energy dissipation in the approximation of irrotational flow. Chandrasekhar (1959; 1961, p. 466) and Reid (1960) attempted to derive more accurate solutions by postulating an exponential dependence on time for the oscillation amplitude. Although the Chandrasekhar-Reid solution is usually considered exact, and Lamb's result only a low viscosity approximation, it will be shown below that in reality both results are approximations valid in the final and early stages of the motion respectively. The physical reason for this is the gradual thickening of the layer in which viscosity is important, which makes physically significant a description in terms of constant frequency and damping parameter only when this layer is very small or very large. Between these two stages the damping and the frequency of oscillation are functions of time. This effect of diffusion of vorticity is a distinctive feature of the class of flows discussed here.

We consider a nearly spherical free surface $\Sigma(t)$ separating two incompressible, viscous, immiscible fluids that fill the entire space. Assuming that the deviation of the surface from the spherical shape is small, we solve the linearized flow problem and derive the general equations of motion for $\Sigma$. As an example of the application of this theory, the oscillations of a liquid drop are considered in some detail, and an asymptotic expansion of the solution valid for short times is obtained. For what concerns the limits of validity of the linearized analysis in spherical geometry, it may be observed that in at least one instance (Plesset and Chapman, 1972) it is known to be accurate for quite large values of the perturbation parameter.

## 2. Preliminaries

In the following the subscripts 1 and 2 will be attached to all quantities pertaining to the inner and outer region respectively. When no subscript is indicated, reference can be made indifferently to either region.

In the absence of body forces, the Navier-Stokes equations and the incompressibility condition are:

$$\frac{\partial \vec{U}}{\partial t} + \frac{1}{2}\,\vec{\nabla}(\vec{U}\cdot\vec{U}) + (\vec{\nabla}\times\vec{U})\times\vec{U} = \frac{1}{\rho}\,\mathrm{div}\,\sigma$$

$$\vec{\nabla}\cdot\vec{U} = 0$$

where $\vec{U}$ and $\rho$ denote velocity and density and the stress tensor $\sigma$ is given in terms of the pressure $p$ and viscosity $\mu$ by:

$$\sigma_{ij} = -p\,\delta_{ij} + \mu\left(\frac{\partial U_i}{\partial x_j} + \frac{\partial U_j}{\partial x_i}\right) \qquad (1)$$

The surface $\Sigma$ can be represented by a superposition of spherical harmonics. To first order in the perturbation of the spherical symmetry, however, the equations for the different modes are uncoupled, so that we may let, in spherical coordinates:

$$\Sigma(t): \quad F(r, \theta, t) \equiv r - R(t) - \epsilon\, a(t)\, P_n(\cos\theta) = 0 \qquad (2)$$

where $0 < \epsilon \ll 1$ and $P_n$ is a Legendre polynomial of degree $n \geq 2$. In writing Eq. (2) we have assumed for simplicity (and in practice with little loss of generality) that the surface maintains an axial symmetry.†

In the following developments only terms of first order in $\epsilon$ will be retained. To this approximation the outward unit normal $\vec{n}$ at every point of $\Sigma$ is:

$$\vec{n} = \vec{e}_r - \epsilon \frac{a}{R} \frac{dP_n}{d\theta} \vec{e}_\theta$$

where $\vec{e}_r$, $\vec{e}_\theta$ are unit vectors in the radial and azimuthal direction respectively. On the free surface the kinematical boundary conditions are (Batchelor, 1967, pp. 60, 148):

$$\frac{\partial F}{\partial t} + (\vec{U} \cdot \vec{\nabla})\, F = 0 \qquad (3)$$

$$\vec{U}_{t_1} = \vec{U}_{t_2} \qquad (4)$$

where the subscript $t$ denotes the tangential component of the velocity to the free surface. If one of the two fluids is inviscid, only

---

† This assumption can be avoided by splitting the velocity field into its toroidal and poloidal components (Chandrasekhar, 1961, p. 622).

the first condition applies. The dynamical boundary conditions stipulate that there should be no discontinuity in the tangential stresses:

$$\vec{n} \times [(\sigma_2 - \sigma_1)\vec{n}] = 0 \tag{5}$$

and that the discontinuity in the normal stress should equal the surface tension T times the total curvature:

$$\vec{n} \cdot [(\sigma_2 - \sigma_1)\vec{n}] = T\,\vec{\nabla} \cdot \vec{n} \tag{6}$$

In these equations the stress tensors $\sigma_1$ and $\sigma_2$ are evaluated on the inner and outer sides of $\Sigma$ respectively. To the above boundary conditions the requirements of regularity at infinity and at the origin (possibly with the exception of a source-like singularity†) are added.

It is convenient to introduce a velocity potential $\varphi$ and a stream function $\psi$ through the definitions:

$$U_r = \vec{U} \cdot \vec{e}_r = \frac{\partial \varphi}{\partial r} + \frac{\epsilon}{r^2 \sin\theta} \frac{\partial \psi}{\partial \theta}$$

$$U_\theta = \vec{U} \cdot \vec{e}_\theta = \frac{1}{r} \frac{\partial \varphi}{\partial \theta} - \frac{\epsilon}{r \sin\theta} \frac{\partial \psi}{\partial r}$$

Because of the solenoidal character of $\vec{U}$, $\varphi$ is harmonic and is found to be (Plesset, 1954):

$$\varphi_1 = \varphi_1^o + \epsilon\varphi_1' = -\dot{R} R^2/r + \epsilon b_1 r^n P_n$$

$$\varphi_2 = \varphi_2^o + \epsilon\varphi_2' = -\dot{R} R^2/r + \epsilon b_2 r^{-n-1} P_n$$

---

† It may be remarked here that if $R(t)$ is not a constant, a source or sink must be present inside $\Sigma$. In spite of its apparent artificiality, this is in many instances a very good schematization (Plesset and Mitchell, 1956).

where dots denote differentiation with respect to time. The constants $b_1$ and $b_2$ are determined by the kynematical boundary condition (3) as:

$$n\, b_1 = R^{-n+1} (\dot{a} + 2a \dot{R}/R)$$

$$(n+1)\, b_2 = - R^{n+2} (\dot{a} + 2a \dot{R}/R)$$

The same boundary condition requires, to first order in $\epsilon$:

$$\frac{\partial \psi}{\partial \theta} (R(t), \theta, t) = 0 \qquad (7)$$

To solve the problem it is convenient to split velocity and pressure into three parts as follows:

$$\vec{U} = \vec{u}^o + \epsilon (\vec{u}' + \vec{u}'')$$

$$p = p^o + \epsilon (p' + p'')$$

where:

$$\vec{u}^o = \vec{\nabla}\varphi^o = \dot{R}(R^2/r^2)\vec{e}_r \qquad \vec{u}' = \vec{\nabla}\varphi'$$

$$u_r'' = \frac{1}{r^2 \sin\theta} \frac{\partial \psi}{\partial \theta} \qquad u_\theta'' = - \frac{1}{r \sin\theta} \frac{\partial \psi}{\partial r}$$

and $p''$ is such that:

$$\vec{\nabla} \left( \frac{1}{2} \vec{u}^o \cdot \vec{u}^o + \epsilon \vec{u}^o \cdot \vec{u}' + \frac{p^o + \epsilon p'}{\rho} \right) = 0 \qquad (8)$$

In view of the incompressibility condition and of the fact that the velocity field $\vec{u}^o + \epsilon \vec{u}'$ is irrotational, the Navier-Stokes equations reduce then to:

$$\frac{\partial \vec{u}''}{\partial t} + \nabla (\vec{u}^o \cdot \vec{u}'' + \frac{p''}{\rho}) + (\vec{\nabla} \times \vec{u}'') \times \vec{u}^o = \nu \nabla^2 \vec{u}'' \qquad (9)$$

where $\nu = \mu/\rho$ is the kynematic viscosity.

3. Solution of the fluid mechanical problem

Define the vorticity as:

$$\epsilon \vec{\omega} = \vec{\nabla} \times \vec{U} = \epsilon \vec{\nabla} \times \vec{u}'' \qquad (10)$$

and take the curl of (9) to obtain:

$$\frac{\partial \vec{\omega}}{\partial t} + \vec{\nabla} \times (\vec{\omega} \times \vec{u}^o) = \nu \nabla^2 \vec{\omega}$$

The solution of this equation is found to have the form:

$$\vec{\omega} = \Omega(r,t)\, P_n^1 (\cos \theta)\, \vec{e}_\varphi$$

where $P_n^1 (\cos \theta)$ is an associated Legendre polynomial, $\vec{e}_\varphi = \vec{e}_r \times \vec{e}_\theta$, and $\Omega(r,t)$ is the solution of:†

$$\frac{\partial \Omega}{\partial t} - \nu \frac{\partial^2 \Omega}{\partial r^2} + \frac{1}{r} \left( \frac{R^2 \dot{R}}{r} - 2\nu \right) \frac{\partial \Omega}{\partial r} + \frac{1}{r^2} \left[ \nu n(n+1) - \frac{R^2 \dot{R}}{r} \right] \Omega = 0 \qquad (11)$$

The boundary conditions for this equation are that $\Omega(r,t)$ should equal a (still unknown) function $\Omega_o(t)$ at $r = R(t)$, and that $\partial \Omega_1 / \partial r$ vanish at the origin and $\Omega_2$ at infinity. The boundary data $\Omega_{o1}(t)$, $\Omega_{o2}(t)$ will be determined by the conditions at the interface. We shall also assume $\Omega(r, 0) = 0$.

---

† In writing these equations the effect of the boundary condition (6) has been partially anticipated in that the separation constant has been set at $\nu n(n+1)$ instead that at $\nu k(k+1)$, with $k$ an integer to be determined.

The stream function $\psi$ is now easily obtained from (10) as:

$$\psi(r,\theta,t) = \frac{n(n+1)}{2n+1}\,\Psi(r,t)\,[P_{n-1}(\cos\theta) - P_{n+1}(\cos\theta)]$$

with

$$\Psi(r,t) = \frac{r^{-n}}{2n+1}\Big[c(t) - \int_R^r s^{n+2}\,\Omega(s,t)ds\Big] + \frac{r^{n+1}}{2n+1}\Big[\int_R^r s^{-n+1}\Omega(s,t)ds - \frac{c(t)}{R^{2n+1}}\Big]$$

One of the integration constants has been eliminated with the aid of condition (7), and the value of the second one, $c(t)$, can be determined by imposing the regularity requirements at the origin and at infinity to obtain:

$$c_1(t) = -\int_o^R s^{n+2}\,\Omega_1(s,t)ds$$

$$c_2(t) = R^{2n+1}\int_R^\infty s^{-n+1}\,\Omega_2(s,t)\,ds$$

The condition (4) of continuity of the tangential velocity across the free surface reduces to:

$$c_1 - c_2 = \frac{2n+1}{n(n+1)}\,R^{n+2}\left(\dot{a} + 2a\frac{\dot{R}}{R}\right) \qquad (12)$$

It is now possible to compute $p''$ with the result:

$$\frac{p''}{\rho} = -\vec{u}^{\,o}\cdot\vec{u}'' + \frac{n(n+1)}{2n+1}\Big\{\Big[d(t) + \int_R^r s^{-n-2}\,\Omega(s,t)ds\Big]\,r^n + \Big[e(t) - \int_R^r s^{n-1}\,\Omega(s,t)ds\Big]\,r^{-n-1}\Big\}\,R^2\dot{R}\,P_n(\cos\theta)$$

The integration constants are found to have the following values:

$$nd_1(t) = (2n+1)\left[\nu_1 R^{-n-2}\dot{R}^{-1}\Omega_1(R,t) + R^{-2n-4}\int_o^R s^{n+2}\,\Omega_1(s,t)ds\right]$$

$$- (n+1)\,R^{-2n-1}\int_o^R s^{n-1}\,\Omega_1(s,t)ds$$

$$e_1(t) = -\int_o^R s^{n-1}\,\Omega_1(s,t)ds$$

$$d_2(t) = -\int_R^\infty s^{-n-2}\,\Omega_2(s,t)ds$$

$$(n+1)e_2(t) = (2n+1)\left[-\nu_2 R^{n-1}\dot{R}^{-1}\Omega_2(R,t) + R^{2n-2}\int_R^\infty s^{-n+1}\,\Omega_2(s,t)ds\right]$$

$$- nR^{2n+1}\int_R^\infty s^{-n-2}\,\Omega_2(s,t)ds$$

To complete the solution of the fluid mechanical problem, Eq. (8) must be integrated. The following results are readily found (Plesset, 1954):

$$p^o = P(t) + \rho\left(R\ddot{R} + \frac{3}{2}\dot{R}^2\right)$$

$$np_1' = -\rho_1\left[R\ddot{a} + 3\dot{R}\dot{a} + (n+2)\ddot{R}a\right]P_n(\cos\theta)$$

$$(n+1)\,p_2' = \rho_2\left[R\ddot{a} + 3\dot{R}\dot{a} - (n-1)\ddot{R}a\right]P_n(\cos\theta)$$

The functions $P(t)$ are two integration constants which are supposed to be known; the function $P_2(t)$ has the additional meaning of pressure at infinity.

4. Equations of motion of the interface

Now that the fluid mechanical problem is solved we are in a position to apply the dynamical boundary conditions (5), (6), and to derive the equations of motion of the interface. If the tangential stresses on both sides of $\Sigma$ are evaluated according to (1) and substituted into (5) one obtains:

$$2R^{-n-3}[\mu_1 c_1(t) - \mu_2 c_2(t)] + \mu_1 \Omega_1(R,t) - \mu_2 \Omega_2(r,t) =$$

$$= \frac{2}{R}\left[\left(\frac{n+2}{n}\mu_1 - \frac{n-1}{n+1}\mu_2\right)\frac{\dot{R}}{R}\,a - \left(\frac{n-1}{n}\mu_1 - \frac{n+2}{n+1}\mu_2\right)\dot{a}\right] \tag{13}$$

This equation, together with (12), can be used (at least in principle) to express the boundary data $\Omega_{o1}(t), \Omega_{o2}(t)$ in terms of $R(t)$ and $\underline{a}(t)$. The remaining boundary condition, Eq. (6), plays then the logical role of a consistency requirement, and can be used to obtain the equations governing the motion of $R(t)$ and $\underline{a}(t)$(Plesset, 1954). Upon substitution of the expressions for the normal stresses, and separation of the $\epsilon$-dependent terms, it yields:

$$R\ddot{R} + \frac{3}{2}\dot{R}^2 = \frac{1}{\rho_2 - \rho_1}\left[P_1(t) - P_2(t) - 4(\mu_2 - \mu_1)\frac{\dot{R}}{R} - 2\frac{T}{R}\right] \tag{14}$$

$$\frac{(n+1)\rho_1+n\rho_2}{n(n+1)}\ddot{a} + \left[3\frac{(n+1)\rho_1+n\rho_2}{n(n+1)}\frac{\dot{R}}{R} - 2(n-1)(n+2)\frac{\mu_2-\mu_1}{R^2}\right]\dot{a}$$

$$+ \left[\frac{(n+1)(n+2)\rho_1-n(n-1)\rho_2}{n(n+1)}\frac{\ddot{R}}{R} + (n-1)(n+2)\frac{T}{R^3} + 2(n-1)(n+2)(\mu_2-\mu_1)\frac{\dot{R}}{R^3}\right]a$$

$$+ (n-1)(n+1)\frac{\mu_1}{R}\,\Omega_1(R,t) - n(n+2)\frac{\mu_2}{R}\,\Omega_2(R,t) \qquad (15)$$

$$+ n\rho_2\,\dot{R}R^{n-2}\int_R^\infty (s^3-R^3)\,s^{-n-2}\,\Omega_2(s,t)ds$$

$$- (n+1)\,\rho_1\,\dot{R}R^{-n-3}\int_o^R (s^3-R^3)s^{n-1}\,\Omega_1(s,t)ds = 0$$

The first equation governs the motion of a sphere of radius $R(t)$, the zero order approximation to the shape of the free boundary. The second equation determines the motion of the first-order correction to the shape of the free boundary; in the limit of vanishing viscosity and vorticity it reduces to the equation obtained by Plesset (1954). The set of equations (12), (13), (14), and (15), with $\Omega(r,t)$ solution of (11), is the complete set of equations determining the free surface problem. The solution of this system is in general a matter of great complexity, so that it is useful to derive approximate equations. In practice two limiting cases are of interest, which we shall term the "drop" and "bubble" approximations.

The drop approximation

In this approximation the mechanical effects of the exterior fluid are negligible, except for the fact that it provides a uniform ambient pressure. Setting $\mu_2 = 0$, $\rho_2 = 0$ we get:

$$\ddot{R}R + \frac{3}{2}\dot{R}^2 = \rho_1^{-1}[P_2(t) - P_1(t) + 2T/R] - 4\nu_1 \dot{R}/R$$

$$\ddot{a} + [3\dot{R}/R + 2n(n-1)(n+2)\nu_1/R^2]\,\dot{a}$$

$$+[(n+2)\ddot{R}/R + n(n-1)(n+2)\,T/(\rho_1 R^3) - n(n-1)(n+2)\,\dot{R}\nu_1/R^3]\,a \qquad (16)$$

$$+ n(n-1)(n+1)(\nu_1/R)\Omega_1(R,t) - n(n+1)\dot{R}R^{-n-3}\int_0^R (s^3 - R^3)s^{n-1}\Omega_1(s,t)ds = 0$$

$$\Omega_1(R,t) - 2R^{-n-3}\int_0^R s^{n+2}\,\Omega_1(s,t)ds = 2R^{-1}[(n+2)a\,\dot{R}/R - (n-1)\dot{a}]/n \qquad (17)$$

The next to the last term in (16) represents the diffusion of vorticity from the moving boundary, and the last one the effect of convection on this process. As already mentioned in Section 2, the condition of continuity of tangential velocity, Eq. (12), does not apply in this case, and $c_2(t) = 0$.

The bubble approximation

In this approximation $\mu_1 = 0$, $\rho_1 = 0$ and the equations become:

$$R\ddot{R} + \frac{3}{2}\dot{R}^2 = \rho_2^{-1}[P_1(t) - P_2(t) - 2T/R] - 4\nu_2 \dot{R}/R \qquad (18)$$

$$\ddot{a} + [3\dot{R}/R - 2(n-1)(n+1)(n+2)\nu_2/R^2]\dot{a}$$

$$+ [-(n-1)\ddot{R}/R + (n-1)(n+1)(n+2)T/(\rho_2 R^3) + 2(n-1)(n+1)(n+2)\nu_2\dot{R}/R^3]a$$

$$- n(n+1)(n+2)(\nu_2/R)\Omega_2(R,t) + n(n+1)\dot{R}R^{n-2}\int_R^\infty (s^3-R^3)s^{-n-2}\Omega_2(s,t)ds = 0$$

$$\Omega_2(R,t) + 2R^{n-2}\int_R^\infty s^{-n+1}\Omega_2(s,t)ds = 2R^{-1}[(n-1)a\dot{R}/R - (n+2)\dot{a}]/(n+1)$$

Eq. (18) is well known in the field of bubble dynamics (Plesset, 1949; Hsieh, 1965). If $P_1 = 0$ and viscosity is negligible it becomes the equation describing the collapse of an empty cavity obtained by Besant (1859). The condition of continuity of the tangential velocity does not apply in this case either, and $c_1(t) = 0$.

5. Application to the oscillations of a drop

As an application of the theory developed above we shall now briefly consider the free oscillations of a liquid drop about the spherical shape. This problem has been discussed by Chandrasekhar

(1959; 1961, p. 466) and Reid (1960) who, assuming an exponential time dependence for the oscillations of the form $e^{-\sigma t}$, with $\sigma$ a complex constant, derived an equation for $\sigma$. It will be shown here that this solution is only valid as $t \to \infty$; the physical reason for this has been discussed in Section 1.

In the case of an oscillating drop, R is independent of time, so that the equations of the drop approximation further simplify to:

$$\ddot{a} + 2n(n-1)(n+2)(\nu/R^2)\dot{a} + n(n-1)(n+2)(T/\rho R^3)\, a + \\ + n(n-1)(n+1)(\nu/R)\, \Omega(R,t) = 0 \tag{19}$$

$$\Omega(R,t) - 2R^{-n-3} \int_0^R s^{n+2} \Omega(s,t) ds = -2(n-1)\dot{a}/nR \tag{20}$$

where the subscript 1 has been dropped. The function $\Omega(r,t)$ is now the solution of:

$$\frac{\partial \Omega}{\partial t} - \nu \frac{\partial^2 \Omega}{\partial r^2} - \frac{2\nu}{r} \frac{\partial \Omega}{\partial r} + \frac{\nu}{r^2} n(n+1)\, \Omega = 0 \tag{21}$$

subject to the initial condition $\Omega(r,0) = 0$, and to the boundary condition $\Omega(R,t) = \Omega_o(t)$.

Observe first that by combining (19) and (20) one gets:

$$\ddot{a} + 2(n-1)(2n+1)(\nu/R^2)\, \dot{a} + n(n-1)(n+2)\, (T/\rho R^3) a \\ + 2n(n-1)(n+1)\, \nu\, R^{-n-4} \int_0^R s^{n+2}\, \Omega(s,t)\, ds = 0$$

If $\Omega(r,t)$ is so small that the approximation of irrotationality can be made, the last term can be neglected and we can read directly from the equation the frequency $\omega_o$ and the decay constant $\tau_d$ of the oscillations:

$$\omega_o^2 = n(n-1)(n+2)\, T/\rho R^3$$

$$\tau_d^{-1} = (n-1)(2n+1)\, \nu/R^2$$

The first of these equations is the result obtained by Rayleigh (1896) for the oscillations of an inviscid drop, the second coincides with the expression derived by Lamb (1932, p. 640) in the approximation of irrotational flow.

Eq. (21) for $\Omega(r,t)$ can readily be solved by taking its Laplace transform with the result:

$$\tilde{\Omega}(r,p) = \left(\frac{R}{r}\right)^{\frac{1}{2}} \tilde{\Omega}_o(p) \quad \frac{I_{n+\frac{1}{2}}(r(p/\nu)^{\frac{1}{2}})}{I_{n+\frac{1}{2}}(R(p/\nu)^{\frac{1}{2}})}$$

where tildas denote the image functions and $p$ is the variable in the transformed plane. The unknown function $\Omega_o(t)$ is now determined by Eq. (20) and is found to be:

$$\tilde{\Omega}_o(p) = -\frac{2}{R}\,\frac{n-1}{n}\,\tilde{a}(p)\left[1 - \frac{2}{q}\,\frac{I_{n+3/2}(q)}{I_{n+\frac{1}{2}}(q)}\right]^{-1}$$

where $q = R(p/\nu)^{\frac{1}{2}}$. Substitution into (19) and application of the convolution theorem for the Laplace transform yields:

$$\ddot{a} + 2\tau_d^{-1}\,\dot{a} + \omega_o^2\, a - 2\nu R^{-2}\,\beta_n \int_o^t Q(t-\tau)\,\dot{a}(\tau)d\tau = 0 \qquad (22)$$

where $\beta_n = (n-1)^2(n+1)$ and the Laplace transform of $Q(t)$ is:

$$\tilde{Q}(p) = \frac{2I_{n+3/2}(q)}{I_{n+\frac{1}{2}}(q) - 2I_{n+3/2}(q)}$$

On physical grounds we expect the solution of (22) to have the form of modulated oscillations. We therefore let:

$$a(t) \propto e^{-\sigma(t)\, t}$$

The only information that we have on the function $\sigma(t)$ at this stage is that:

$$\sigma(t=0) = \sigma_o = \tau_d^{-1} \pm i(\omega_o^2 - \tau_d^{-2})^{\frac{1}{2}} \qquad (23)$$

Let now:

$$u(t) = \exp\{-[\sigma(t) - \sigma_o]\, t\} \qquad (24)$$

with $\sigma_o$ given by (23), so that

$$a(t) = e^{-\sigma_o t}\, u(t)$$

and $u(t=0) = 1$, $\dot{u}(t=0) = 0$. The Laplace transform of $u(t)$ is found to be:

$$\tilde{u}(p) = \frac{p + 2(\tau_d^{-1} - \sigma_o) - 2(\nu/R^2)\beta_n \tilde{Q}(p-\sigma_o)}{p^2 + 2(\tau_d^{-1} - \sigma_o)p - 2(\nu/R^2)\beta_n (p - \sigma_o)\tilde{Q}(p-\sigma_o)}$$

In view of the complexity of this expression it is practically impossible to obtain an exact expression for $u(t)$, but a solution valid for small values of time can nevertheless be found by an asymptotic expansion as $p \to \infty$. When this is compared with (24) we find:

$$\sigma(t) = \sigma_o\{1 + \beta_n[\frac{32}{15\pi^{\frac{1}{2}}}\ (\frac{\nu t}{R^2})^{3/2} - \frac{2}{3}(n-1)(\frac{\nu t}{R^2})^2 + O(\frac{\nu^{3/2}\sigma_o t^{5/2}}{R^3}, \frac{\nu^{5/2}t^{5/2}}{R^5})]\}$$

To investigate the behaviour of $a(t)$ for large values of time it is convenient to let:

$$a(t) \propto e^{-\sigma_\infty t}\, v(t)$$

with $\sigma_\infty$ a constant to be determined in such a way that:

$$\lim_{t \to \infty} v(t) = \text{constant} \qquad (25)$$

The Laplace transform of $v(t)$ can be expanded near $p = 0$ with a result of the form:

$$\tilde{v}(p) \sim \frac{A + Bp}{C + Dp}$$

where A, B, C, D, are functions of $\sigma_\infty$, n and the other parameters of the problem. To satisfy (25) we must then require that $C = 0$. This condition, written out in full, reads:

$$\sigma_\infty^2 - 2\tau_d^{-1}\sigma_\infty + \omega_o^2 + 2\beta_n \frac{\nu}{R^2}\ \sigma_\infty \frac{2J_{n+3/2}(x)}{xJ_{n+\frac{1}{2}}(x) - 2J_{n+3/2}} = 0$$

$$x = R(\sigma_\infty/\nu)^{\frac{1}{2}}$$

which coincides with the equation obtained by Chandrasekhar and Reid.

## 6. The equation for the vorticity

We now turn to the solution of (11) for the vorticity and to some related problems. The equation is of such a complexity that it is extremely difficult if not impossible to find a general solution. Very often, however, one can take advantage of the exponential decay of vorticity on both sides of $\Sigma$ to obtain adequate approximate solutions.

Consider first the simple case in which $|R\dot{R}| \ll \nu$. Equation (11) then reduces to Eq. (21), the solution of which in the inner region has already been given in Section 5. In the outer region one finds:

$$\tilde{\Omega}_2(r,p) = \left(\frac{R}{r}\right)^{\frac{1}{2}} \tilde{\Omega}_2(R,p) \; \frac{K_{n+\frac{1}{2}}(r(p/\nu)^{\frac{1}{2}})}{K_{n+\frac{1}{2}}(R(p/\nu)^{\frac{1}{2}})}$$

where the tildas denote the Laplace-transformed function, $p$ is the transformed variable, and $K_\nu$ is the modified Bessel function regular at infinity.

In the general case, let us operate the following change in the dependent variable:

$$\Omega(r,t) = r^{-2} \; \frac{R^3}{R_o^3} \exp\left[-\nu[n(n+1)-2]\int_o^t R^{-2}(u)\,du\right] U(r,t)$$

(where $R_o$ is the initial condition for (11)) and adopt Langrangian coordinates:

$$h = (r^3 - R^3)/3 \qquad t = t \; ;$$

equation (11) becomes:

$$\frac{\partial U}{\partial t} - \nu r^4 \; \frac{\partial^2 U}{\partial h^2} + \{\nu[n(n+1)-2](r^{-2} - R^{-2}) + 3R^2\dot{R}(R^{-3} - r^{-3})\}\, U = 0 \tag{26}$$

This equation can now be solved by means of a perturbation method based on a boundary layer approximation. To this end, introduce the dimensionless variables:

$$h_+ = h/\epsilon_1 \ell^3 \qquad t_+ = \nu t/\epsilon_1^2 \ell^2 \qquad r_+ = r/\ell \qquad R_+ = R/\ell$$

where $\ell$ is a typical length, for instance $\ell = R_o$, and $0 < \epsilon_1 \ll 1$, and let:

$$U(h,t) = U^o(h,t) + \epsilon_1 U^1(h,t) + \ldots \tag{27}$$

Dropping the subscript +, we obtain the following set of equations:

$$\frac{\partial U^o}{\partial t} - R^4 \frac{\partial^2 U^o}{\partial h^2} = 0$$

$$\frac{\partial U^1}{\partial t} - R^4 \frac{\partial^2 U^1}{\partial h^2} = 4R \frac{\partial^2 U^o}{\partial h^2} - 9 \frac{h}{R^4} \frac{dR}{dt} U^o$$

. . . . . .

The boundary conditions are:

$$U^o(0,t) = \frac{R_o^3}{R} \exp\left[\nu\,[n(n+1)-2] \int_o^t R^{-2}(u)du\right] \Omega(R,t)$$

$$U^i(0,t) = 0 \quad \text{for } i \geq 1$$

$$U_2^j(h,t) \to 0 \text{ as } h \to \infty \quad \text{for } j \geq 0$$

$$U_i^j(h,t) = 0 \quad \text{at } h = -R^3/3$$

The solution is most easily obtained in terms of the new time variable:

$$\tau_+ = \int_0^{t_+} R_+^4 (u_+)\, du_+ \tag{28}$$

by means of a Laplace transform. For the outer region we have:

$$U_2^o (h, \tau) = \int_o^\tau \frac{U_2^o(0, \lambda)h}{2\pi^{\frac{1}{2}}(\tau - \lambda)^{3/2}} \exp\left[ - \frac{h^2}{4(\tau - \lambda)}\right] d\lambda$$

$$U_2^i(h, \tau) = \int_{-\infty}^{\infty} dy \int_o^\tau \frac{G_i(y, \lambda)}{2\pi^{\frac{1}{2}}(\tau - \lambda)^{\frac{1}{2}}} d\lambda \quad \text{for } i \geq 1 \tag{29}$$

where:

$$G_1(h, \tau) = \text{sgn}(h)\, \frac{h}{R^3} \left(4 \frac{\partial^2}{\partial h^2} - 9R^{-5} \frac{dR}{dt}\right) U_2^o(|h|, t)$$

. . . . . .

For the inner region the expressions get more complicated because of the boundary condition at the origin instead that at infinity. For example:

$$U_1^o (h, \tau) = \frac{9}{R^3} \frac{\partial}{\partial r^3} \int_o^\tau U_1^o (0, \lambda)\, \theta_4\left(\frac{r^3}{2R^3} \,\middle|\, \frac{9i\pi(\tau-\lambda)}{R^6}\right) d\lambda$$

where $\theta_4(v|a)$ is Jacobi's theta function of the fourth type.

In this more general case the computation of the integrals entering into Eqs. (13), (15) cannot be carried out in closed form, but an approximate method is described in the Appendix. Very often, for

phenomena of a sufficiently short duration, the first term $U^o(h, \tau)$ will be an adequate approximation, and the boundary condition on $U_1^o$ can be imposed at $h \to -\infty$, thus obtaining an expression similar to (29). Strictly speaking, $U^o$ is a good approximation to the solution only near the interface $\Sigma$, so that some error will be involved in using it in integrals extending to large distances. In view of the exponential dependence on $h^2$ in general this error can be expected to be small. If a greater accuracy is required, however, the above expansion for $U$ should be considered as an inner expansion and supplemented by an outer expansion in an obvious way.

Appendix

We consider here the problem of computing integrals like those entering into the definitions of $c(t)$ when $R(t)$ is not a constant. Expressions of general validity cannot be obtained, and we shall content ourselves with some approximate results. In practice the interest in this case arises when the conditions for the validity of the bubble approximation are met, so that we shall further restrict our analysis accordingly.

Consider the integral:

$$I_k = \int_R^\infty s^{-k+1}\, \Omega_2(s,t)\, ds \qquad (A1)$$

and expand $\Omega_2(r,t)$ in a series analogous to (27):

$$\Omega_2(r,t) = \Omega_2^o(r,t) + \epsilon_1 \Omega_2^1(r,t) + \ldots$$

where

$$\Omega_2^i(r,t) = r^{-2}\, f(t)\, U_2^i(r,t)$$

$$f(t) = (R/R_o)^3 \exp\left[-\nu[n(n+1)-2] \int_o^t R^{-2}(u)\, du\right]$$

From (29) it is easily found that:

$$\Omega_2^o(r,t) = \frac{h}{2(\pi\nu)^{\frac{1}{2}}} \frac{R^2}{r^2} \int_o^\tau \frac{\Omega_2(R,\lambda)}{(\tau-\lambda)^{3/2}} \exp\left[-\frac{h^2}{4\nu(\tau-\lambda)}\right] d\lambda \qquad (A2)$$

where the time variable $\tau$ is connected to the dimensionless one $\tau_+$ by:

$$\tau = (\epsilon_1^2 \ell^6/\nu)\, \tau_+$$

After substitution of (A2) into (A1) and interchange of the order of integration we find:

$$\Omega_2^o(r,t) = \frac{R^{-k+5}}{4(\pi\nu)^{\frac{1}{2}}}\int_o^\tau \frac{\Omega_2(R,\lambda)}{(\tau-\lambda)^{3/2}} J_k(R^6/4\nu(\tau-\lambda)\, d\lambda$$

where:

$$J_k(u) = \int_o^\infty (1+3y^{1/2})^{-k/3-1} \; e^{-uy}\, dy$$

This can be approximated by the following asymptotic series obtained with the aid of Watson's lemma:

$$J_k(u) \sim \sum_{m=2}^{\infty} 3^{m-2}\binom{-k/3-1}{m-2} \Gamma(m/2)u^{-m/2}$$

If $R^6/4\nu\tau$ is large enough so that only the first term needs be retained we obtain:

$$c_2^o(t) = R^{2n+1}(t)\int_R^\infty s^{-n+1}\Omega_2^o(s,t)ds \simeq (\nu/\pi)^{\frac{1}{2}}R^n(t)\int_o^\tau \Omega_2(R,\lambda)(\tau-\lambda)^{-\frac{1}{2}}d\lambda$$

To this order the last integral in (18) vanishes; if another term is kept in the asymptotic series the result is:

$$\int_R^\infty (s^3-R^3)s^{-n-2}\,\Omega_2^o(s,t)ds \simeq 3\nu R^{-n-4}(t)\int_o^\tau \Omega_2(R,\lambda)\, d\lambda\,.$$

## REFERENCES

Batchelor, G. K. 1967 An Introduction to Fluid Dynamics. Cambridge University Press.

Besant, W. 1859 Hydrostatics and Hydrodynamics. Cambridge University Press.

Birkhoff, G. 1954 Note on Taylor Instability. Quart. Appl. Math. 12, 306.

Birkhoff, G. 1956 Stability of Spherical Bubbles. Quart. Appl. Math. 13, 451.

Chandrasekhar, S. 1959 The Oscillations of a Viscous Liquid Globe. Proc. London Math. Soc. 9, 141.

Chandrasekhar, S. 1961 Hydrodynamic and Hydromagnetic Stability. Clarendon Press.

Hsieh, D. Y. 1965 Some Analytical Aspects of Bubble Dynamics. J. Basic Eng. 87, 991.

Lamb, H. 1932 Hydrodynamics, 6th Ed. Dover Reprint, 1945.

Plesset, M. S. 1949 The Dynamics of Cavitation Bubbles. J. Appl. Mech. 16, 277.

Plesset, M. S. 1954 On the Stability of Fluid Flows with Spherical Symmetry. J. Appl. Phys. 25, 96.

Plesset, M. S. and Chapman, R. B. 1971 Collapse of an Initially Spherical Vapor Cavity in the Neighborhood of a Solid Boundary. J. Fluid. Mech. 47, 283.

Plesset, M. S. and Mitchell, T. P. 1956 On the Stability of the Spherical Shape of a Vapor Cavity in a Liquid. Quart. Appl. Math. 13, 419.

Lord Rayleigh 1896 The Theory of Sound, 2nd Ed., Art. 364. Dover Reprint, 1945.

Reid, W. H. 1960 The Oscillations of a Viscous Liquid Drop, Quart. Appl. Math. 18, 86.

Thomson, W. 1890 Oscillations of a Liquid Sphere. In Mathematical and Physical Papers, vol. 3, p. 384. C. J. Clay and Sons, Cambridge University Press.